PERFORMANCE EVALUATION OF ASPHALT CONCRETE PAVEMENTS IN ETHIOPIA, THE APPLICATION OF HDM-4 ROAD DETERIORATION SUB-MODEL

By

Abiyou Gebru Kassa

A Thesis Submitted in Partial Fulfillment for the Award of the Degree of Master of Science in Civil Engineering in the University of Nairobi

Department of Civil and Construction Engineering

Supervisor:

Professor Gichaga Francis J.

MAY 2013

Declaration

This Thesis is my original work and has not been presented for a degree in any other University.

Signature ……. Date …….

Abiyou Gebru Kassa (F56/64444/2010)

This Thesis has been submitted for examination with my approval as University Supervisor

Signature ……. Date …….

Professor Gichaga Francis J.

ABSTRACT

Many road performance models have been developed and used as important inputs for design and evaluation of pavements especially in the Post-AASHO Road Test era. The Highway Development and Management model (HDM-4), a computer model originally developed by the World Bank, is particularly useful because it integrates pavement performance models to the initial construction, maintenance and road user cost models thereby enabling economic and financial evaluation of a project or alternative projects. This research focused on a level two calibration of the road deterioration sub-model of HDM-4, specifically the models of asphalt concrete (AC) on granular base pavements to the conditions in Ethiopia, taking Addis-Modjo-Awasa Road as a case study.

To meet the objectives of the study, a thorough evaluation of historical data of the road was conducted and suitable calibration pavement sections identified. A methodology for field data collection was crafted. The field data collection includes measurement of pavement deflection using a Benkelman Beam and the measurement of pavement conditions of roughness, rutting and cracking using automated survey vehicle.

The calibration process includes prediction of pavement deterioration taking the calibration factor as unity and scaling to match the observed level of deterioration. The procedure of calibration is based on the provisions of the HDM-4 calibration manual prepared by Bennett and Paterson in the year 2000.

The results showed that the calibration factors are well within the typical values of factors included in the calibration manual of HDM-4 (Paterson and Bennett 2000) indicating that the road deterioration models are generally applicable to the asphalt concrete pavements to the Ethiopian conditions. The prediction of cracking initiation and progression and the collected data generally show wider dispersion, resulting in higher calibration factors especially for cracking initiation. The predictions of rutting and roughness progression are more stable, and the calibration factors are close to unity. The study also showed that local condition of material quality, workmanship and the environmental effects of drainage affect deterioration rates more than traffic loading.

ACKNOWLEDGMENT

I would like take this opportunity to thank my Supervisor, Professor Gichaga, for his valuable advice, encouragement and patience in moulding this thesis from its inception to the final shape.

I am also very grateful to the Ethiopian Roads Authority (ERA) specifically Ato Haddis Tesfaye, the Director of Asset Management, and his team for providing me the necessary equipment and manpower for the study, without their help it could be very difficult to materialize this study. I also thank Ato Eshite Mulat of Metaferia Consulting Engineers, Ato Asnake Abate of Omega Consulting Engineers, Ato Shimeles Tesfaye of Spice Consulting Engineers and Eng. Peter Nduati of GIBB Africa for providing materials relevant to the study. I wish to thank all of you, who I did not call by name, for your valuable support and advice.

Finally, I would like to thank my family to their patience and continued support in the lengthy exercise of this thesis.

TABLE OF CONTENTS

Declaration ..... **i**

Abstract ..... **ii**

Acknowledgment ..... **iii**

Abbreviations and Acronyms ..... **ix**

Chapter 1. Introduction **1**

1.1 Overview 1
1.2 Background 3
1.2.1 Location 3
1.2.2 Climate 3
1.2.3 Traffic 4
1.2.4 Pavement History 5
1.3 Problem Statement 6
1.4 Objectives of the Study 7
1.4.1 Overall Objective 7
1.4.2 Specific Objectives 7
1.5 Hypothesis 7
1.6 Scope and limitations of the study 8

Chapter 2. Literature Review **9**

2.1 Studies Leading to the Development of the HDM-4 Model 9
2.1.1 AASHO Road Test 9
2.1.2 The HDM SERIES 11
2.2 Input parameters to HDM Road Deterioration Models 13
2.2.1 Pavement Strength 13
2.2.2 Pavement Classification 18
2.2.3 Traffic Loading 20
2.2.4 Construction Quality 21
2.2.5 Environmental Factors 21
2.2.6 Pavement History 22
2.3 HDM Paved-Road Deterioration Models 23
2.3.1 Cracking 26
2.3.2 Ravelling 38
2.3.3 Potholing 38
2.3.4 Rutting 42
2.3.5 Roughness 45
2.4 HDM-4 Studies in Ethiopia and Neighbouring Countries 51
2.5 Statistical Methods of Data Analysis 53
2.6 Summary of Literature Review 55

Chapter 3. Methodology of Data Collection **57**

3.1 Introduction 57
3.2 Levels of Data Collection and Calibration 57
3.3 Desk Top Studies 58
3.4 Analysis for Establishing Calibration Sections 59
3.4.1 Analysis for Environmental Classification of the Study Area 59
3.4.2 Analysis for Pavement Strength Classification of the Study Area 62
3.4.3 Analysis for Classification of Study Area Based on Traffic Loading 68
3.4.4 Classification of the Study Area Based on Pavement Condition 70
3.1.4 Matrix of Calibration Sections 71
3.5 Preliminary Field Studies, Requirements of HDM-4 and Constraints 73
3.6 Availability of a Permanent Referencing 73
3.7 Specific HDM-4 Requirements 73
3.8 Selected Calibration Sections 73
3.9 Field Data Collection 75
3.9.1 Deflection Measuring Equipment and Procedure 78
3.9.2 Pavement Condition Data Collection 81
3.9.3 Traffic Study 89
Chapter 4. Data Analysis and Results 90
4.1 Introduction 90
4.2 Preparation of Model Input Data 90
4.2.1 Analysis of Pavement Strength of the Calibration Sections 90
4.2.2 Traffic Loading 94
4.2.3 Materials Quality and Construction Standards of the Roads 94
4.3 Analysis and Calibration of the HDM-4 Deterioration Models 99
4.3.1 Crack Initiation Adjustment Factor 99
4.3.2 Cracking Progression 103
4.3.3 Rutting Progression 106
4.3.4 Roughness Progression 110
Chapter 5. Discussion of Results 116
5.1 Discussion on Analysis of Input Data 116
5.1.1 Climatic Classification 116
5.1.2 Traffic Loading 117
5.1.3 Pavement Strength 118
5.1.4 Quality of Construction and Quality of Drainage 119
5.2 Interaction of Pavement Strength, Traffic Loading and Road Deteriorations 119
5.2.1 Addis Ababa-Modjo Pavement Segment 120
5.2.2 Modjo-Meki Pavement Segment 121
5.2.3 Meki-Zeway Pavement Segment 122
5.3 Discussion of Results of HDM-4 Models Calibration 124
5.3.1 Cracking Initiation Model and Calibration Factor 124
5.3.2 Cracking Progression Model and Calibration Factor 124
5.3.3 Rut Depth Progression Calibration Factor 125

5.3.4 Roughness Progression Calibration Factor 125
5.4 Comparison of Calibration Factors in the Region 126
5.5 Summary Key Findings 127
Chapter 6. Conclusions and Recommendations 129
6.1 Conclusions 129
6.2 Recommendations 130
References 132
APPENCICES 136
APPENDIX 1- Pavement Strength Calculations 137
APPENDIX 2- Traffic Volume and Loading Calculations 144
APPENDIX 3-Compaction Index Calculations 149
APPENDIX 4- HDM-4 Road Deterioration Models Calibration 152

List of Tables

Table 1-1 Pavement Structure of Addis-Modjo and Modjo-Awasa Roads 5
Table 2-1: Values of exponent p for calculating SNP 17
Table 2-2 Pavement classification system of HDM-4 19
Table 2-3 HDM-4 Environmental classification 22
Table 2-4 Mode and Type of Distresses 23
Table 2-5: HDM-4 Sensitivity Classes 25
Table 2-6 Ranking of Impacts of Road Deterioration factors 25
Table 2-7 Material characteristics and loading condition on fatigue life 31
Table 2-8 Summary of Roughness Measuring Systems 46
Table 3-1 Thornthwaite moisture index calculation of Akaki town 63
Table 3-2: Thornthwaite moisture index calculation of Modjo town 64
Table 3-3 Thornthwaite moisture index calculation of Awasa town 65
Table 3-4 Damaging factor of vehicles in the study area 69
Table 3-5 Calibration Section Identification Matrix 72
Table 3-6: Matrix of Calibration Sections 72
Table 3-7 Location of Selected Calibration Sites 74

Table 3-8 HDM-4 calibration site selection requirement versus actually adopted 76
Table 3-9: Sample spread sheet from HAWKEYE Processing Toolkit 87
Table 4-1 Mean monthly rainfall (mm) records of towns in the study area 93
Table 4-2 Eighth year traffic loading for the three segments 94
Table 4-3 Project Specification for Unbound Pavement Layers 95
Table 4-4 Project Specification of Bituminous Pavement Layer 96
Table 4-5 Recovered binder content of Addis Ababa-Modjo road segment 98
Table 4-6 Asphalt binder content of Modjo-Meki-Zeway road segments 98
Table 4-7 Cracking initiation adjustment factor (K_{cia}) 101
Table 4-8 Wide cracking initiation calibration factor (K_{ciw}) 103
Table 4-9 Model Coefficients for the different roughness components 113
Table 5-1 Observed Deterioration versus Traffic Loading and Deflection 117
Table 5-2 Comparison of calibration factor of the study area versus typical range 126
Table 5-3: HDM-4 Calibration Factors used in Kenya 127

List of Figures

Figure 1-1 Structure of HDM-4 Model 2
Figure 1-2 Location map of the study area 4
Figure 2-1: Chronology of HDM Development 14
Figure 3-1 Graph for estimating pavement temerature 67
Figure 3-2 Graph for estimating temperature adjustment factor (F) 67
Figure 3-3 Classification into homogenous strength sections 68
Figure 3-4 Annual equivalent standard axle load (ESAL/lane/year) 70
Figure 3-5: Global visual index (I_s) rating of Addis-Modjo road segment 71
Figure 3-6 Deflection measurement using Benkelman Beam on Progress 79
Figure 3-7 Adjusting the Benkelman in preparation for measurement 81
Figure 3-8 Traffic management during measurement 81
Figure 3-9: ARRB Automated Survey Vehicle 82
Figure 3-10 Onlooker Live View 83

Figure 3-11 Addis-Modjo road segment measured roughness 84
Figure 3-12 Modjo-Meki road segment measured roughness 84
Figure 3-13 Meki-Zeway pavement segment measured roughness 85
Figure 3-14 Rutting of Addis Ababa-Modjo road segment 86
Figure 3-15 Rutting of Modjo-Meki road segment 86
Figure 3-16 Rutting of Meki-Zeway road segment 86
Figure 3-17 Photo frame captured with ARRB Hawkeye survey vehicle 88
Figure 3-18 Rut depth measurement 89
Figure 3-19 Visual estimation of cracking area 89
Figure 4-1: Corrected deflection for Addis-Modjo road segment 91
Figure 4-2 Corrected deflection for Modjo-Meki road segment 91
Figure 4-3 Corrected deflection for Meki-Zeway road segment 92
Figure 4-4 Side drain Condition on Addis-Modjo Road Segment 93
Figure 4-5 Observed versus predicted and calibrated crack initiation ages 102
Figure 4-6 Sigmoid curve fitting for determining time to 30% cracking 105
Figure 4-7 Linear regression of predicted versus observed mean rut depths 110
Figure 4-8 Predicted versus observed roughness of the study area 115
Figure 5-1 Plot of mean pavement condition versus chainage 119
Figure 5-2 Addis Ababa-Modjo right lane Pavement condition versus chainage 120
Figure 5-3 Addis Ababa-Modjo left lane pavement condition versus chainage 121
Figure 5-4 Modjo-Meki right lane pavement conditions versus chainage 122
Figure 5-5 Modjo-Meki left lane pavement conditions versus chainage 122
Figure 5-6 Meki-Zeway left lane pavement conditions versus chainage 123
Figure 5-7 Meki-Zeway left lane pavement conditions versus chainage 123

ABBREVIATIONS AND ACRONYMS

A1, A7	Road classification system, A1: Addis-Djibouti, A7: Modjo-Awasa
Addis	Addis Ababa
AADT	Average Annual Daily Traffic
AASHTO	American Association of State Highway and Transportation Officials
ARRB	Australia Road Research Board
AC	Asphalt Concrete
CBR	California Bearing Ratio
CDB	Construction Defects Indicator for base
CDS	Construction Defects Indicator for surfacing
COTO	Committee of Transport Officials of South Africa
CRRI	Central Road Research Institute of India
CRT	Crack Retardation Factor
ELANE	Effective number of lanes
ERA	Ethiopian Roads Authority
ESAL	Equivalent Single Axle Load
DEF	Deflection from Benkelman Beam
FWD	Falling Weight Deflctometer
GCS	Graded Crushed Stone
HDM	Highway Development and Management
HCM	Highway Cost Model
IRRE	International Road Roughness Experiment
IRI	International Roughness Index
LTPP	Long-Term Pavement Performance
MIT	Massachusetts Institute of Technology
MMP	Mean Monthly Precipitation
NMA	National Meteorological Agency of Ethiopia
OBC	Optimum Binder Content
OTCI	Observed Time of cracking Initiation
PSR	Present Serviceability Rating
PSI	Present Serviceability Index
PTCI	Predicted time to cracking Initiation
P_t	Terminal Serviceability Index

RSDP	Road Sector Development Program of Ethiopia
SN(C)	Structural number/Modified Structural Number
TRB	Transportation Research Board
TRRL	British Transportation and Road Research Laboratory
YAX	Flow of all vehicles Axles per year
YE4	Equivalent single axles load per/lane/ year, HDM-4 system
RTIM	Road Transport Investment Model of TRRL
ISOHDM	International Study of Highway Development and Management Tools
SNP	Adjusted Structural Number
ARS	Average rectified slope
RDME	Road Design and Maintenance Effects
RQCS	Reference quarter car simulation
RTRRMS	Response Type Road Roughness Measuring System
RMSE	Root Mean Square Error
PSD	Power spectrum density
RAS_{80}	Rectified Average Slope at a speed of 80km/h
VOC	Vehicle Operating Cost
SNSG	Structural number contribution of the sub grade

Chapter 1. Introduction

1.1 Overview

Studying the performance of road pavements under the action of traffic loading and environmental effects is of paramount importance to save the huge initial public investment, road user and maintenance costs resulting from early road deterioration.

Many pavement performance models are developed and used as inputs for design and evaluation of pavements especially in the Post-AASHO Road Test era. The Highway Development and Management model (HDM), a computer model developed by the World Bank, is particularly useful because it integrates pavement performance models to the initial construction, maintenance and user cost models thereby enabling economic and financial evaluation of alternatives of a project or multiple projects for a given set of construction and maintenance standards. The model is a further improvement of its predecessors, HDM-III and HDM-II, which were respectively the third and second versions of the then Highway Design and Maintenance Standards Series and its first version of the series known as the Highway Cost Model (HCM).

HDM model consists of three broader sub-models namely Construction Cost, Road User Effects, and Road Deterioration and Maintenance Effects sub-models. Figure 1-1 show the process of cost prediction using the HDM-4 model (Bennett and Paterson 2000).

This study focused on the road deterioration sub-model of HDM-4, specifically on deterioration models of asphalt concrete (AC) surfacing on granular base pavements. The sub-model as described by Watanatada et.al (1987a) estimates the combined effects of traffic, environment and age on the condition of the road, given data on its construction and materials, and proceeds to predict the annual change of surface condition under specified maintenance and rehabilitation policies throughout the course of the analysis period.

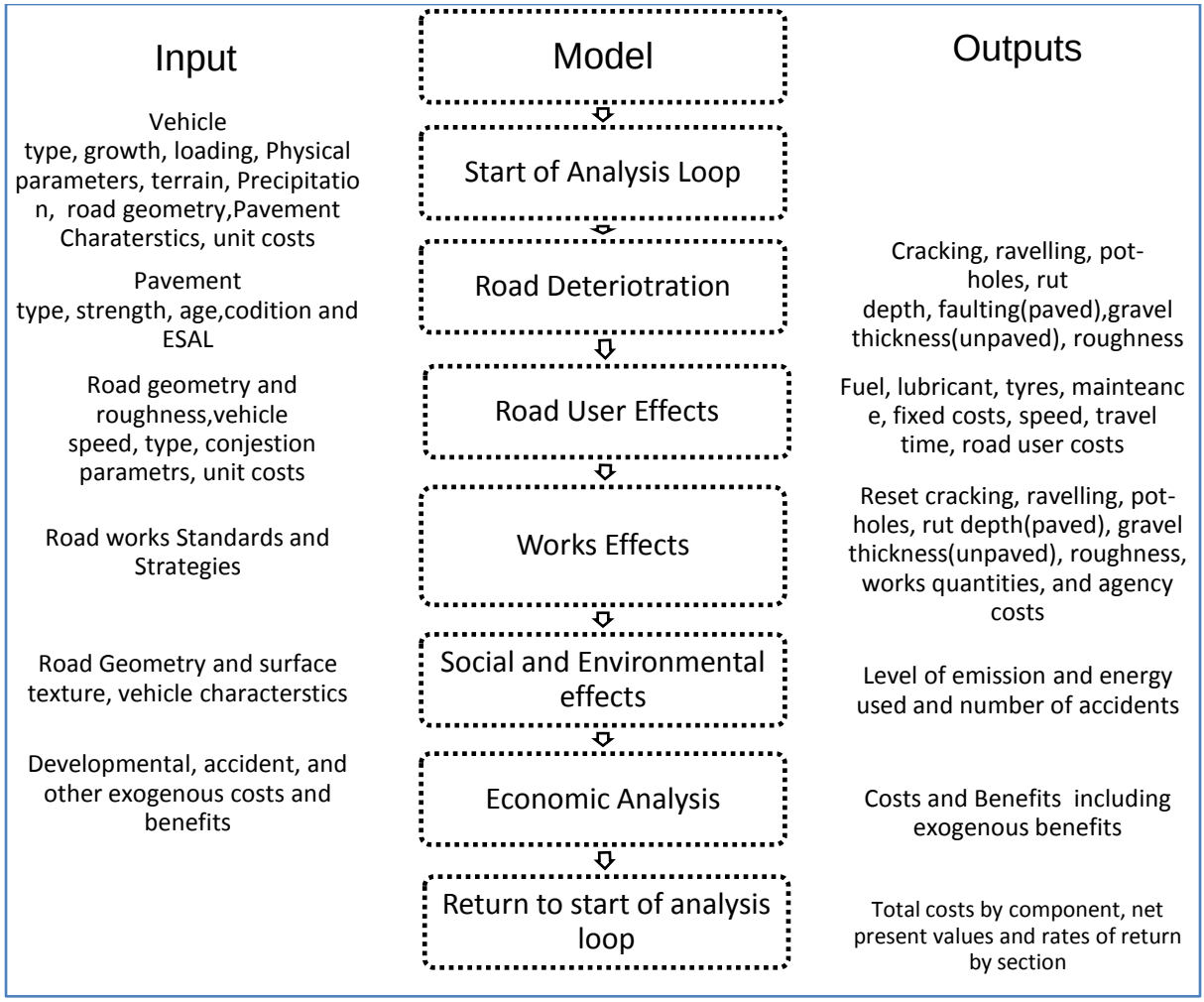

Figure 1-1 Structure of HDM-4 Model

Source: Bennett and Paterson(2000)

The study has tested the applicability of the HDM-4 road deterioration models and calibrated their adjustment factors for asphalt concrete pavements in Ethiopia, particularly to the conditions of three sampled road segments on Addis-Modjo and Modjo-Awasa Roads. The two roads are selected to represent the different levels of traffic loading and to represent the different climatic conditions in Ethiopia as per the required specification for the calibration of the road deterioration sub-model of HDM-4. The roads are also representative of the asphalt concrete surfacing on GCS base pavements, which is the dominant type of pavement structure of Ethiopian Roads (Africon, 2009).

The researcher believes that lessons learnt from this performance study especially the findings from the initial calibration process of the HDM-4 road

deterioration models will be a basis for the planning of the maintenance strategies of the project under consideration or for the overall initial planning, implementation and operation of other rehabilitation and new projects in Ethiopia and regional countries. The findings of the pavement performance study are also equally important to make improvement to the applicable pavement design procedures/manuals of Ethiopia.

1.2 Background

1.2.1 Location

Addis-Modjo and Modjo-Awasa roads stretch from Central to Southern Ethiopia and are parts of the trunk roads that connect the Ethiopian capital, Addis, to the two neighboring countries of Djibouti and Kenya. Addis-Modjo road, 70 km long, is part of the trunk road A1 that connects Addis Ababa to the Port of Djibouti where the bulk of the country's import and export is passing through. Modjo-Awasa road, 206 km long, is part of the classified trunk road A7 and is leading to Moyale located at the border with Kenya. Figure 1-2 shows the location of the road links studied.

1.2.2 Climate

According to the records of the National Meteorological Agency of Ethiopia (NMA, 2009), the study area close to Modjo can be classified as warm climate with a maximum temperature slightly above 30 ^{0}c for most of the year. It also exhibits high diurnal temperature changes with 8.1 ^{0}c as the lowest temperature. The diurnal temperature change in Awasa is relatively small with average maximum and minimum temperature of 27 ^{0}c and 20 ^{0}c. The area close to Addis is the coolest of all with maximum average temperature of 23 ^{0}c and minimum of 11 ^{0}c. In all locations, the maximum temperature occurs in the months of January to May, the dry season, and minimum occurs in October immediately after the rainy season. Addis has the highest rainfall exceeding 1000mm/year, and Ziway located halfway between Modjo and Awasa gets the least rainfall of 739.3mm/year. In all places of the study area maximum rainfall occurs in the months of June to September, during the rainy season which covers most of Ethiopian territory.

Figure 1-2 Location map of the study area

Source: https://www.cia.gov/library/publications/cia-maps-publications/map-downloads/Ethiopia

1.2.3 **Traffic**

In terms of traffic volume and loading Addis-Modjo road is the most heavily trafficked road in Ethiopia as it is the last link of the road network from the Southern and Eastern parts of Ethiopia. Most importantly, it is the last link of the route from the port of Djibouti where the bulk of Ethiopia's import and export is passing through. The traffic census of ERA in the year 2010 showed that Addis Ababa-Modjo road section has AADT of 16,299 vehicles. According to the same study, Modjo-Awasa's road traffic is considered of medium volume of 6,934 vehicles per day in the same year of 2010. In terms of traffic composition, heavy trucks and truck trails account for 29% and 22% of total traffic for Addis-Modjo and Modjo-Awasa Roads respectively. It shall be noted that traffic along the 300

km of Addis-Modjo-Awasa Road vary from section to section and the volume and composition indicated here are only for the sections where this research is focused. Detailed traffic volume and composition of traffic are included in Annex 2.

1.2.4 **Pavement History**

The age of pavements in both cases is more than 10 years, where road deteriorations such as cracking are visible. It was in the year 1999 that the Addis -Modjo Highway was last rehabilitated. Modjo-Awasa Highway was, however, rehabilitated and opened to traffic in the years 2000 and 2001. Although a routine maintenance for both roads is undertaken from time to time, for this study only road sections which did not receive maintenance were selected. Studies for rehabilitation of the two roads were conducted in the years 2008 and 2009 and were used as a basis for this study.

The engineering reports from these studies (Metaferia and Omega, Metaferia and Spice, 2009) indicate that the pavement structure in both cases consists of an average of 10 cm thick asphalt concrete surfacing on top of 20 cm thick crushed stone base and sub-base ranging from 20-30 cm of milled asphalt mixed with cinder material. Subgrade soil for Addis-Modjo road is predominantly black cotton soil with small sections of bedrock and silty clay soil. Modjo-Awasa road's subgrade soil is dominantly clayey silt and silty clay.

Table 1-1 Pavement Structure of Addis-Modjo and Modjo-Awasa Roads

Pavement Layer	Thickness(mm)	
	Addis-Modjo	Modjo-Awasa
Surfacing	100	100
Base	200	100-200
Sub-base	200	200-300
Capping layer	100-300	

Source: Metaferia and Omega, Metaferia and Spice (2009)

1.3 **Problem Statement**

Ethiopia is a country where expansion of road infrastructure is growing at a very fast rate. The Ethiopian Roads Authority and the Regional Road Authorities responsible for the expansion and maintenance of highways and rural roads respectively have expanded the road network of Ethiopia from 26,500 km at the start of the Road Sector Development Program (RSDP) in year 1996/1997 to 54,000 km in year 2010 (www.ethiopianreporter.com, 07 January 2012).The effort so far has been on the upgrading and construction of the road network and it is now timely to focus on the maintenance requirement. For proper maintenance strategy it is important to evaluate the performance of the already constructed road network. HDM-4 model is currently the model used worldwide including Ethiopia for pavement performance, economic and financial appraisal of road projects. As has been discussed in the introductory part of this study the output of the HDM's road deterioration sub-model together with maintenance standards, construction and user costs is used as a basis for comparing alternative maintenance/rehabilitation/re-construction strategies and to select the best alternative in terms of cost-benefit ratio and economic internal rate of return. Calibrating the model to suit to the conditions of the different climatic and topographical conditions of each country is important and it is with this understanding that there is a provision in HDM-4 to calibrate the model in the form of calibration factors; where in the case of Ethiopia this has not been done so far. Moreover the Ethiopian Roads Authority is now developing its pavement management system using HDM-4 as a performance and condition monitoring tool for each road in the network. The Ethiopian Roads Authority is now keen to supplement its effort of applying HDM-4 with research geared at calibrating the road deterioration models.

Therefore, the aim of this research in this regard is to fill the gap in knowledge by testing the applicability of HDM-4 road deterioration sub-model and calibrating the adjustment factors of each distress model to the conditions of study area in Ethiopia.

1.4 Objectives of the Study

HDM-4 road deterioration sub-model predicts the condition of the pavement on an incremental basis from initial condition to a condition at a certain time during its service life. The change of the pavement condition in HDM- 4 model is represented by 5 distress types. The five road distress types representing flexible pavements are cracking, rutting, potholing, ravelling and roughness. The modeling of cracking, potholing and ravelling are again divided into initiation and progression phases. Separate models are developed for each of the distress types and each of them is provided with default calibration adjustment factor. The objectives of this study with this respect and in line with the problem statement are therefore the following

1.4.1 Overall Objective

Evaluate the performance of HDM's road deterioration sub-model and calibrate the adjustment factors for the conditions of Ethiopia.

1.4.2 Specific Objectives

- Test the validity of each distress model embedded in the road deterioration sub-model of HDM-4 to the conditions of Ethiopia
- Determine the rate of pavement deterioration
- Calibrate the adjustment factors of each distress model of HDM-4 to suit to the conditions of Ethiopia

1.5 Hypothesis

The research is expected to produce the following results

- Better understanding of the HDM-4 road deterioration sub-model
- Factors of road deterioration sub-model calibrated to the condition of Ethiopia and used as input for performance prediction and economic evaluation of a project or alternative projects
- The research methodology and analysis techniques used in this study will be a basis for further studies

1.6 Scope and limitations of the study

The road deterioration models are again different for a different surfacing and base material types and it would be overwhelming to cover all in this research due to financial and time constraints. Hence, the research is limited only to asphalt concrete surfacing on GCS base. The rate of deterioration is also dependent on the type of maintenance works; models developed for the effects of maintenance on rate of deterioration are vast and is not covered in this research.

A Full calibration of the HDM-4 road deterioration sub-model requires data collection on input variables and pavement condition for a long period of time. Many countries have understood the need for this process and collected data in a program known as Longer–Term Pavement Performance (LTTP) studies. However, for the Ethiopian road network sufficient time series data are not available, and hence the methodology adopted for this study is limited only to a 'slice-in-time' meaning slicing of pavements of different ages, strengths and traffic loadings at a certain instant of time, where studies show that the result is not very satisfactory due to the naturally non-homogenous behavior of pavements.

Chapter 2. Literature Review

In this chapter first pavement performance studies which lead to the development of the HDM-4 road deterioration sub-model will be discussed. In an effort to fully understand the HDM-4 road deterioration models, required input parameters and the theoretical and empirical basis in the development of each distress model will be discussed. A review of similar studies conducted in Ethiopia and the regional countries will be discussed and finally statistical techniques used for data analysis and calibration process will be discussed.

2.1 Studies Leading to the Development of the HDM-4 Model

2.1.1 AASHO Road Test

The AASHO Road test, the last of a series of road tests conducted by State Highway Agencies and the Bureau of Public Roads in the United States starting in the 1920s (TRB,2007), is a pioneer in pavement performance studies. The primary purpose of the road test was to determine the relationship between axle loading, pavement strength and pavement performance. The tests were conducted by applying traffic of different axle loading on pavements of different thicknesses and material types.

The test was the basis for the development of the pavement serviceability concept widely used in AASHTO Pavement Design guides. The pavement serviceability measured by the Present Serviceability Rating (PSR) is a subjective rating of the pavement riding quality conducted as part of the road test, by a panel of raters consisting of both truck and automobile drivers on 138 sections of pavements in three states of United States (TRB, 2007). The rating goes from 0 and 1 as very poor to 4 and 5 very good. While numerical ratings were conducted, other test crew was measuring the condition of the pavement in terms of roughness, cracking, rutting and patching. Using regression analysis, a relationship was developed to predict the present serviceability index (PSI) from the physical measurements. Currently the PSI is the primary measure of the pavement serviceability with a rating ranging from 0 (impassable road) to 5 (perfect road).

The primary design philosophy of the AASHTO design guide (AASHTO, 1993) is the performance-serviceability concept, which provides a means of designing a pavement structure based on specific total traffic volume and a minimum level of serviceability desired at the end of the performance period. Selection of the lowest allowable PSI or terminal serviceability index (p_t) is based on lowest index that will be tolerated before rehabilitation, resurfacing or reconstruction becomes necessary. AASHTO (1993) recommended a PSI index of 2.5 for major highways and 2.0 for less traffic volume roads.

In addition, the AASHO Road Test was the basis for the development of the equivalent single axle load (ESAL) and the pavement structural number (SN) concepts which are the two important inputs for predicting the deterioration of pavements in HDM-4.

However, Watanatada et.al (1987a) argued that the application of the results of AASHO road test is severely limited to the conditions of the developing countries due to the following reasons

- The test was conducted in partly freezing climate, which is quite different from tropical and subtropical climate of most developing countries.
- The range of pavement types of strong asphalt concrete and rigid pavement of the study is quite different to the usually thin surface treatment or thin asphalt concrete of the developing countries. The study also does not include gravel and earth roads which are quite common in developing countries.
- It is not quite certain how the relationships derived from accelerated and experimentally controlled loading are applicable to mixed lightly and heavy traffic and lightly traffic roads of the developing countries.
- In order to evaluate the effects of different maintenance actions, intervention criteria and standards to be evaluated it is desirable to predict the trends of roughness, rut depth and cracking separately rather than the composite serviceability index.
- The effects of alternate maintenance policies on deterioration were not considered in the AASHO test.

Moreover, the AASHO Road Test is applied on pavement structure placed only on subgrade soil of CBR 3, and the structural number(SN) determined does not take into account the different subgrade-soil strength encountered elsewhere.

2.1.2 **The HDM SERIES**

In an attempt to develop a computer model capable of evaluating alternative project options by predicting pavement performance and overall project costs, and which is applicable to the conditions of the developing countries, the World Bank launched the Highway Design and Maintenance Standards Series in 1969. The first prototype model known as the Highway Cost Model (HCM) was developed by Moavenzadeh et.al from the Massachusetts Institute of Technology in 1971(Watanatada, 1987a). As explained by Moavenzadeh et.al (1971) much of the data on rate of paved road pavements deterioration was derived from AASHO Road test, on the other hand, engineering judgment and general information in the literature were used for predicting deterioration of unpaved road surfaces.

Watanatada et al (1987) discussing on the limitation of the first version of the study indicated that of the three basic sets of relationships, construction, road deterioration/maintenance and road user costs it was evident that most of what was needed was already known about estimating construction costs, but far too little was known about the relationships of user costs, road deterioration and maintenance costs to road design and maintenance policies.

Moavenzadeh et.al (1971) in their conclusion recommended empirical work and modification of model parameters by collecting actual field data especially on vehicle operating costs and road deterioration. Therefore in order to represent the actual pavement condition in developing countries and to represent different geographical areas and by doing so to quantify the road user cost and road deterioration models adequately input data has been collected from field studies conducted in Kenya, Caribbean, Brazil and India (Watanatada,1987a).

The first of such study was conducted in Kenya from 1971 to 1975 by the British Transport and Road Research Laboratory (TRRL) in collaboration with Kenya Ministry of works and the World Bank. Part of the study focused on determining model relationships on road user costs and the other part focused on road

deterioration models. The variety of topographical and climatic conditions in Kenya, typical for large number of developing world, had been the main reason for conducting the research in Kenya (Hodges and Jones, 1975). The result of the study has been the basis for the development of the TRRL's Road Transport Investment Model (RTIM).

In 1976, the World Bank awarded a research contract to MIT to produce an extended version of RTIM which is capable of carrying out economic analysis directly by automatically sub-dividing road link into homogenous sections (Parsley and Robinson, 1982). This work resulted in the production of the second version of the HDM series (HDM-II) in 1982.

Further field studies on vehicle operating cost has been conducted in the Caribbean, Brazil and India. Additional major road deterioration study was conducted in Brazil. The result of these studies combined from the experience in the use of HDM-II resulted in the development of the HDM-III model in 1987.

Later it was recognized that the HDM-III model needed improvement in the following areas (Lea, 1995), (Watanatada, 1987a)

- The vehicle and tyre technology in the VOC studies are different to those of modern vehicles
- Some cost components are modelled in a simplistic manner
- HDM-III does not consider congestion, environmental effects or traffic safety
- The RDME models do not encompass all of the pavement types or maintenance treatments commonly found in developing or developed countries
- The RDME models were not validated for freezing climates
- the RDME do not cover rigid pavements
- HDM-III does not consider pavement texture effects

In order to address the limitations and to improve the HDM software further, an international collaborative study known as the International Study of Highway Development and Management Tools (ISOHDM) was launched in 1993 (N.D Lea, 1995b). The study produced the draft HDM-4 model in 1996, and the first

version of HDM-4 released in 2000. The products of this version are the basis for this research. Figure 2-1 shows the chronology of HDM development.

2.2 Input parameters to HDM Road Deterioration Models

2.2.1 Pavement Strength

The strength of a pavement is quantified either by the modified structural number (SNC) or from deflections measured using commonly used methods such us Benkelman Beam or Falling Weight Deflctometer (FWD). The modified structural number, originally developed after AASHO road test, is an equivalent thickness parameter which is the sum of individual pavement thicknesses weighted by layer strength coefficients plus insitu subgrade contribution as estimated by Hodges and others (1975). According to Watanatada (1987a) SNC is found to be the most statistically significant measure of pavement strength affecting the deterioration of pavements, and is thus the primary strength parameter in the prediction of relationships.

Conceptually, SNC is a measure of the resistance of the pavement to a permanent deformation and is an indicator of the shear strength. It requires good knowledge of the layer-strength coefficients, CBR of the unbound pavement layers, in-situ CBR of the subgrade and the effect of moisture on the strength of each layer. The calculation of structural number requires laboratory testing and field measurement of the pavement characteristics.

If pavement structural characteristics are available, SNC is estimated from equation (2-1) that was developed after AASHO road test. Later Hodges and others (1975) modified it in order to take into account of sub-grade contribution

$$SNC = 0.0394\sum_{i=1}^{n} a_i H_i + SNSG \qquad (2\text{-}1)$$

Where SNC = Modified Structural number (inches)

a_i = Strength coefficient of the i^{th} layer

H_i = Thickness of the i^{th} pavement layer (mm)

n = Number of pavement layers

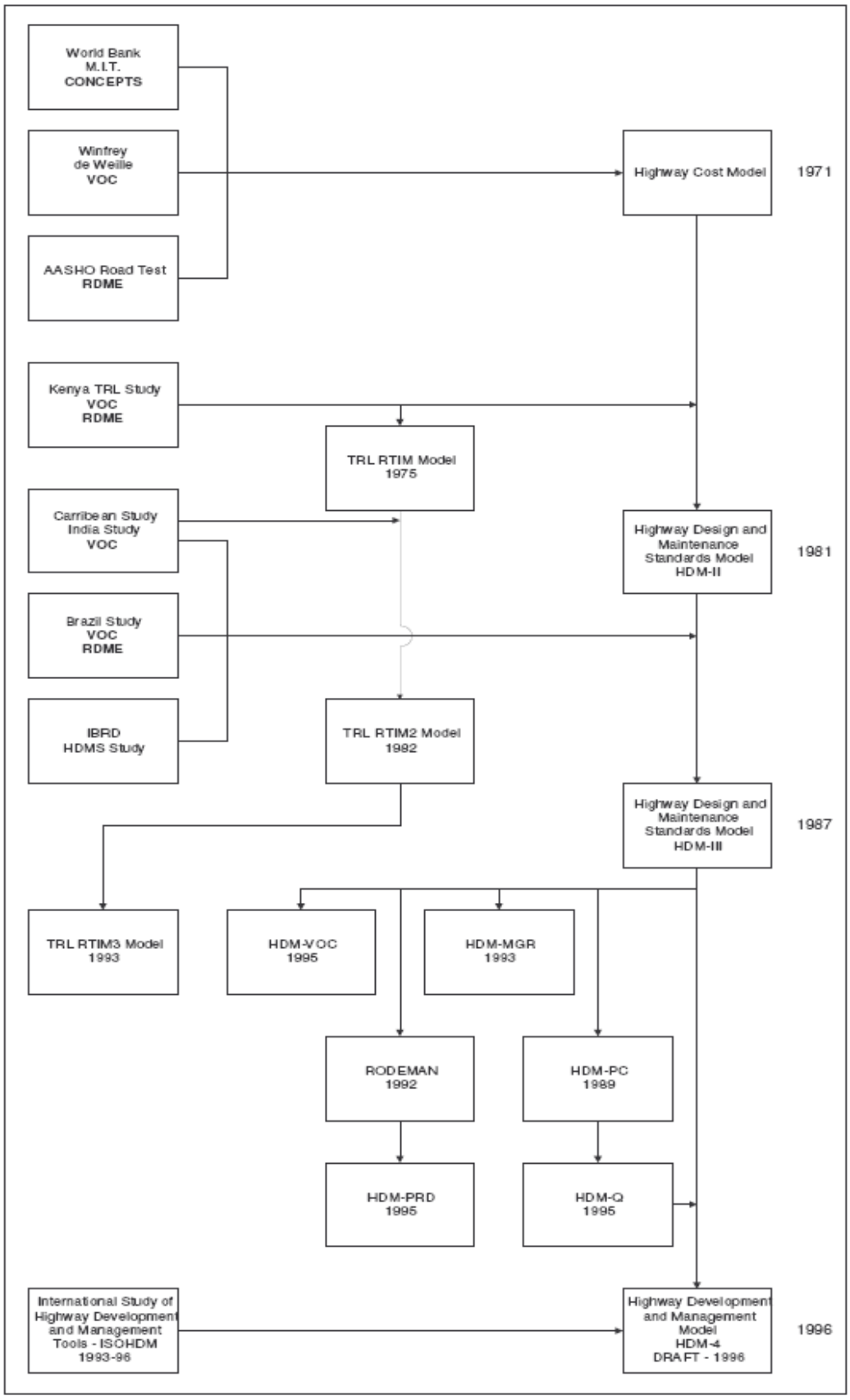

Figure 2-1: Chronology of HDM Development

Source : Lea 1995 (b)

$SNSG$ = Structural number contribution of the sub grade given by

$$SNSG = 3.5\log_{10} CBR - 0.85\ \log_{10} CBR^{\ 2} - 1.43 \qquad (2\text{-}2)$$

Where

CBR = California Bearing Ratio of the sub grade at the in situ condition of moisture and density in percent.

According to Watanatada et.al (1987a) equation (2-1) gives good predictions for pavements of less than 700mm thickness. For predicting conditions when pavement thickness is greater than 700mm a new relationship was developed (Parkman and Rolt, 1997) and is currently incorporated in the HDM-4 model in using equations (2-3) through equation (2-6) (Odoki and Kerali, 2000).

$$SNPs = SNBASU_s + SNSUBA_s + SNSUBG_s \qquad (2\text{-}3)$$

Where

$$SNBASU_s = 0.0394\sum_{i=1}^{n} a_{is} h_i \qquad (2\text{-}4)$$

$$SNSUBA_s = 0.0394\sum_{j=1}^{m} a_{js} \left\{ \left(\frac{b_0 exp(-b_3 z_j)}{-b_3} + \frac{b_1 exp(-(b_2+b_3) z_j}{b_2+b_3} \right) - \left(\frac{b_0 exp\ -b_3 z_{j-1}}{-b_3} + \frac{b_1 exp(-(b_2+b_3) z_{j-1})}{b_2+b_3} \right) \right\} \qquad (2\text{-}5)$$

$$SNSUBG_s = b_0 - b_1 exp(-b_2 z_m)\ \ exp(-b_3 z_m) \left[\begin{array}{c} 3.51 log_{10} CBR_s - \\ 0.85(log_{10} CBR_s)^2 - 1.43 \end{array} \right] \qquad (2\text{-}6)$$

Where

SNP_s = Adjusted Structural Number of the pavement for season s

$SNBASU_S$ = Contribution of Surfacing and Base layers for season s

$SNSUBA_S$ = Contribution of the sub-base or selected fill layers for season s

$SNSUBG_S$ = Contribution of the Sub grade for season s

n = Number of surfacing and base layers (i=1, 2... n)

a_{is} = Layer coefficient for base or surfacing layer i for season s

h_i = Thickness of base or surfacing layer i

m = Number of sub-base and selected fill layers (j=1, 2... m)

z = Depth parameter measured from the top of the sub-base in mm

z_j = Depth to the underside of the j^{th} layer (z_0=0) in mm

CBR_S = In situ sub-grade CBR for season s

a_{js} = Layer coefficient for sub-base or selected fill layer j for season s

b_0, b_1, b_2, b_3 = Model coefficients, where $b_0 = 1.6$, $b_1 = 0.6$, $b_2 = 0.008$, $b_3 = 0.00207$

If pavement structural characteristics are not available, the measurement of the pavement deflection using the Benkelman Beam is the other method of determining the pavement strength, which in the case of the HDM could be inputted together with the SNC or can be used to determine the modified structural number. Watanatada et.al (1987a) indicated that peak deflection is a weak predictor of pavement performance, though it is the convenient and quick method of assessing pavement strength.

The deflection is an indication of the pavement stiffness and depends on the resilient stiffness and thickness of each layer of the pavement. As discussed by Paterson (1987), the correlation between SNC and maximum deflection is good but not high because each measure different attribute of the pavement.

The relationships (2-7) and (2-8), are used to convert the Benkelman beam deflection measurements to modified structural number (Watanatada et al., 1987a)

If the base is not cemented

$$SNC = 3.2DEF^{-0.63} \quad (2\text{-}7)$$

If base is cemented

$$SNC = 2.2DEF^{-0.63} \quad (2\text{-}8)$$

Where

SNC = As defined earlier

DEF = Benkelman beam deflection in mm

Seasonal and Drainage Effects on Pavement Strength

Drainage and seasonal changes of moisture content influence the pavement strength and hence its effect is included in the HDM-4 adjusted structural number (SNP) prediction model. Once the adjusted pavement strength (SNP) for a particular season is calculated using relationships (2-3) to (2-8), to be inputted into the HDM pavement deterioration model the average adjusted structural number of the year has to be calculated as a percentage of the dry season structural number using equations (2-9) and (2-10) of (Odoki and Kerali, 2000).

$$SNP = f_s SNP_d \qquad (2\text{-}9)$$

Where

SNP = Average annual adjusted structural number

$$fs = \frac{f}{[(1-d)+d(f^{p})]^{(1/p)}} \qquad (2\text{-}10)$$

SNP_d = Dry Season SNP

$f = \frac{SNPw}{SNP_d}$ Ratio

SNP_w = Wet Season SNP

d = Length of dry season as a fraction of the year

p = Exponent of SNP specific to the distress type

As can be seen from Table 2-1 the value of exponent p is different for the models of different distresses.

Table 2-1: Values of exponent p for calculating SNP

Distress	**Model**	**p**
Cracking	Initiation of structural cracking	2
Rut depth	Initial densification	0.5
	Structural deformation	1
Roughness	Structural component	5

Source: Odoki and Kerali (2000)

If there is some form of pavement deterioration and data for only one season is available, equation (2-11) is used to determine the wet to dry modified structural number ratio a function of the mean monthly rainfall, percentage area of cracking and potholing (Odoki and Kerali, 2000).

$$f = kf\left\{1-\frac{\left[1-\exp\ a_0\, MMP\ \right]}{a_1}\ 1-a_2 DF_a\quad 1+a_3 ACRA_a + a_4 APOT_a\ \right\} \qquad (2\text{-}11)$$

Where

$f = \frac{SNPw}{SNP_d}$ Ratio as defined earlier

MMP = Mean Monthly precipitation (mm/month)

DF_a = Drainage factor at the start of the analysis year.

$ACRA_a$ = Total area of cracking at the start of the analysis year (% of total carriageway area)

$APOT_a$ = Total area of potholing at the start of the analysis year (% of total carriageway area)

K_f = Calibration factor for wet to dry SNP ratio

a_0, a_1, a_2, a_3, a_4 = are model coefficients, where $b_0 = 10$, $b_1 = 0.25$, $b_2 = 0.02$, $b_3 = 0.05$

According to the work of Kerali and Odoki (2000), the drainage factor, DF, ranges from 1(Excellent) to 5(very poor) and depends on the quality of drain, where the lined drains are the best and unlined shallow seated V-ditches are the worst.

2.2.2 **Pavement Classification**

HDM-III road deterioration modeling was applicable to both flexible paved and unpaved road categories. But neither rigid nor block surfaced road types were included in the HDM-III version of the model. However, in HDM-4 the scope of pavements to be considered has been significantly expanded and it was necessary to develop a systematic pavement classification system (N.D. Lea, 1995b). The classification of the bituminous surfaced roads is included in this

report as it is applicable to the theme of the research. Table 2-2 summarizes the HDM-4 pavement classification system.

Table 2-2 Pavement classification system of HDM-4

Surface type	Surface	Base type	Base material	Pavement type
AM	AC	GB	CRS	AMGB
	HRA		GM	
	PMA	AB	AB	AMAM
	RAC	SB	CS	AMSB
	CM		LS	
	PA	AP	TNA	AMAP
	SMA		FDA	
ST	CAPE	GB	CS	STGB
	DBSD		GM	
	SBSD	AB	AB	STAB
	SL	SB	CS	STSB
	PM		LS	
		AP	TNA	STAP
			FDA	

Source: Bennett and Paterson, 2000

AM-Asphalt Mix

AC-Asphalt Concrete

HRA-Hot Rolled Asphalt

PMA-Polymer Modified Asphalt

RAC-Rubberized Asphalt Concrete

CM-Soft Bitumen Mix(Cold Mix)

PA-Porous Asphalt

SMA-Stone Mastic

ST-Surface Treatment

CAPE- Cape Seal

DBSD-Double Bituminous surface Dressing

SBSD-Single Bituminous Surface Dressing

GB-Granular Base

AB-Asphalt Base

AP-Asphalt Pavement

SB-Stabilized Base

CRS-Crushed Stone

GM-Natural Gravel

CS-Cement Stabilization

LS-Lime Stabilization

TNA-Thin Asphalt Surfacing

FDA-Full depth Asphalt

PM-Penetration Macadam

SL-Slurry Seal

2.2.3 **Traffic Loading**

The purpose of designing a pavement structure is to provide a smooth and strong platform to carry the expected volume and loading of traffic throughout its service life with acceptable rate of deterioration. In HDM road deterioration models there are two ways of inputting the traffic parameter, the flow of all vehicle axles per year expressed in the model as (YAX) and number of equivalent standard axles of 80KN per year, expressed in the model as YE4.

Equation (2-12) which was developed after the AASHO road test is used to convert the number of axles of all vehicles in the traffic stream to a number of equivalent single axle loads (N.D. Lea, 1995b)

$$\frac{N_s}{N_P} = \left(\frac{P}{P_s}\right)^n \qquad (2\text{-}12)$$

Where N_s = the number of applications of a standard axle load

N_p = Number of applications of the load of interest

P = the load of interest

P_s = the standard load

n = load equivalence factor, taken as 4 in HDM model.

Bennett and Paterson (2000) defined the total number of vehicle axles (YAX_k) for a particular vehicle class k as a product of the volume and number of axles of vehicle k expressed in millions/lane/year which is expressed in equation form of (2-13).

$$YAX_k = \frac{(T_k * Num - Axles_k)}{(ELANES * 10^6)} \qquad (2\text{-}13)$$

The total vehicle axles for vehicles (k=1, K=2….K=n) is given by

$$\mathrm{YAX} = \sum_{K=1}^{K=n} \mathrm{YAX_k} \qquad (2\text{-}14)$$

Where

YAX_k = Annual total number of axles of vehicle type K (millions/lane/year)

T_k = Annual traffic volume of vehicle type k (K=1…..n)

$NUM\text{-}Axles$ = Number of axles per vehicle type k

$ELANES$ = Effective number of lanes for the road section, which depend on the width of carriageway

YAX = Annual total number of axles of all vehicle classes (millions/lane/year)

2.2.4 Construction Quality

The effect of construction quality on pavement deterioration has been accounted for in HDM-III model by automatically dividing the link under consideration into weak, medium and strong sections before starting simulation (Watanatada, 1987a). This assumption is expressed in terms of the occurrence distribution factor, F, appearing in each relationship to predict the time at which cracking or ravelling starts. That is, these subsections employ the same basic distress initiation models but with different occurrence distribution factors to account for the different rates of deterioration (Watanatada, 1987a). In HDM-4 such classification of construction quality is not used, instead an average level of construction defects indicator, different for surfacing and base, are used (Odoki and Kerali, 2000). They are termed as construction defects indicators for surfacing (CDS) and construction defects indicator for base (CDB).

2.2.5 Environmental Factors

The environmental factors of temperature and rainfall affect the performance of flexible pavement. The temperature plays a role in the rate of hardening of the asphalt concrete surfacing which is termed as aging. The hardening of the asphalt concrete makes the surface susceptible to embrittlement; thereby increasing the rate of cracking and together with the precipitation hastens the deterioration of the pavement in the forms of rutting, potholing and roughness.

In HDM-4 the environment is classified by a combination of the annual precipitation, Thornthwaite moisture index and temperature. Table 2-3 shows HDM-4's climate classification. The Thornthwaite moisture index is the measure of the available net moisture in the soil. When the precipitation of an area is more than the evapotranspiration, the case during the rainy season or the temperature

is cool not to cause excessive evapotranspiration, there will be excess moisture in the soil to support vegetation. The reverse is true during the dry season where there will be moisture deficit in the soil. According to carter (1954), in regions where the water deficiency is large with respect to the need or potential evapotranspiration then the climate is dry and where water is excess then it will be moist climate.

2.2.6 **Pavement History**

According to Odoki and Kerali (2000), the pavement history refers to the age of the pavement with reference to the last maintenance, rehabilitation or re-construction. According to the same reference, there are four variables that define the age of the pavement used in the HDM-4 models.

AGE1-Referred as preventive treatment age, is defined as the number of years since the last preventive treatment, reseal, overlay (rehabilitation), pavement re-construction or new construction activity.

AGE2-Referred as surfacing age, is defined as the number of years since the last re-seal, overlay (rehabilitation), pavement re-construction or new construction activity.

AGE3-Referred as the rehabilitation age, is defined as the number of years since the last overlay (rehabilitation), pavement re-construction or new construction activity.

AGE4-Referred as the base construction age, is defined as the number of years since the last reconstruction that involve construction of new base or new construction activity.

Table 2-3 HDM-4 Environmental classification

Temperature Classification	Description	Typical Temperature range(^{0}C)
Tropical	Warm temperature in small range	20 to 35
Subtropical- hot	High day, cool night temperatures and hot-cold seasons	-5 to 45
Sub-tropical cool	Moderate day temperatures, cool winters	-10 to 30
Temperate cool	Warm summer, shallow winter freeze	-20 to 25
Temperate-Freeze	Cool Summer, deep winter freeze	-40 to 20

Moisture classification	Description	Typical moisture index	Typical annual precipitation(mm)
Arid	Very low rainfall, High evaporation	-100 to -61	<300
Semi-arid	Low rainfall	-60 t0 -21	300 to 800
Sub-humid	Moderate rainfall, or strongly seasonal rainfall	-20 to 19	800 to 1600
Humid	Moderate warm rainfall season	20 to 100	1500 to 3000
per humid	High rainfall, or very many wet days	>100	>2400

Source: Bennett and Paterson (2000)

2.3 HDM Paved-Road Deterioration Models

As has been discussed in the introductory part of this report pavement deterioration is expressed by distress modes and types which are classified as follows.

Modes of Distress

According to Paterson (1987) the defects on pavements, usually quantified through pavement condition survey, can be classified into three major modes of distress, namely

1. Cracking (fracture)

2. Disintegration

3. Permanent deformation

Table 2-4 summarizes the classification of distress types and the major causes of distress.

Table 2-4 Mode and Type of Distresses

Mode	Type	Brief Description	Primary cause
Cracking	Crocodile(Alligator)	Interconnected polygons of less than 300mm diameter	Traffic
	Longitudinal	Line cracks longitudinal along pavement	Material/Climate
	Transverse	Line cracks transverse across pavement	Material/Climate

	Irregular	Unconnected cracks without distinct pattern	Material/Climate
	Map	Interconnected polygons more than 300mm	Material/Climate
	Block	Intersecting line cracks in rectangular pattern at spacing	Material/Climate
Disintegration	Ravelling	Loss of stone particles from surfacing	Material/Climate
	Potholes	Open cavity in surfacing (>150mm diameter, >50mm depth	Traffic
	Edge Break	Loss of surfacing at edge of	
Deformation	Rut	Longitudinal depression in wheel	Traffic
	Depression	Bowl-shaped depression in	Material/Climate
	Mound	Localized rise of surfacing	Material/Climate
	Ridge	Longitudinal rise in surfacing	Material/Climate
	Corrugation	Transverse depressions at close spacing	Material/Climate
	Undulation	Transverse depression at long spacing(>5m)	Material/Climate
	Roughness	Irregularity of pavement surface in wheel paths	Traffic/Material/Climate

Source: Paterson (1987), AASHTO (1993)

From the distresses types identified and included in Table 2-4 only cracking, ravelling, potholing, rutting, and roughness are modeled and implemented in HDM-III deterioration model. In HDM-4 in addition to the five, edge break and texture depth are modeled. The five distresses were included in the HDM-III and later in HDM-4 due to their high sensitivity which is quantified by the impact elasticity. Impact elasticity is simply the ratio of the percentage change in a specific result to the percentage change of the input parameter holding other parameters constant as a mean value. The HDM-4 sensitivity classes are presented in Table 2-5.

Table 2-5: HDM-4 Sensitivity Classes

Impact Level	Sensitivity Class	Impact Elasticity
High	S-I	>0.50
Moderate	S-II	0.20-0.50
Low	S-III	0.05-0.20
Negligible	S-IV	<0.05

Source: Bennett and Paterson (2000)

As recommended by Bennett and Paterson (2000), the S-III to S-IV class models shall only be studied when time and resources are available and the default calibration factors generally give satisfactory model predictions, but the seven models in Table 2-6 are found to be more sensitive than others and need to be calibrated. From Table 2-6 it is evident that the roughness due to environment is the most sensitive model with a net impact of 10% followed by the cracking initiation and progression models of each 6% net impact.

Table 2-6 Ranking of Impacts of Road Deterioration factors

Deterioration factor	Impact Elasticity	Typical Value of Factor	Net Impact (%)	Sensitivity class
Roughness-age-Environment	0.2	0.2-5.0	10	High
Cracking Initiation	0.25	0.5-2.0	6	
Cracking Progression	0.22	0.5-2.0	6	
Rut depth Progression	0.10	0.5-2.0	3	Low
Roughness progression-general	0.09	0.8-1.2	1	
Potholing Progression	0.03	0.3-3.0	2	
Ravelling initiation	0.01	0.2-3.0	1	

Source: Bennett and Paterson (2000)

In this research, distress types relevant for triggering maintenance and which are included in Table 2-6 will be further studied. As can be seen from the table, rutting and roughness progression, potholing progression and ravelling are of low sensitivity, and as can be confirmed later in chapter four, the calibration factors of

rutting and general roughness progression are more stable and values after calibration are close to the default value of 1.

2.3.1 Cracking

Cracking is defined as the appearance of fracture on the pavement surface caused by traffic related fatigue, defects in material and construction quality, environment related ageing and ingress of moisture into the pavement structure. As discussed by Paterson (1987), cracking occurs at a certain age of the pavement (initiation phase) and once it occurs it increases in extent, severity and intensity eventually leading to disintegration (progression phase). The ingress of water into the pavement structure through the crack will accelerate not only the rate of cracking but also the progression of rutting, potholing and ultimately roughness.

According to Lea (1995) cracking can initiate at the surface and progress downward, begin at the bottom or at an intermediate depth of the bituminous layer and progress upward, or begin in an underlying layer and ultimately propagate upward through the entire thickness of the bituminous surface.

Classification of Cracking

In addition to the six types included in Table 2-4, Paterson (1987) classified cracking is as follows

By pattern

1. Network Cracking- crocodile or map cracking ;i.e., interconnected polygons
2. Line cracking-Longitudinal or transverse or line cracks interconnected in rectangular pattern
3. Irregular cracking- Unconnected cracks or interconnected by irregular pattern.

By location

1. Wheel path cracking
2. Non-wheel path cracking

By Mechanism of cracking

Fatigue, shrinkage, reflection, low temperature, settlement, ageing

By traffic

1. Traffic related cracking
2. Non-traffic related cracking

Paterson (1987) states that the intention in all these classifications is to provide information on the probable cause of cracking, which in turn provides more reliable prediction and provides a rational basis for selecting and designing appropriate maintenance.

The collection and inputting of cracking data into HDM-4 models requires understanding and interpreting of the mechanism, pattern, and quantity of cracking.

Measure of Cracking

Many methods of measuring are developed, both quantitative and qualitative, but there is no internationally agreed standard or correlation between the different methods (Paterson, 1987). Quantitatively cracking is measured by the following parameters

Extent- Paterson (1987) defined extent of cracking as the sum of pavement surface covered by cracking as a percentage of the surfacing area over a defined unit such as a lane or pavement width by a convenient sample length in the range of 100 to 1,000 m. For example in the Brazil-UNDP study the area is measured as sum of rectangular areas surrounding individual cracking networks measured in square meters and eventually reported as a percentage of the subsection area (one lane-width by 320 m length) and for linear cracks, the area was defined by a 0.5 m wide strip extending the length of the crack. Contrary to the area measurement, TRL (1999) defines extent of cracking as the length of blocks affected by cracking expressed as percentage of defined length.

Intensity- Similar to the method used for the Kenya road deterioration study (Hodges and Rolt, 1975), the intensity of cracking in HDM is expressed as the total length of cracks in a unit area (m/m^2) or as an average spacing of the cracks (considering cracking as a nominally square-grid network). In the TRL (1999) intensity is defined in terms of six scale rating where no cracking is rated as 0 to 5 for severe crocodile cracking with blocks rocking under traffic.

Severity –It is a measure of the width of crack, usually represented by classes. The following classes were used during the AASHO road test and later in the Brazil-UNDP Cost study (Paterson, 1987)

Class 1- Hairline cracks of width 1mm or less

Class 2- Crack widths of 1mm- 3 mm

Class 3- Crack widths greater than 3 mm without spalling

Class 4- Spalled cracks, fragments of the surfacing adjacent to the crack were lost

When quantifying cracking, therefore one needs to know the extent, intensity and severity of cracking together with at least one or two types of cracking classification. For example during the Brazil-UNDP cost study cracking data was collected based on class (severity), extent (area) and type(crocodile, irregular, block, transverse or longitudinal) the same as the system adopted from AASHO Road Test and condition survey templates which were used in Texas and South Africa (Paterson, 1987).

Concepts of Crack Modeling in HDM

The concept of cracking initiation and progression for each class has been developed first by the Texas Research Development Foundation (TRDF) (Paterson, 1987). Those concepts show that each severity class of cracking can be represented by separate functions but according to Paterson (1987) it was quite difficult to apply the separate functions for planning purposes and instead a cumulative numeric CR_i, which represents the sum of areas of cracking with severity class i was defined and used for the Brazil road deterioration study.

$$CR_i = \sum_{j=1}^{4} CL_j \qquad (2\text{-}15)$$

Where CR_i= Cracking area numeric of level i

CL_j= Area cracked of class j, j=1 to j=4

When the TRDF concept was applied to the Brazil-UNDP study and later included in the HDM-III and HDM-4 models CR_2 represents the sum of “all cracking” that is the sum of cracking area of severity class 2, 3, and 4. CR_4 on the

other hand represents only the area of “wide cracking” i.e. severity of class 4. According to Paterson (1987), the area of cracking of class 1(hairline crack), was omitted in the study because it was difficult to observe and has little mechanical impact on pavement behavior.

Again to limit the number of models for cracking prediction a summary index, CRX, combining all severities was defined by the World Bank as follows (Paterson, 1987)

$$CRX = \sum_{j=1}^{j=4} (iCL_j) / 4 \qquad (2\text{-}16)$$

Where

CRX = Area of indexed cracking, in percent of total surfacing area.

i = Weighing factor which equals to width of crack in mm, in this case large crack width contributes more to the index for its more contribution for water ingress.

In the Brazil-UNDP study the cracking index was estimated from CR_2 and CR_4 using the following relationship (Paterson, 1987)

$$CRX = 0.62CR_2 + 0.39CR_4 \qquad (2\text{-}17)$$

Where

CRX = As Defined earlier

CR_2 = Sum of “all cracking” that is the sum of cracking of severity class 2, 3, and 4.

CR_4 = Area of “wide cracking” i.e. severity of class 4

According to Paterson (1987) during the TRRL Kenya cost study cracking was quantified in terms of average intensity, without classifying severity and with indirect measure of extent. Cracking length was measured for sample areas at 100 m interval for 1000 m length of road and then the intensity of each section added and averaged. The area of cracking was calculated based on defined minimum criterion for applying maintenance; say greater than 5m/m^2.

Cracking Mechanisms

Fatigue

Pell (1978) defined fatigue cracking as cracking of the pavement surface unaccompanied by deep seated deformation of pavement structure resulting from repeated cumulative traffic loading. It is characterized by crocodile pattern and is usually confined to the wheel path. According to Pell (1978) investigations of fatigue phenomenon of bituminous pavements has shown that strain is a good indicator of fatigue performance both in the laboratory and in-situ.

The following equation represents the relationship between N and ε (Paterson, 1987)

$$N_f = K * \varepsilon_t^{-n} \qquad (2\text{-}18)$$

Where N_f = Number of repetitions of load in flexure to the incitation of fatigue cracking

ε_t = Maximum horizontal tensile strain in the bituminous material under the applied load

K, n = Constants depending primarily on material characteristics of stiffness and binder content.

Laboratory estimates of k and n show variation depending on material characteristics and loading conditions (Paterson, 1987). According to Tangella et.al (1990), fatigue life also depends on compaction during construction and on the mode of loading. According to Paterson (1987), under controlled strain loading which generally applies in thin flexible pavements the fatigue life is two to three times longer than at comparable strain level under controlled stress loading which generally applies to thick stiff pavements. Table 2-7 summarizes material characteristics and their impact on fatigue life for the controlled stress and controlled strain modes of loading.

Table 2-7 Material characteristics and loading condition on fatigue life

Factor	Change in factor	Effects on Stiffness	Effect on fatigue life under	
			Controlled stress loading	Controlled strain loading
Asphalt Viscosity-	Increase	Increase	Increase	Decrease
Asphalt Content	Increase	Increase	Increase	Increase
Aggregate gradation	Open to dense grading	Increase	Increase	Decrease
Air Void Content	Decrease	Increase	Increase	Increase
Temperature	Decrease	Increase	Increase	Decrease

Source: Tangella et.al, 1990

Paterson's analysis of the strain, pavement layer stiffness and surfacing thickness using data from Brazil-UNDP study shows that tensile strain on surfacing increases sharply when the stiffness of base decreases due to either poor base material quality (low strength), water penetration or poor compaction and causes early fatigue failure. The result of the same study also shows that thin pavements are more sensitive to base stiffness variation than thick pavements. A plot of surface strain versus interface(with base) strain for pavements of different thickness shows that, at thickness less than 40mm the surface strain is higher than the interface, showing that maximum strain on thin pavements is on the exposed pavement surface. This concept is more important for fatigue life when considered together with ageing.

Again according to Paterson (1987) a research using layered structure analysis, experimental fatigue relationships and field experiments show that thin pavements of less than 50 mm thickness when they are produced as flexible are having longer fatigue life than surfacing of 60-80mm thickness. When the thickness of surfacing is more than 100 mm, the structural contribution of the surfacing becomes significant in reducing the induced tensile strain and hence will result in longer fatigue life.

Ageing

Ageing in bituminous pavements is the hardening of the binder material due to the oxidizing effect of the environment. According to Dickson (1984) the rate of ageing depends on the resistance to oxidation of the bituminous binder (depending on chemical composition and source of the crude oil), the film thickness (the length of oxidation path) and on temperature. High binder content (thick film) and low air voids has a beneficial effect by lengthening the oxidation path and excluding air and high temperature has an effect of accelerating oxidation and hence ageing. Dickinson (1984) has also noted that a pavement cracks due to ageing when the binder reaches a critical viscosity beyond which the binder can no longer take the low strain level associated with daily thermal movements. According to Paterson (1987) cracking by "aging" usually has the form of irregular or map cracking pattern with spacing greater than 0.5 meters and, once initiated, is likely to progress rapidly over the full area of surface.

Interaction of Ageing and Fatigue

According to Paterson (1987), the time to initiation of fracture depends on the material design and the interaction of traffic related fatigue and environment related ageing. At the early years of the surfacing, the fatigue life at the surfacing is more than at the underside. But as time progresses the fatigue life at the underside will be greater than the surfacing and fracture normally happens at the surfacing due to traffic and ageing. Fracture at the underside will then happen due to increased traffic loading. According to Paterson's work fracture due to thermal variation and ageing will normally happen at about 11 years if the traffic loading is smaller compared to the pavement strength.

Reflection Cracking

It occurs when the underlying cracking propagates upwards to the newly overlaid surfacing. It normally takes the pattern of the underlying cracking. According to Paterson (1987) it occurs due to concentration of stress at the tip of the internal crack or flaw, which reduces the available fatigue life of the surfacing considerably.

Longitudinal and Transverse Cracking

Non-wheel path longitudinal cracking and transverse cracking will occur due to shrinkage of treated base material or naturally-occurring cementing materials such as calcretes, ferricretes, lateraites etc. According to Paterson cracking occurs typically at 3m but varying from 1.5-12 m depending on tensile strength (increases spacing and crack width) and daily or seasonal temperature ranges(decrease spacing or increase width).

Longitudinal edge cracking occurs due to moisture movements through the shoulder. Sealing the shoulder or good drainage will control this type of cracking.

Settlement of the foundation or embankment will cause either a longitudinal or a long curved crack.

Crack Modeling Methodology

The methodology adopted in the TRRL Kenya deterioration study combines crack initiation and progression in one model as represented by equations (2-19) and (2-20) (Robinson and Linda 1982).

$$C + P = 300\left[SN - 4 + \frac{72N}{SN^{SN}} \right] \quad \text{for } \mathrm{SN}<4.0 \text{ and } \mathrm{c+p}\geq 0 \tag{2-19}$$

$$C + P = \frac{21600N}{(SN)^{SN}} \quad \text{for } \mathrm{SN}\geq 4.0, \mathrm{C+P}\geq 0 \tag{2-20}$$

Where

C+P= Sum of areas of cracking of intensity exceeding 5m/m^2, and patching in m^2/km/lane

SN = Modified structural number

N = Cumulative number of equivalent standard axle load since recent surfacing, in million ESAL

According to Paterson (1987), the disadvantage of such model forms is that they constrain rate of progression by the time to the initiation of distress. For example

the Texas model forces long surviving pavements to have a rapid rate of progression once cracking initiates.

Other prediction model types comprise of separate initiation and progression phase models. The Brazil UNDP and Arizona ADOT studies resulted in such type of models (Paterson, 1987). According to Paterson separate models have the advantage of predicting initiation and progression independent of each other. The approach adopted in the development of HDM-III and HDM-4 deterioration models is a separate initiation and progression phase using the probabilistic failure time modeling principles.

Probabilistic Failure Time Modeling

Due to the variability of material character, construction quality and environment cracking will occur at different times even in a nominally homogenous section. As explained by Paterson (1987), typically when a uniform cross-section of different pavements with a range of different ages, strengths and loading conditions are observed over a period of time or "window", the actual timing of cracking initiation will not be observed in every case. Some of the surfacings may have cracked before the study began and some may only crack later after the study has finished.

Cracking Initiation

Paterson (1987) defined cracking initiation as a discrete event in time when cracking appears on the surface, a definition consistent to the many condition survey methods used in pavement management systems. For research purposes it is defined as the time cracking begins in bound layer. In the succeeding progression phase cracking increases in extent, severity and intensity.

Crack initiation is defined as the age of pavement at cracking extent of 0.5% of the carriageway area of the section under consideration. This means that a minimum of $5m^2$ cracking for each 320 m by 3.5 m of standard section. This length of section is adequate to give a consistent result of measurement during a condition survey.

Cracking of bituminous pavements is primarily caused by traffic related fatigue and environment related aging, which is termed as structural cracking. The

initiation of cracking also depends on the pavement strength, quality of the base layer, the stiffness of the bituminous bound layer, the bituminous content, the thickness of the surfacing, air void content and construction quality which is measured by the relative compaction. Paterson (1987) using the probabilistic time failure concept and combinations of at least three explanatory variables developed crack initiation models from data collected during the Brazil-UNDP study. As explained by Paterson, a model of more than three explanatory variables was not developed due to the limited range of data available and hence he developed the following models

$$TY_{cr2} = 4.21\exp\left(0.139SNC - 17.1\frac{YE_4}{SNC^2}\right) \quad (2\text{-}21)$$

$$TY_{cr2} = 8.61exp\left(-\frac{24.4YE_4}{SNC^2}\right) \quad (2\text{-}22)$$

$$TY_{cr2} = 8.38\exp\left(1.21BNO - 18.6\frac{YE_4}{SNC^2}\right) \quad (2\text{-}23)$$

$$TY_{cr2} = 16.5\exp(-0.098HS + 0.00081HS^2 + 0.438SNC - 1.82YE_4^{0.5} \quad (2\text{-}24)$$

Where,

TY_{cr2} = Expected or mean age of surfacing at initiation of cracking

YE_4 = Annual traffic loading, million ESA_4/ lane/ year

HS = Thickness of the bituminous layer in mm

BNO = Excess bituminous content with respect to optimum bitumen content in fraction and given by equation (2-25)

$$BNO = 1 - BC / OBC \quad (2\text{-}25)$$

BC = Recovered binder content conforming to Marshal Criteria for dense graded mixtures estimated by the following approximate algorithm

$$OBC \approx 7.8 - 0.1D_{95} \quad (2\text{-}26)$$

$OBC =$ Optimum Binder Content

D_{95} = Maximum stone size of the mix aggregate in mm

According to Paterson (1987), model (2-21), which shows a strong decay of predicted life as the traffic loading rate increases or pavement strength decreases is generally accepted for planning purposes and is included in both HDM-III and HDM-4 models, with models (2-22) and (2-24) as good alternatives.

The model of HDM-4 crack initiation has some differences to that of HDM-III, for it includes a factor for construction defects indicator and the effect of maintenance.

Initiation of Wide Cracking

Initiation of wide cracking is considered when wide cracking (CR_4) reach 0.5% of the carriageway area and according to Paterson (1987), can be modeled independently as a function of initiation of all cracking. The independent models however have the disadvantage that the prediction wide cracking initiation can happen before the initiation of narrow cracking with some combinations of explanatory variables. Therefore, according to Paterson (1987), predictions are more reliable when expressed as a function of initiation of narrow cracking, linearly in the form of equation (2-27).

$$TY_{cr4} = a_0 + a_1 TY_{cr2} \quad (2\text{-}27)$$

Regression of the Brazil-UNDP data gave model (2-28) for the initiation of wide cracking

$$TY_{cr4} = 2.46 + 0.93 TY_{cr2} \quad (2\text{-}28)$$

Where

TY_{cr4} = Initiation age of wide cracking (years) and TY_{cr2} is as defined earlier.

According to Paterson (1987) the interval between the initiation of narrow and wide cracking is relatively constant and is between 2 and 2.5 years.

Progression of Cracking

Similar to the initiation, the probabilistic maximum likelihood procedure was also used to develop models for progression of cracking so as to include the effect of "censored" data (Paterson, 1987), using the time of progression of cracking from

0-30% and 30-60% of carriageway area as dependent variables to be modeled. The progression of cracked area was found in the empirical study to be a non-linear, S-shaped function the rate of progression depending on the area of cracking and the time since cracking initiation, without significant effect of either traffic loading or pavement strength (Watanatada, 1987a). In HDM-III, the progression of cracking is given by the following equation (Paterson, 1987).

$$CR_{it} = 1 - z\ 50 + z\left[zabt_{ci} + z\ 0.5^{\ b} + 1 + z\ 50^{b} \right]^{\frac{1}{b}} \quad (2\text{-}29)$$

Where,

CR_{it} = Area of cracking at time t

t_{ci} = Time since initiation of CR_i cracking in years and given by

$$t_{ci} = \frac{[(1 - zz)50^{b} + zzSCR_{i}t^{b} - 0.5^{b}]}{ab} \quad (2\text{-}30)$$

z = 1, when $t_{ci} \leq t_{50}$ and $z = 1$, otherwise

SCR_{it} = minimum $[CR_{it}, 100\text{-}CR_{it}]$ (2-31)

The incremental area of cracking during the period Δt, ΔCR_{it} is given as

$$\Delta CR_{it} = zz\left[zz\ a\ b\Delta t + SCR_{it}^{b} \right]^{1/b} - SCR_{it} \quad (2\text{-}32)$$

The time to 50% cracking area is given by

$$t_{50} = \frac{(50^{b} - 0.5^{b})}{ab} \quad (2\text{-}33)$$

zz=1, when $CR_{it} \leq 50, otherwise\ zz = -1$

a= Estimated model coefficient which is a function pavement type, traffic loading and pavement strength estimated to be 1.84 for all cracking and 2.94 for wide cracking of original asphalt concrete pavements

b= A constant equal to 0.45 for all cracking and 0.56 for wide cracking of asphalt concrete pavements

In HDM-4, the general form of the model for the progression of all structural cracking is generally similar to that derived by Paterson, except that it is adjusted for construction quality indicator and crack retardation factor, which will be discussed further in Chapter four.

2.3.2 **Ravelling**

Ravelling is a loss of stone particles from pavement surface by the mechanical effect of fracture of the binder film or the loss of adhesion between the binder and stone. Mechanical fracture of the binder film around a stone particle occurs when the binder has become too brittle or the film is too thin to sustain the stresses imposed by a moving traffic. Loss of adhesion is usually caused by the presence of water or contamination by dust. Therefore the controlling of ravelling is through controlling of material and work quality specifications. According to Paterson (1987) ravelling has a negligible effect on roughness but has serious structural implications when the surfacing is thin and could potentially lead to potholing. It usually triggers maintenance (patching or re-surfacing) as a preventive measure against more serious types of distress such as potholes and skid resistance and against penetration of moisture to the lower layers.

Ravelling Initiation and Progression

Similar to cracking, initiation of ravelling is modeled by the principles of probabilistic failure time because all conditions which are appropriate for crack initiation are also applicable for ravelling. Similar to cracking, in HDM-III and HDM-4, ravelling is modeled by separate initiation and progression phases. Initiation of ravelling is considered when 0.5% of the carriageway area is raveled. The progression of ravelling is also modeled using the non-linear sigmoidal function.

Ravelling has a negligible effect on the structural performance of thick surfacings and hence in HDM-III and HDM-4 road deterioration models, ravelling is limited to thin surfacings like surface treatments. The details of the models will not be discussed in this report because the study area’s pavement surfacing is asphalt concrete of thickness 100mm.

2.3.3 **Potholing**

Paterson (1987) defined potholing as a cavity on the road surface which is 150 mm or more in average diameter and 25 mm or more in depth. Later Lea (1995) estimated the size of the potholes to be 0.07m^2 or 300mm in diameter and in HDM-4 (Odoki and Kerali, 2000) the size of the pothole is accepted to be 0.1 m^2 and a volume of 10 liters which means a depth of 0.1m. If the depth of the cavity is less than 25mm, it is considered as ravelling. Lea (1995) defined potholing as a local loss of material from the pavement which penetrates through the asphalt layers into the unbound layers. This definition is the minimum which affect the motion of a car wheel and measured roughness significantly. If the loss of materials is limited only to the bituminous layers then it is termed as delaminations, a distress term between raveling and potholing levels. Potholes develop from either or both of cracked and raveled pavement surfaces, whereby the presence of water accelerates the rate of pothole enlargement. The unit of measurement in both cases is the number of o.1m^2 potholes/ delaminations per km/ lane.

Prediction of Potholing Initiation and Progression

Paterson (1987) explained that even though potholing normally triggers automatic routine maintenance and is the least predictable form of distress, for an economic evaluation of a differed maintenance, some form of quantification is necessary.

The HDM-III pothole model was derived from studies in Brazil, St. Vincent, Ghana and Kenya and predicts the initiation and progression potholing resulting from wide cracking or ravelling (Lea, 1995)

In HDM-III, the initiation of cracking was estimated as function of all vehicle axles (YAX), type of base material, and thickness of surfacing separate for cemented and un-cemented base layers. The model for un-cemented material is represented by equation (2-34)

Un-cemented base layer

$$TMIN = MAX\left[2 + 0.04HS - 0.5YAX; 2\right] \quad (2\text{-}34)$$

Where

$TMIN$ = Predicted time between the initiation of either wide cracking or ravelling whichever occurs earliest and the probable initiation of potholing (in years)

HS = Total thickness of bituminous surfacing, (in mm)

YAX = Annual number of vehicle axles, (in million axles per lane per year)

In HDM-4, the model form is changed where the construction defects indicator for base (CDB), MMP and YAX are the explanatory variables.

In HDM-4, the potholing initiation due to cracking is given by equation (2-35) of Odoki and Kerali (2000)

$$PTI = K_{pi} a_0 \left[\frac{1 + a_1 HS}{1 + a_2 CDB \quad 1 + a_3 YAX \quad 1 + a_4 MMP} \right] \tag{2-35}$$

Where

PTI = Time between the initiation of wide structural cracking and the initiation of potholes (years)

HS = Total thickness of bituminous surfacing

CDB = Construction defects indicator for base

YAX = Annual number of axles of all motorized vehicle types on the analysis year (millions/lane/year)

MMP = Mean monthly precipitation (mm/month)

K_{pi} = Calibration factor for potholing initiation

a_0, a_1, a_2, a_3, a_4 = Model coefficients, where in the case of AMGB pavements $a_0 = 2$, $a_1 = 0.05$, $a_2 = 1.0$, $a_3 = 0.5$, $a_4 = 0.01$

Potholing Progression

Paterson (1987) sited many studies, which show the progression rate of potholing varying between 0.1 to 9 percent per year. Therefore, in the modeling of potholing progression 10 percent is considered as the upper limit.

$$\Delta APOT = MIN \left(\Delta APOT_{cr} + \Delta APOT_{rv} + \Delta APOT_{pe}, 10 \right) \tag{2-36}$$

Where

$\Delta APOT$ = Predicted change in total area of potholing due to deterioration in the analysis year

$\Delta APOT_{cr}$ = Predicted change in potholing area due to cracking

$\Delta APOT_{rv}$ = Predicted change in potholing area due to ravelling

$\Delta APOT_{pe}$ = Predicted change in potholing area due to pothole enlargement

In HDM-4, the annual increase in the number of pothole units due to cracking, ravelling and enlargement of existing potholes is given by equation (2-37) of Odoki and Kerali (2000)

$$dNPT_i = K_{pp} * a_0 * ADIS_i \; TLF \left[\frac{1 + a_1 CDB \quad 1 + a_2 YAX \quad 1 + a_3 MMP}{1 + a_4 HS} \right] \qquad (2\text{-}37)$$

Where

$dNPT_i$ = Additional number of potholes/km derived from distress type i(wide structural cracking, ravelling or enlargement of existing potholes) during the analysis year

$ADIS_i$ = Percentage area of wide structural cracking at the start of the analysis year, or the percentage area of ravelling at the start of the analysis year or number of existing potholes per km at the start of the analysis year

TLF = Time lapse factor which depend on the time lapse between occurrence of potholes and patching, value varying between TLF=0.02 for time lapse of two weeks to TLF=1 for time lapse of 12 months.

$$dNPT = \sum_{i=1}^{3} dNPT_i \qquad (2\text{-}38)$$

$dNPT$ = Total number of additional potholes per km during the analysis year

K_{PP} = Calibration factor for potholing progression

a_0, a_1, a_2, a_3, a_4 = Model coefficients, where in the case of AMGB pavements $a_0 = 1$, $a_1 = 1.0$, $a_2 = 10.0$, $a_3 = 0.005$, $a_4 = 0.08$

It shall be noted that in HDM-III potholing progression was estimated in the unit of area and in HDM-4 in unit of number of potholes.

2.3.4 **Rutting**

Rutting is defined as the permanent or unrecoverable traffic-associated deformation within pavement layers which, if channelized into wheel paths, accumulates over time and becomes manifested as a rut(Lea, 1995)

Mechanisms of Rutting

The causes of rutting can be classified as traffic associated and non traffic associated causes and Paterson (1987) noted the following

- The mechanism of deformation associated with traffic loading could be either densification or plastic flow. Densification involves change in material volume resulting from tighter packing of the material particles and sometimes also from the degradation of the particles into smaller sizes.
- Plastic flow on the other hand does not involve volume change and gives rise to shear displacement in which both depression and heave are manifested. It occurs when the shear stress induced exceed the shear strength of the material or are sufficient to induce creep. It is controlled by selecting materials by the measure of their shear strength like CBR for soils and Marshall Test for bituminous materials.

According to Lea (1987), the above mechanisms are manifested into rutting in three phases.

Initial Consolidation-The relatively rapid initial increase in rutting on a newly constructed pavement once it is opened to traffic.

Constant rate of deformation-During this phase the rate of deformation (strain) tends to stabilize, resulting in a constant rate of increase in deformation over time or traffic load.

Accelerating deformation-This is the final phase of deformation characterized by an increased rate of deformation (strain). The increased rate of deformation is

mainly influenced by traffic loading, pavement strength, material type and environmental influences

Rut depth Prediction Approaches

According to Paterson (1987), two approaches have been used in pavement design methods

1. Excessive deformation beyond a specified failure limit is prevented through applying criteria derived from empirical correlation to pavement performance. These criteria are either empirical or mechanistic. The commonest empirical criterion is the CBR which correlates the layer thickness to material shear strength and applied wheel load. Mechanistic criteria are commonly based on limiting the vertical compressive strain in the subgrade to the level dependent upon traffic loading using the elastic theory. These methods do not show the trend of deformation accumulation.
2. The second type of approach predicts the trend of deformation under repeated loading either mechanistically, based on laboratory material characterization and theoretical structural analysis of the stresses and strains induced in each layer under the traffic loading, or empirically, by correlation between field data of rut depth trends and explanatory parameters representing the pavement and loading.

The approach adopted in the development of the HDM rutting models is using statistical analysis of data collected during the Brazil-UNDP cost study. In HDM-III, the rutting prediction models developed were incremental and cumulative types. Paterson recommended the cumulative type than incremental type because of the large errors associated with the manual method of rutting measurement which strongly affect predictions of the incremental models. However, the incremental model was included in HDM-III and later in HDM-4 to be consistent with the recursive, incremental model structure of the deterioration and maintenance models of HDM-III and later HDM-4 (Lea, 1995). It shall also be

noted that while the rutting progression model in HDM-III is a summary incremental model with one calibration factor, in HDM-4 the incremental model is the sum of four component models each with its own calibration factor. Another noticeable difference between HDM-III and HDM-4 models is that in HDM-III the standard deviation of rut depth is predicted with the same variables as the mean rut depth, but in HDM-4 the standard deviation of rut depth is predicted just as a function of mean rut depth. The coefficients in HDM-III and HDM-4 are also different due to the different straight edge length adopted.

Determination of Compaction Index

The compaction achieved during construction influences the amount of rutting due to initial densification. Therefore it is necessary to establish a standard compaction reference profile which decreases with depth in order to be compatible with specification practices, which are calculated as follows (Paterson, 1987)

A reference profile of nominal compaction is defined as

$$C_{nom,i} = 1.02 - 0.14 z_i \tag{2-39}$$

Relative compaction achieved for each layer i (RC_i) was defined as

$$RC_i = \min\left[1, C_i / C_{nom,i}\right] \tag{2-40}$$

Where

$C_{nom,i}$ = Nominal specification of compaction to be achieved inlayer i with respect to the relevant standard as a fraction

Z_i = Depth at the bottom of layer i in meters, Z≤1

RC_i = Relative compaction i.e. the ratio of the compaction measured in the field to the nominal compaction as a fraction

C_i = Compaction of layer i defined by

$$C_i = \frac{DD_i}{MDD_i} \tag{2-41}$$

DD_i = Insitu dry density of layer i

MDD_i = Maximum dry density of layer i determined in the laboratory to the relevant compaction standard

The relative compaction index ($COMP$) for the full pavement depth is then defined as the average relative compaction weighed by layer thickness over a 1m depth as follows

$$COMP = \sum_{i=2,n} RC_i \left(\frac{H_i}{\sum_{i=2,n} H_i} \right) \quad (2\text{-}42)$$

Where $COMP$ = Relative Compaction over the full pavement depth (%)

H_i = Thickness of layer i in mm

The compaction index is calculated only to the untreated base and sub-base layers because they are the likely source of densification.

In HDM-4, rut depth modeling has four components (Odoki and Kerali, 2000). These are initial densification, structural deformation, plastic deformation and wear from studded tires; models are discussed in chapter four.

2.3.5 **Roughness**

Roughness is the measure of the variation in the longitudinal surface profile of the road considering a true planar surface as datum. It will be significant if the magnitude of variation affect the dynamics of vehicle operation and motion and influence road users' perception of the riding quality. Sayers, Gillespie and Quiroz (1986) defined roughness as "the variation in surface elevation that induces vibrations in traversing vehicles". Similarly Lea (1995) defined roughness as irregularities in the pavement surface that gives most concern to road users.

As rightly said by Paterson (1987) and as shown in all the definitions above a relevant measure of roughness should consider three elements, namely road surface profile, the vehicles and road users (drivers and occupants).

Paterson (1987) further explained that the deviation of the longitudinal surface profile from true planar surface tends to be random in nature consisting waveforms of various spectrums of amplitude and wave lengths, but to eliminate surface texture in the very short range and the vertical gradient in the very long

range, a practical range for surface roughness is limited between 0.1m to 100m wave length and 1mm to 100mm wave amplitude. According to COTO (2007) the wave lengths that have greatest effect on road user's comfort are limited between 1m and 30m.

In order to extract useful roughness numeric from original surface profile measurements, Sayers, Gillespie and Quiroz (1986) used the statistical power spectrum density (PSD) which is mathematically defined as the variance of the variable measured (elevation, slope) distributed over wave number expressed in unit of (Quantity measured)^2/wave number. The plot of elevation variance (PSD) expressed in units of (m^3/cycle) to wave numbers (cycles/m) showed that the amplitude is higher in longer wavelengths (smaller wave numbers) and vice versa.

According to the same study and later described by Paterson (1987), the spectrum of wavebands also tends to vary with surface type. Asphalt surfaced roads will have much of its roughness from longer wave lengths, because the short wave lengths will be eliminated during construction, in contrary to surface treatment (or chip seal) surfaces which have a much more variable spectrum with more roughness found at the short wavelengths below 2 m.

Method of Measurement

Early measures were subjective ratings values between 0 and 10 with 10 being a perfect surface and 0 the roughest indicating lower riding qualities (Lea, 1995). Because subjective ratings are variable with the expectations of the individuals who do the rating, mechanical methods of measuring roughness were developed each with its own measuring scale. Table 2-8 show the category and instruments used for measuring roughness

Table 2-8 Summary of Roughness Measuring Systems

Category	Method and Example
Absolute profile	Measure profile elevation relative to a true horizontal datum, e.g., rod-and-level survey, "Dipstick" profiler, British profile beam (measures in 3m segments)

Category	Method and Example
Moving datum profile instruments	Measure deviations of profile relative to a datum moved along the road, e.g., sliding straightedge, rolling straightedge, profilographs
Vehicle motion instruments(road meters)	Measure 1: Relative displacement between axle and body of car, summing upward, or upward and downward, movements with readout at regular distances giving a slope statistic (displacement/length), e.g., m/km, mm/km, inch/mile) e.g., Maysmeter, Cox meter, NAASRA meter, Bump Integrator (trailer or car-mounted) Measure 2: Accelerations of axle or body by accelerometer, and integrate signal, e.g., ARAN (Automatic Road Analyzer).
Dynamic profile Instruments	Measure profile elevations electronically relative to an artificial "horizontal" datum providing elevation-distance data, at intervals depending on electronic sampling rate, and filtered to span a practical range of frequencies; e.g., General Motors research (GMR) and K. J. Law profilometers (accelerometer as inertial reference); French APL (longitudinal profile analyzer) (mechanical inertial reference); British High Speed Road Monitor (HRM) (laser-sensed profile relative to leading sensor)

Source: Paterson (1987)

Standard Method of Measure

The wide differences between the outputs of different devices used throughout the world, and often poor reproducibility of results by the same type of equipment have severely hindered the use of roughness data in decision making, and particularly in research attempting to compare results from different studies (Paterson, 1987). In order to establish correlation between the different roughness measures and to select a standard for calibration, the World Bank convened the International Road Roughness Experiment (IRRE) in 1982 in Brazil, with sponsorship and participation of several international organizations (Sayers, Gillespie and Quiroz, 1986).

The result of the experiment recommended the international roughness index (IRI) as a reference numeric from which all other mechanical road roughness measuring equipment will be calibrated. IRI represents the average rectified slope output (ARS) of the reference quarter car simulation (RQCS) at a speed of 80 km/h, derived from the absolute profile of the road surface.

RQCS is a mathematical vehicle simulation of an ideal response-type road roughness measuring system (RTRRMS) and the roughness obtained is representative of the true longitudinal surface profile.

International Roughness Index (IRI)

This numeric was selected because it closely correlates with RAS_{80} measure obtained by any of RTRRMSs and closely correlates with RAS_{80} of any profile-based numeric.

The IRI was adopted in the IRRE study as an international roughness numeric because of the following advantages (Paterson, 1987)

- It is time-stable and reproducible anywhere from elevation data because it is a mathematical summary statistic of the absolute road profile.
- The origin for a planar surface is zero and the scale is open ended at high roughness levels (equipment-based statistics generally had a nonzero origin due to mechanical imperfection)
- It was the statistic which gave the most consistently high correlations with the output of all road meters on all surfaces at all speeds and also correlated highly with subjective rating.
- It is relevant to the impact of roughness on vehicles and users because the waveband covered, and its sensitivity to amplitude variations within that waveband, are representative of vehicular response and the comfort perceived by users - the bandwidth is predominantly in the frequency range of 1 to 20 Hz or 0.04 to 1 cycles/m (wavelengths of 1 to 25 m).
- It is applicable to all profilometers and road meters, because it can be calculated directly from profile data (and is not limited to specific intervals as are some statistics) and correlates well with all road meters tested

- it is relevant to a wide range of traffic conditions from slow speeds to fast speeds and for a variety of vehicle types: even though the specific bandwidth included in the statistic applies primarily to uncongested, interurban highway travel with speeds in the order of 80 km/h (which represent the most prevalent conditions for highway networks in both industrialized and developing countries)
- The statistic also correlates extremely highly with the roughness perceived by vehicles at both slower speeds (under congestion) and faster speed (motorways or freeways).

The following had been noted as short comings

- It does not give a direct measure of the accelerations affecting the riding comfort perceived by users, although it correlates very highly with them.
- There is concern that the vehicle characteristics embodied in the IRI mathematical model may not be specifically representative of all vehicle classes or of future vehicle technology.

Modeling Roughness Progression

Roughness as discussed above is the measure of the longitudinal road surface irregularities resulting from the structural effects of traffic loading and pavement strength, surface condition (cracking, rutting and ravelling), ageing (time) and environmental factors. The prediction of roughness, which is the dominant criterion of pavement performance in relation to both economics and quality of service, in HDM-III and later in HDM-4, therefore, draws together the impacts of these factors and maintenance on road roughness (Paterson, 1987).

The AASHO performance equation, which is the result of the AASHO controlled road test, is cited by Paterson as the first comprehensive roughness progression model predicted as a function of traffic loading and pavement strength in a dimensionless damage parameter g expressed as

$$g_t = \frac{(p_o - p_t)}{(p_o - p_r)} = \left(\frac{N_t}{\rho}\right)^{\beta} \qquad (2\text{-}43)$$

Where

g_t = Dimensionless damage parameter defining the functional loss of serviceability incurred prior to time t (Note that when $P_t = P_r$, $g_t = 1$)

p_o = Serviceability Index at time t= 0

p_t = Serviceability Index at time t, where

$$p_t = 5.03 - 1.91\log 10\ (1 + SV\ ) - 1.38RD^2 - 0.01\ (C + P\ )^{0.5} \quad (2\text{-}44)$$

P_r = Terminal serviceability criterion, at which rehabilitation or reconstruction is deemed necessary

N_t = Cumulative number of equivalent 80 KN standard axle loads to time t

ρ, β = Functions of axle type, axle load and pavement strength parameters, including the structural number and later a soil support parameter

SV = Slope Variance, a measure of longitudinal roughness

RD = Mean rut depth expressed in inches

$C + P$ = Areas of class 2 and 3 cracking plus patching in ft/1,000ft^2

The strong effects of pavement strength and loading on roughness progression has also been verified on in-service roads in Kenya (Parsley and Robinson, 1982) as defined by the following equation

$$R = R_0 + mN \quad (2\text{-}45)$$

Where

R = Roughness at time t

R_o = Initial roughness of the road

N = Number of millions of standard axles which have passed over the road

m = Function of modified structural number

Paterson in his work also included other models developed from studies conducted on in-service pavements which are unable to identify any structural effects of pavement strength or traffic loading but which relate roughness progression directly to time and pavement age.

All the above discussed models are basically showing the effect of either structural (traffic/pavement strength) or time related factors on roughness progression independently.

To address these limitations, Paterson (1987) developed a model based on mechanistic concepts, and taking into consideration of the main independent variables of traffic, pavement strength, age, environment, maintenance effects and surface distresses into one model, which is basically the roughness progression model included in HDM-III and later HDM-4. Two sets of models, an incremental and summary type, have been developed. The two types of models developed are discussed in chapter four, because calibrations of the models require analysis of data using the models.

2.4 HDM-4 Studies in Ethiopia and Neighbouring Countries

In Ethiopia, Alebachew (2005) tried to identify the causes of pavement distress for Addis Ababa Arterial Roads and recommended maintenance alternatives. In his work Alebachew pointed out that 75% of the distresses observed on the Addis Ababa Arterial roads are ravelling, corrugation, bumps and sags. This is quite different from the distresses of Interurban highways where most of the distresses are cracking, rutting and potholing which are associated mainly with heavy traffic loading. His findings are expected in cities of high traffic volume of light loading. The findings show that the causes of deterioration are more related to poor material and construction quality and poor drainage conditions.

A study which focused on HDM-4 was conducted by Africon, a consultant employed by ERA. The main objective of the study was to integrate HDM-4 into ERA's Pavement Management System and level two calibration of the model to Ethiopian conditions (Africon, 2009). While Africon has developed guidelines for calibration of the road deterioration models of HDM-4, there was no suggestion on initial calibration factors to be adopted. Although Africon in the same report

concludes that the HDM-4 Road deterioration Models are applicable to Ethiopian Conditions, no study has been cited to support its conclusion. In a similar report, Africon classified the Ethiopian Road Network into different climatic zones prevalent in the country. From the description of Africon the method used for classification is by superimposing the Road Network on the “Atlas of Ethiopian Rural Economy”, a map prepared by the International Food Policy Research Institute, the Ethiopian Central Statistics Agency and Ethiopian Development Research Institute. After superimposing the map, the climatic classification of the map is correlated with the HDM-4 method which is based on values of Thornthwaite Moisture Index, annual precipitation and average temperature. According to Africon the Ethiopian Road network is classified into four climatic Zones. However, the classification shall be re-conformed using the method of HDM-4, which is the recommended approach in the calibration manual of HDM-4.

Many studies have been conducted in Kenya on topics related to pavement performance. Gichaga (1971) evaluated the elastic response of pavements to traffic loading by conducting measurements of Benkelman Beam Deflection, precise leveling, traffic study and plate loading tests on flexible pavements of Thika, Mombasa and Langata roads which are sampled to represent the conditions of Eastern Africa. Murunga (1983) also conducted similar studies where he correlates the rebound deflection of pavements to rainfall, traffic and pavement conditions of cracking and rutting. An important work on ageing of bitumen for pavements in tropical condition has been conducted by Bezabeh (1992).

As previously discussed and explained by Hodges and Jones (1975) a major road performance study was conducted in Kenya by TRRL in collaboration with the Kenyan Government and the World Bank as part of a larger study designed to provide suitable relationships for use in computer model capable of estimating the construction costs, maintenance costs and road user costs throughout the life of the road in a developing country. The study was designed to improve the deficiencies of the model developed by Moavenzadeh et.al of the Massachusetts Institute of Technology (MIT) by conducting direct field studies in Tropical and Sub-Tropical countries (Hodges and Jones, 1975). The result of the study

becomes the basis for the development of the TRRL Road Transport Investment Model (RTIM) and HDM-II model.

A study focusing on the calibration of the HDM-4 models was conducted in 2008 in Kenya as part of the Road Sector Investment Program (RSIP) (Carl Bro, Grontmij and Gath Consultants, 2008). The study titled “HDM-4 Workspace Calibration Report and Guideline” focuses mainly on the calibration of Road User Cost and to some degree on the calibration of road deterioration models. The methodology adopted for the study is based on the procedure included in the HDM-4 calibration manual prepared by Bennett and Paterson for a level one calibration. Data for such level of calibration is collected from desk studies or minimal field surveys.

Similar to the Ethiopian study by Africon, the Kenyan study used the Agro-Climatic map classification of Kenya as a basis and re-classified the climate according to the HDM-4 system (Carl Bro, Grontmij and Gath Consultants, 2008). Calibration to Kenyan condition was conducted for the environmental coefficient (m), cracking initiation and cracking progression factors, which are the most sensitive models recommended by Bennett and Paterson (2000) for initial calibration. Default calibration factors are adopted for rutting, potholing, ravelling and general roughness models. The result of the study on calibration factors adopted is further discussed in Chapter five in comparison with the results from research.

In Tanzania, however, a study on the calibration of the HDM-III model has been conducted (Mrawira, 1995). The study focused on establishing a database of input data and preparation of guidelines for the calibration of the HDM-III models. The method of calibration suggested by Mrawira (1995) is based on interviews of field personnel which is equivalent to the HDM-4’s level one calibration methodology. This study however includes values of environmental coefficient (m) for the different regions of Tanzania. However, the method used for determining this coefficient is not clearly explained. The environmental coefficient of the different regions of Tanzania varies between 0.023 and 0.035 for rainfall in the range of 400-1600mm/year. The findings of Mrawira (1995) are consistent with the findings of this study for annual rainfall of the specified range.

2.5 Statistical Methods of Data Analysis

HDM road deterioration models were developed using the mechanistic theory of pavement performance as a basis and statistical techniques of regression to correlate the deteriorations (dependent variables) with the influencing factors (independent variables). The processing of the input data and the calibration of the models also require the use of statistical techniques. The most common statistical techniques of mean, standard deviation, variance etc are not discussed instead the techniques which were directly used in the process of calibration are discussed.

Root mean Square Error (RMSE)

The calibration of the HDM-4 road deterioration models requires scaling of the predicted data to match the observed data. The calibration factor therefore is the ratio of observed data to the predicted data. The calibration process requires rotation and translation of the predicted data so that the regressed line's slope becomes unity.

The process requires minimization of the distance between the predicted and observed data. This is mathematically expressed as

$$RMSE = \sqrt{\frac{\sum Y - y^{2}}{n}} \qquad (2\text{-}46)$$

Where,

Y = Observed data

y = predicted data

n = Number of observation data points

Outliers

An outlier is a response (predicted) data point that does not follow the general trend of the rest of the data. An outlier is influential if it unduly influences the outcome of a regression. Identification of outliers is very important because any prediction based on a data that is far from the general trend of scatter will pull the

regression line towards the outlier and hence affect the slope of the regression line (calibration factor).

To identify the outliers some statistical analysis of predicted versus observed data is required and is conducted as follows.

a) Check if the data point has high leverage. According to (http://online.stat.psu.edu) leverage (h_{ii}) is a measure of the distance between the x value for the i^{th} data point and the mean of the x values for all n data points.

Leverage at $X_i = h_{ii} = \frac{1}{n} + \frac{X_i - \bar{}^2}{\sum X_i - \bar{}^2}$ (2-47)

Where X_i the observed response and n is the number of observations

The average of the leverage points is given by $\frac{2}{n}$ and a data is said to have high leverage if its leverage is more than twice the average leverage.

b) Find the residual between the predicted and observed responses

$$e_i = y_i - \hat{y} \quad (2\text{-}48)$$

c) Calculate the standardized residual for each data point, i=1…n as an ordinary residual divided by its standard deviation.

$$e_i = \frac{e_i}{s\ e_i} = \frac{e_i}{\sqrt{MSE\ 1 - h_{ii}}} \quad (2\text{-}49)$$

Where MSE is the mean square error, $s(e_i)$ is the standard deviation

An observation with a standardized residual that is larger than 3(in absolute value) is generally deemed an outlier.

2.6 **Summary of Literature Review**

The above discussions showed how the current model, HDM-4 released in 2000, has evolved throughout the years starting from its first version (HDM-I) in 1971 to its second version (HDM-II) in 1982 and third version (HDM-III) in 1987. It has been shown that the first models of HDM road deterioration models had been in a form of simple linear regression models where the developed models had been

site specific and were not transferable when conditions change. HDM-III and HDM-4 were developed to curb the limitations of their predecessors and are developed to be transferable by the inclusion of adjustable calibration factors. The models were developed using the mechanistic theory of pavement behavior and statistical analysis of pavement condition data collected from countries representative of the different geographical and climatic conditions.

The HDM-4 Road deterioration input parameters were discussed and was shown how these parameters could be quantified. The empirical and theoretical bases for the development of HDM-4 road deterioration models of cracking, rutting, potholing, roughness were also discussed.

Finally similar studies in Ethiopia and the region were discussed. It has been shown that although a level one calibration which relies on data from desk study was conducted specifically in Kenya and Tanzania but a second level calibration using actual field survey data was not conducted in either Ethiopia or the region. This study tried to fill the gap in knowledge by calibrating the HDM-4 road deterioration models using data collected from the field.

Chapter 3. Methodology of Data Collection

3.1 Introduction

In order to meet the objectives of the study a concise method of data collection has to be devised and implemented to get a reasonable quality output. Therefore for calibrating the HDM-4 road deterioration model, which is the main objective of this study, input data on traffic volume and axle loading, Pavement strength parameters, age of the pavement, materials and construction quality, climatic and environmental conditions, maintenance standards, present and past pavement conditions has been collected.

The input data as described by Hodges, Rolt and Jones (1975) could be from a database established by monitoring test sections from the time of initial construction to their ultimate failure, the information capable of showing complete pavement deterioration history, or from data sampled from set of road population at any instant of time. Though the first method has the advantage of showing complete pavement deterioration and is more accurate for formulating deterioration models it requires gathering data for long period of time, which especially for low volume roads deterioration is not achieved quickly. The data in the second method on the other hand could be collected by cross-sectioning (slice in time) of pavements of different ages at any instant of time, but due to stochastic variability in the material and construction quality the result of the analysis of the collected data will be very scattered.

The input data for this research is collected using the second method, due to unavailability of periodically recorded pavement condition data for the study area.

3.2 Levels of Data Collection and Calibration

Bennett and Paterson (2000) state that the amount and quality of data to be collected depend on the level of calibration to be achieved which is governed by the time and resources available to collect the data. Accordingly they classified into low, moderate and major level of data collection, each being defined as follows

Low level of data collection-For basic application

The data for this level are collected from desk studies, best estimates or minimal field surveys. The calibration for this level determines the values of required basic input parameters, adopts mainly default values, and calibrates the most sensitive parameters.

Moderate level of data collection-For Calibration

This level requires, in addition to the data to be collected at low level, measurement of additional parameters and moderate field surveys to calibrate key predictive relationships to local conditions.

High level of data collection-For Adaptation

This level requires major field surveys and controlled field experiments to enhance the existing predicting relationships or to develop new and locally specific relationships for substitution in the source code of the model.

However, due to the limitations of time and resources the data for this study is collected by the combination of the first two levels so that a level two model calibration is achieved to the conditions of the study area. The onetime field data collected based on this method from pavements of different age, strength and traffic loading is not sufficient for complete calibration of the model due to the natural non homogeneity of pavements. According to Bennett and Paterson (2000), for complete model calibrations, a long term preferably 5 years of data collection with major commitment to good quality, structured field research and statistical analysis is required. The methodology adopted to achieve a level two calibration is described as follows.

3.3 Desk Top Studies

The desk study has been used for establishing the pavement's history since the last maintenance, rehabilitation or reconstruction by reviewing literature specific to the study area. The literature includes design and as built drawings, engineering reports, traffic studies, climatic and metrological records. The following historical data have been collected from literature and by consulting relevant institutions.

- Equivalent standard axle loads
- Age of pavement and maintenance history
- Pavement strength parameters like pavement structural number (SNC), CBR
- Thickness of each pavement layer and material type used for surfacing, base and sub-base
- Drainage standards, quality of the lateral drainage provisions, cross drainage structures
- Strength of the sub grade in terms of either CBR or Modulus of Elasticity
- Climatic conditions along the route including the amount of rainfall and temperature
- Initial pavement condition including measurement of the initial roughness
- Construction quality indicators and deterioration retardation factors

The information collected from the desk studies and supplemented by initial field inspection has been used for establishing

a) The pavement history (age, maintenance, thickness, traffic loading, SNC, etc)
b) Calibration sections
c) For supplementing the field collected data

3.4 Analysis for Establishing Calibration Sections

The information collected from the desk studies supplemented by initial field inspection of the study area has been used for classification of the study area into homogenous sections by analyzing climatic, traffic loading, pavement strength and pavement condition data. The requirement for establishing the calibration sections varies with each distress type and this has been fully analyzed and the method of measurement on each section developed before proceeding with data collection.

3.4.1 Analysis for Environmental Classification of the Study Area

As described in the literature review climatic zone in HDM-4 is classified using the mean air temperature, Thornthwaite moisture index and annual precipitation. While the data from meteorological agencies on air temperature and precipitation

are used with minor calculation, the Thornthwaite moisture index requires calculation of the water budget of the area.

The procedure of calculating the water budget and Thornthwaite moisture index is as follows.

1. The monthly unadjusted potential evapotranspiration is estimated using the following equations developed by Thornthwaite and Mather (1955)

$$PET_{monthly} = 16\left(\frac{10T}{I}\right)^{a} \qquad \text{If} \quad 0<T<26.5\ ^{0}C \tag{3-1}$$

$$PET_{monthly} = -415.85 + 32.24T - 0.43T^{2} \qquad \text{If} \quad T> 26.5\ ^{0}C \tag{3-2}$$

Where

T = Monthly mean temperature

I = Annual Heat Index given by $I = \sum_{1}^{12} i$

i = Monthly heat index calculated from $i = \left(\frac{T}{5}\right)^{1.514}$

a= Index calculated using $a = 0.49 + 0.0179I - 0.0000771I^{2} + 0.000000I^{3}$

It should be noted that for a temperature of less than or equal to 0 ^{0}C, there will not be any evapotranspiration, because the heat energy, I, will be zero.

2. Because equation (3-1) and (3-2) are developed for an area experiencing 12 hours of sunlight and a 30-day month, the unadjusted potential evapotranspiration calculated above shall then be adjusted by the monthly average daylight hours and number of days per month using equation (3-3). The daylight hours depend on the location of the area (latitude and longitude). The monthly day light hours for this study is extracted from the Atmospheric Science Data Centre of NASA (http://eosweb.larc.nasa.gov/cgi-bin/sse/sse.cgi?+s01#s01)

$$PET_{adjusted} = PET_{unadjusted}\left(\frac{monthly\ \ days}{30}\right)\left(\frac{day\ \ light\ \ hours}{12}\right) \tag{3-3}$$

3. The excess moisture or moisture deficiency is then calculated from the difference of monthly precipitation and monthly-adjusted potential evapotranspiration.

$$Moisture\ excess\ /\ deficiency\ _{monthly} = Precipitation\ _{monthly} - PET_{adjusted} \quad (3\text{-}4)$$

4. The soil moisture storage is calculated using the tables of Thornthwaite and Mather (1957) for clay loam soil, representative of the study area, supporting a cereal type of crop with a maximum root depth of 400mm. From the table the soil has a maximum storage capacity of 100 mm and the minimum water storage is zero. This is an iterative process started by assuming certain amount of moisture storage at the beginning of the year. The soil moisture storage for a month is then calculated from the soil moisture storage of the previous month plus the excess water/water needed for that month.
5. The actual evapotranspiration (AET) is then calculated from the minimum of the potential evapotranspiration and available moisture content. The potential evapotranspiration is as calculated above and the moisture content is the sum of the previous month soil water storage and the monthly precipitation.
6. The annual moisture surplus(S) and moisture deficit (D) is then calculated from the sum of the monthly water precipitation and actual evapotranspiration. If the monthly precipitation is greater than the monthly actual evapotranspiration, then the excess water is the difference between AET and precipitation. If the monthly precipitation is less than AET then moisture deficit is the difference between PET and AET.
7. Thornthwaite moisture index (MI) is then calculated from the yearly Water surplus(S), yearly water deficit (D) and the Soil water storage capacity estimated to be 100 mm using the following equation.

$$MI = \frac{100\ S - D}{PET} \quad (3\text{-}5)$$

Where S, D and PET are as defined above

8. The Thornthwaite Humidity and Aridity indices are calculated as follows

$$\text{Humidity Index, } HI = \frac{100 * S}{PET} \quad (3\text{-}6)$$

Aridity Index, $A1 = \frac{100 * D}{PET}$ (3-7)

The Thornthwaite moisture index calculated using the above procedure for the three towns of Akaki, Modjo and Awasa which are within the study area is shown in Table 3-1,Table 3-2 and Table 3-3 respectively.

As can be seen from the tables the Thornthwaite moisture index of the three towns range between -20 and 19, which according to HDM-4 environmental classification and included in this report as Table 2-3 falls in sub-humid climatic zone. It is evident from the aridity and humidity Indices of the three towns Akaki is closer to humid climate and Awasa is closer to Semi-arid climate due to its relatively higher mean temperature. The result is based on temperature and rainfall data records collected from the Ethiopian Meteorological Agency.

The temperature of Akaki, Modjo and Awasa towns ranges between 21 ^{o}c to 22 ^{o}c, 18 ^{o}c to 24 ^{o}c and 22 ^{o}c to 26 ^{o}c respectively. Using the HDM-4 temperature classification, Table 2-3 of this report, the three towns generally fall in tropical climatic zone.

Therefore by the combination of the temperature and moisture classification it can be concluded that the study area falls into one homogenous climatic zone, namely sub-humid/tropical climatic zone.

Though it was the interest of the researcher to select study sites falling in at least two environmental zones, the above analysis for the Thornthwaite moisture index has resulted in only one environmental zone. It should however be emphasized that the study area is representative of climatic condition of most roads in the highlands of Ethiopia.

3.4.2 **Analysis for Pavement Strength Classification of the Study Area**

The modified structural number and/or deflection are the parameters used for quantifying pavement strength in HDM-4. For classifying the study area into homogenous strength sections the Benkelman beam deflection data collected in 2008 by consultants hired by ERA for the rehabilitation of the roads has been used. The deflection measurements were taken at 100 m interval staggered on left and right lanes.

Table 3-1 Thornthwaite moisture index calculation of Akaki town

Modjo(Latitude, longitude)	Jan	Feb	Mar	Apr	May	Jun	July	Aug	Sept	Oct	Nov	Dec		
Number of days	31	28	31	30	31	30	31	31	30	31	30	31		
Day light hours	11.6	11.8	12.0	12.3	12.5	12.6	12.5	12.4	12.1	11.9	11.7	11.6		
Mean temperature(^{o}C)	20.7	21.3	22.2	21.7	22.4	20.1	20.3	20.1	21.0	21.7	21.5	21.4		
Precipitation(mm/day)	*1.1*	*0.9*	*1.0*	*3.2*	*2.1*	*4.4*	*8.2*	*7.2*	*5.0*	*0.5*	*0.0*	*0.0*	I	a
Heat Index (i)	8.6	8.9	9.6	9.2	9.7	8.2	8.3	8.2	8.8	9.2	9.1	9.0	106.7	2.3
Monthly Potential evapotranspiration (mm/month)	75.1	80.3	89.0	84.4	90.4	70.1	71.7	70.1	78.1	84.4	82.1	81.7		
Adjusted potential evapotranspiration (mm/month)	75.0	73.7	92.0	86.5	97.3	73.6	77.2	74.8	78.8	86.4	80.0	81.6	976.9	
Precipitation(mm/month)	*34.2*	*24.6*	*31.6*	*96.8*	*64.6*	*132.7*	*254.2*	*221.8*	*148.5*	*14.8*	*1.3*	*0.0*		
Extra water/water need/month	-40.8	-49.1	-60.4	10.3	-32.7	59.1	177.0	147.0	69.7	-71.6	-78.7	-81.6		
Soil storage(mm)	0.0	0.0	0.0	10.3	0.0	59.1	100.0	100.0	100.0	28.4	0.0	0.0	0.0	100.0
Actual Evapotranspiration (mm/month)-AET	34.2	24.6	31.6	86.5	74.9	73.6	77.2	74.8	78.8	86.4	29.7	0.0		
Soil storage/Soil withdrawal(mm)	0.0	0.0	0.0	10.3	-10.3	59.1	40.9	0.0	0.0	-71.6	-28.4	0.0		
Runoff(mm)	0.0	0.0	0.0	0.0	0.0	0.0	136.1	147.0	69.7	0.0	0.0	0.0		
Check	0.0	0.0	0.0	0.0	0.0	0.0	0.0	0.0	0.0	0.0	0.0	0.0		
Water surplus	0.0	0.0	0.0	10.3	0.0	59.1	177.0	147.0	69.7	0.0	0.0	0.0	463.1	Total Surplus
Water deficit	40.8	49.1	60.4	0.0	22.4	0.0	0.0	0.0	0.0	0.0	50.4	81.6	304.6	Total deficit

16.2	MI
47.4	HI
31.2	AI

Table 3-2: Thornthwaite moisture index calculation of Modjo town

Modjo(Latitude, longitude)	Jan	Feb	Mar	Apr	May	Jun	July	Aug	Sept	Oct	Nov	Dec		
Number of days	31.0	28.0	31.0	30.0	31.0	30.0	31.0	31.0	30.0	31.0	30.0	31.0		
Day light hours	11.6	11.8	12.0	12.3	12.5	12.6	12.5	12.4	12.1	11.9	11.7	11.6		
Mean temperature(^{o}C)	19.6	23.0	32.7	22.8	23.6	21.9	17.8	18.8	20.9	19.4	19.4	19.2		
Precipitation(mm/day)	1.8	0.9	2.7	1.0	3.6	4.3	7.2	7.4	3.1	0.3	0.0	0.0	I	a
Heat Index (i)	7.9	10.1	17.1	9.9	10.5	9.4	6.8	7.4	8.7	7.8	7.8	7.7	110.9	2.5
Monthly Potential evapotranspiration (mm/month)	64.1	94.9	178.4	92.9	101.1	84.6	50.9	57.8	75.4	62.5	62.9	61.3		
Adjusted potential evapotranspiration (mm/month)	64.0	87.1	184.3	95.2	108.8	88.8	54.8	61.8	76.1	64.0	61.3	61.2	1007.	
Precipitation(mm/month)	*54.1*	*23.7*	*83.8*	*31.2*	*111.0*	*129.7*	*222.8*	*227.9*	*91.4*	*7.6*	*0.0*	*0.0*		
Extra water/water need/month	-9.9	-63.4	-100.5	-64.0	2.2	40.9	168.0	166.2	15.3	-56.4	-61.3	-61.2		
Soil storage(mm)	0.0	0.0	0.0	0.0	2.2	43.1	100.0	100.0	100.0	43.6	0.0	0.0	0.0	100.0
Actual Evapotranspiration (mm/month)-AET	54.1	23.7	83.8	31.2	108.8	88.8	54.8	61.8	76.1	64.0	43.6	0.0		
Soil storage/Soil withdrawal(mm)	0.0	0.0	0.0	0.0	2.2	40.9	56.9	0.0	0.0	-56.4	-43.6	0.0		
Runoff(mm)	0.0	0.0	0.0	0.0	0.0	0.0	111.1	166.2	15.3	0.0	0.0	0.0		
Check	0.0	0.0	0.0	0.0	0.0	0.0	0.0	0.0	0.0	0.0	0.0	0.0		
Water surplus	0.0	0.0	0.0	0.0	2.2	40.9	168.0	166.2	15.3	0.0	0.0	0.0	392.6	Total
Water deficit	9.9	63.4	100.5	64.0	0.0	0.0	0.0	0.0	0.0	0.0	17.7	61.2	316.7	Total

7.5	MI
39.0	HI
31.5	AI

Table 3-3 Thornthwaite moisture index calculation of Awasa town

Awasa(Latitude, longitude)	Jan	Feb	Mar	Apr	May	Jun	July	Aug	Sept	Oct	Nov	Dec		
Number of days	31.0	28.0	31.0	30.0	31.0	30.0	31.0	31.0	30.0	31.0	30.0	31.0		
Day light hours	11.7	11.9	12.0	12.2	12.4	12.5	12.4	12.3	12.1	11.9	11.8	11.7		
Mean temperature(^{o}C)	24.4	25.2	25.4	24.5	23.8	22.2	21.7	22.0	22.4	23.1	23.1	23.6		
Precipitation(mm/day)	0.9	1.4	2.6	3.9	3.8	3.6	3.8	3.8	4.0	2.5	1.0	0.7	I	a
Heat Index (i)	11.0	11.6	11.7	11.1	10.6	9.5	9.2	9.4	9.7	10.2	10.1	10.5	124.5	2.8
Monthly Potential evapotranspiration (mm/month)	106.5	117.4	120.0	108.4	99.3	81.5	76.4	80.0	84.1	91.8	91.2	97.5		
Adjusted potential evapotranspiration (mm/month)	107.3	108.6	124.0	110.2	106.0	84.9	81.6	84.7	84.8	94.1	89.7	98.2	1174.2	
Precipitation(mm/month)	*28.3*	*40.2*	*80.9*	*115.8*	*116.1*	*106.6*	*118.7*	*117.9*	*120.6*	*76.5*	*29.5*	*22.4*		
Extra water/water need/month	-79.0	-68.4	-43.1	5.6	10.1	21.7	37.1	33.2	35.8	-17.6	-60.2	-75.8		
Soil storage(mm)	0.0	0.0	0.0	5.6	15.7	37.4	74.5	100.0	100.0	82.5	22.3	0.0	0.0	100.0
Actual Evapotranspiration (mm/month)-AET	28.3	40.2	80.9	110.2	106.0	84.9	81.6	84.7	84.8	94.1	89.7	44.7		
Soil storage/Soil withdrawal(mm)	0.0	0.0	0.0	5.6	10.1	21.7	37.1	25.5	0.0	-17.6	-60.2	-22.3		
Runoff(mm)	0.0	0.0	0.0	0.0	0.0	0.0	0.0	7.7	35.8	0.0	0.0	0.0		
Check	0.0	0.0	0.0	0.0	0.0	0.0	0.0	0.0	0.0	0.0	0.0	0.0		
Water surplus	0.0	0.0	0.0	5.6	10.1	21.7	37.1	33.2	35.8	0.0	0.0	0.0	143.5	Total
Water deficit	79.0	68.4	43.1	0.0	0.0	0.0	0.0	0.0	0.0	0.0	0.0	53.6	244.2	Total

-8.6	MI
12.2	HI
20.8	AI

The following procedures have been used for classifying pavements into homogenous sections from deflection surveys (method adopted from Road Note 18 of TRL and Appendix D of the pavement evaluation and asphalt overlay manual of ERA).

- Using the measured pavement surface temperature plus a 5-day air temperature prior to the survey date, the temperature at the centre and bottom of the asphalt pavement layer is determined using Figure 3-1
- The mean pavement temperature is then determined as the average of the temperature at the top, centre and bottom of the pavement.
- The mean pavement temperature is then used for determining the temperature adjustment factor (F) using Figure 3-2.
- The measured deflection is then adjusted to a deflection at a standard temperature of 21^{o}c by multiplying it with F.
- The cumulative sum of deviations from mean deflection is then calculated and plotted against chainage. A section which is homogenous should generally have constant slope and whenever the slope changes another homogenous section is created. The following equation represents the cumulative sum method (TRL, 1999).

$$S_i = X_i - X_m + S_{i-1} \tag{3-8}$$

Where

X_i = Deflection at specific chainage i

X_m = Mean section deflection

S_i = Cumulative sum of the deviations from the mean deflection at chainage i

The level of homogeneity of a section is assessed using the coefficient of variation, which is the ratio of the standard deviation to the mean. In this study a preliminarily identified homogenous section is repeatedly optimized so that the coefficient of variation is within acceptable range. According to TRL (1999), if the coefficient of variation is less than 0.2, the section is in good homogeneity and if it is between 0.2-0.3 the section is of moderate homogeneity and if more than 0.3 it has poor homogeneity.

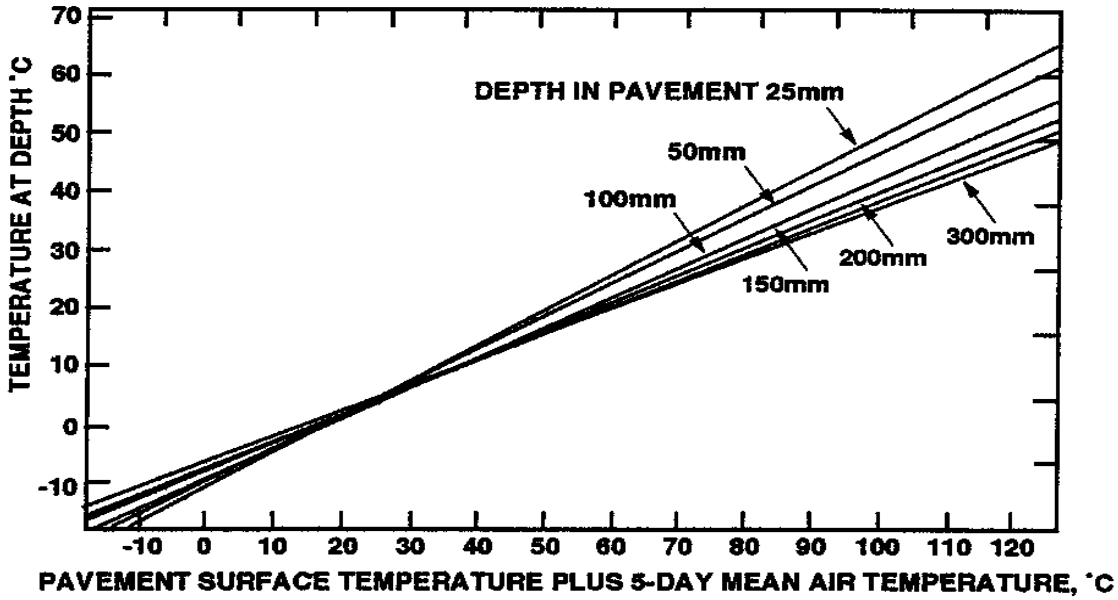

Figure 3-1 Graph for estimating pavement temerature
Source: Pavement Rehabilitation Manual, ERA (2002)

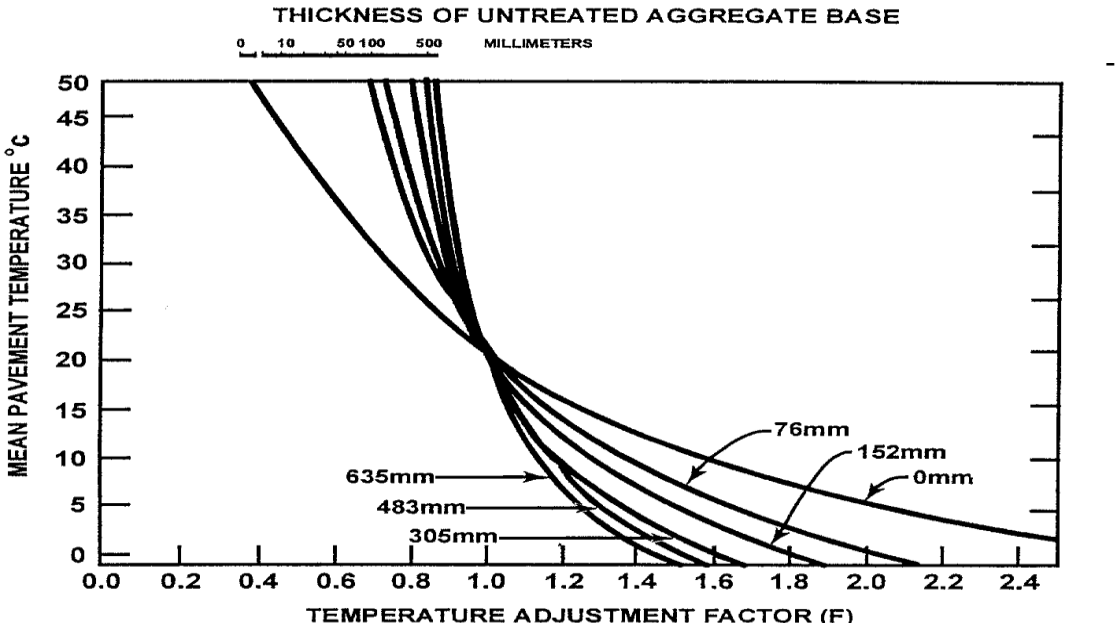

Figure 3-2 Graph for estimating temperature adjustment factor (F)
Source: Pavement Rehabilitation Manual, ERA (2002)

Figure 3-3 shows a plot of pavement strength (SNC) versus chainage, after the analysis of the data using the above procedures is completed. The horizontal lines of zero slopes are representing the homogenous sections for the Addis Ababa-Modjo and Modjo-Awasa road segments. The graph for the left and right

hand side lanes generally have a similar pattern indicating the cross-sectional homogeneity of the pavement.

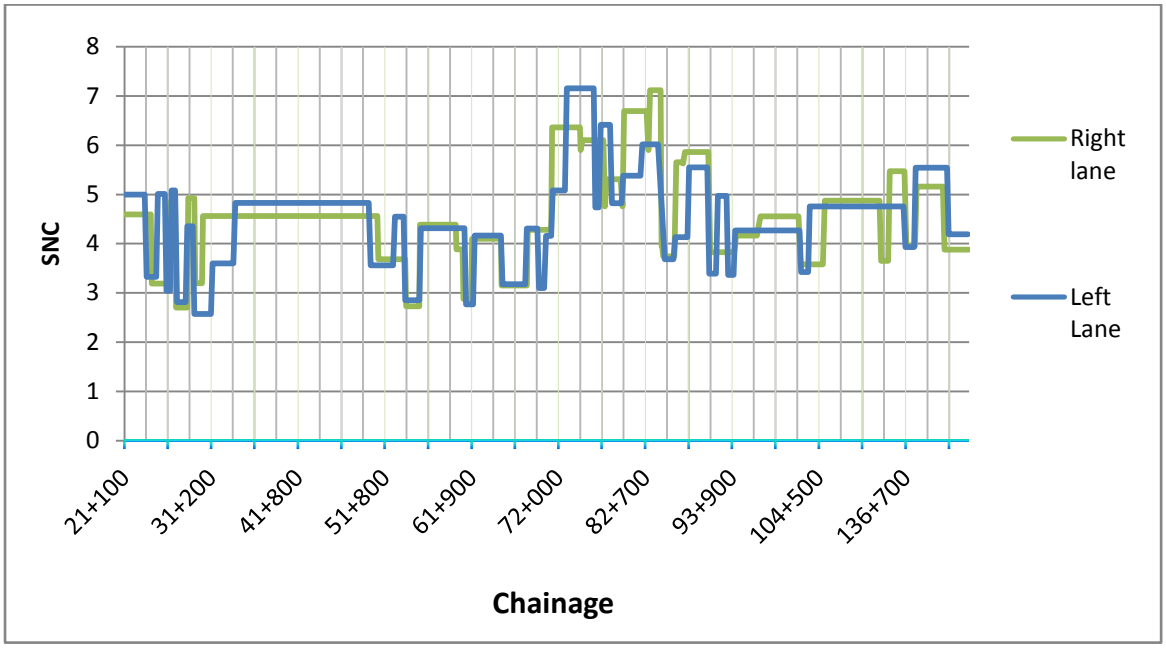

Figure 3-3 Classification into homogenous strength sections

3.4.3 **Analysis for Classification of Study Area Based on Traffic Loading**

The traffic axle loading is one of the most important input variables for any of the deterioration models. The axle loading in terms of the number of equivalent standard axle load can be estimated using the equation developed from the AASHO road test and expresses as

$$\frac{N_s}{N_p} = \left(\frac{P}{Ps}\right)^n \tag{3-9}$$

In HDM-4, n=4, P_S=8.16 ton

p = sum of axle loads for each class of vehicle

The right hand side of the equation represents the vehicle equivalence factor (EF) or damaging factor for each class of vehicle. The number of applications of axle load N_p expressed in terms of the number of applications of Standard axle N_s, will then be given by $N_s = N_p\left(\frac{P}{8.16}\right)^4$. N_p for a period of one year will be the average annual daily traffic multiplied by 365 days. Table 3-4 shows the damaging factor of vehicles operating in the study area after analysis of the axle

load survey data. The damaging factor of cars, land rovers and small buses of less than 12 persons loading capacity are negligible and hence are excluded from the calculation.

Table 3-4 Damaging factor of vehicles in the study area

Type of Vehicle	**EF(Addis-Modjo)**		***EF(Modjo-Awasa)***	
	Modjo Bound	**A.A bound**	**Awasa Bound**	***Modjo Bound***
SB	0.04	0.04	0.06	*0.054*
MB	0.67	0.67	0.70	*0.58*
Large Bus	1.96	1.96	2.04	*1.42*
Small Truck	0.21	0.21	0.20	*0.34*
Medium Truck	0.58	1.59	1.77	*1.27*
Heavy Truck	2.38	6.49	2.24	*8.34*
Truck Trailer	*4.84*	*13.16*	*15.25*	*1.6*

Source: Analysis of data from Metaferia and Omega &Metaferia and Spice (2009)

The damaging factor of vehicles operating on Modjo-Addis Ababa, Modjo-Awasa and Awasa-Modjo road segments had been calculated from axle load surveys conducted in each road segment in the year 2008. The axle load survey of Modjo bound traffic of the Addis-Modjo road however was not conducted because the consultant decides to design the pavement structure using the heavy load in either of the two direction, which in this case is the Addis bound traffic . The origin and destination survey of the same study, however, indicated that 68% of trucks leaving Addis Ababa are empty while 25% of trucks coming to Addis Ababa are empty. It is therefore reasonable to assume that the damaging factor of the Modjo bound traffic is $(\frac{25}{68})$ of the truck damaging factor of Addis bound traffic. This actually represents the reality because the import to export ratio for the country is nearly 75%:25%. From the experience, the damaging factor of buses and small trucks will generally be similar in both directions. Once the damaging factor is established then the annual equivalent standard axle load is calculated by multiplying the damaging factor by the annual traffic volume of each vehicle class.

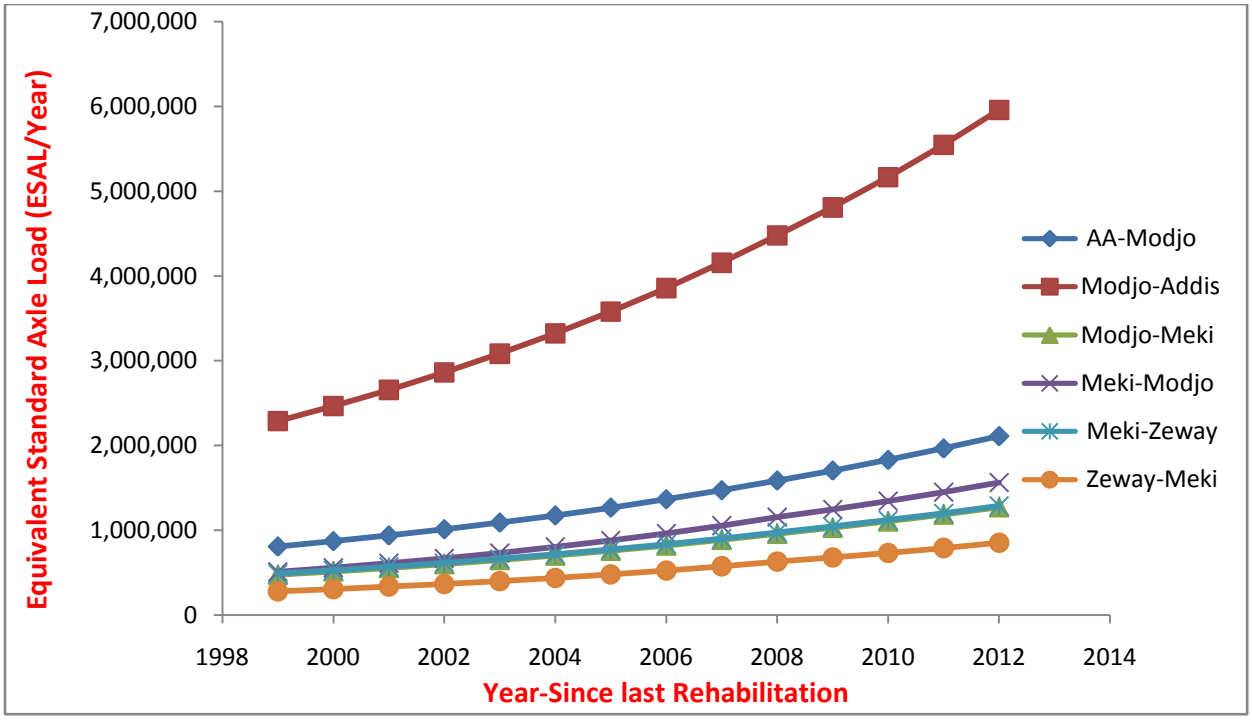

Figure 3-4 Annual equivalent standard axle load (ESAL/lane/year)

From Figure 3-4 Addis bound lane of the Addis-Modjo road is the most heavily trafficked road due to the imports from Djibouti port followed by Modjo bound lane of the same road due to the exports. Modjo bound lane of the Modjo-Meki road is the third heavily loaded primarily contributed by heavy trucks transporting river sand from Meki area to construction sites in Addis Ababa.

Based on the annual axle loading rate of Figure 3-4, the study area is divided into the following homogenous sections

Debrezeit (km 24) –Modjo (km 71)

Modjo (km71)-Meki (km 131)

Meki (km 131)-Ziway (km 159)

3.4.4 Classification of the Study Area Based on Pavement Condition

Pavement condition has been evaluated based on the severity and extent of rutting and cracking as recommended by the pavement rehabilitation manual of ERA. The condition survey conducted in 2008 by consultants hired by ERA has been used for this purpose. An evaluation of the condition survey showed that for Addis Ababa-Modjo road segment, it is well quantified by severity and extent of

cracking and rutting and it was possible to estimate the global visual index (I_S) from a matrix of cracking and rutting ratings contained in the Pavement Rehabilitation Manual of ERA (2002).

According to the manual I_S rating of 1 and 2 indicates that the pavement is in good condition and no maintenance is required. An I_S rating of 3 and 4, represents medium surface condition enough to trigger maintenance and an I_S rating of 5, 6 or 7 implies that the surface is in poor condition requiring major maintenance or rehabilitation. Though complete Field condition survey data was not available for the whole study area. Table 3-5 shows the result of the analysis of the Addis-Modjo road segment of the study area.

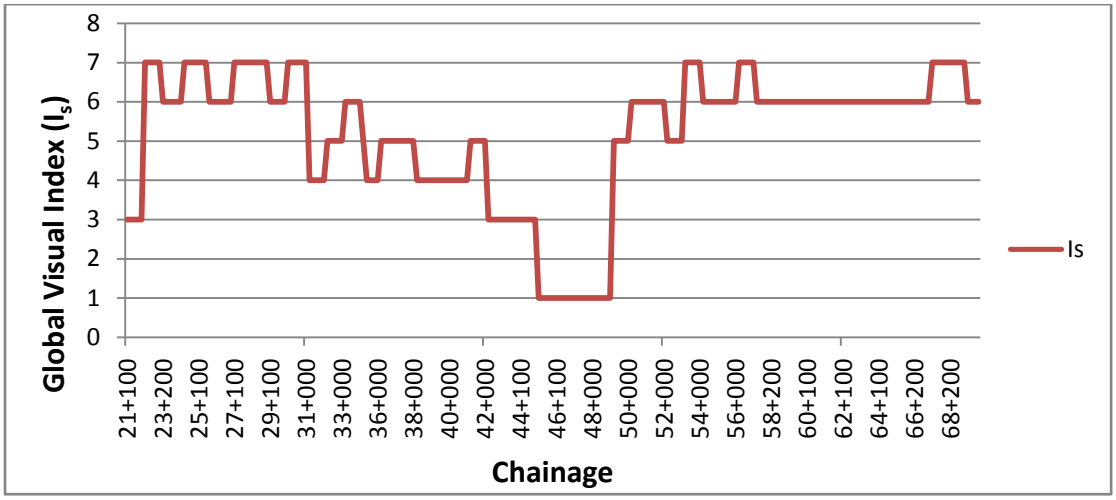

Figure 3-5: Global visual index (I_S) rating of Addis-Modjo road segment

Table 3-5, the section between chainage 42+000 and 50+000, is in perfect surface condition. The section between chainage 22+000- 31+000 and between 54+000-70+000 is in very poor surface condition. The condition shows a very strong correlation with pavement strength (SNC). When Table 3-5 and Figure 3-3 are compared very good surface condition is correlated with high pavement strength and vice versa.

3.1.4 Matrix of Calibration Sections

Once the study area is classified according to climatic zones, pavement strength, traffic loading and pavement surface condition, sample calibration section are picked from a matrix built using the following criteria. In each climatic zone and in

each of traffic loading regime sections are picked having characteristics included in Table 3-5.

Table 3-5 Calibration Section Identification Matrix

Pavement characteristics	**criterion**		
	Strength	**Condition**	**Drainage**
Strong pavement, good surface condition	SNC>5	rating 0-1	
Strong pavement, poor surface condition	SNC>5	rating 2-3	
Strong Pavement, good drainage condition	SNC>5		rating 0-1
Strong Pavement, poor drainage condition	SNC>5		rating 2-3
Weak pavement, good surface condition	SNC<3	rating 0-1	
Weak pavement, poor surface condition	SNC<3	rating 2-3	
Weak Pavement, good drainage condition	SNC<3		rating 0-1
Weak Pavement, poor drainage condition	SNC<3		rating 2-3

Table 3-6 show locations in the study area meeting the criterion of Table 3-5.

Table 3-6: Matrix of Calibration Sections

Sub-humid/Tropical Environmental Zone			
Pavement strength and surface Condition	**Homogenous traffic loading sections (km)**		
	Addis-Modjo	**Modjo-Meki**	**Meki-Zeway**
Strong pavement, good surface condition	48-49	74-75	148-149
Strong pavement, poor surface condition	51-52	82-83	
Strong Pavement, good drainage condition	46-47	75-76	
Strong Pavement, poor drainage condition		96-97	138-139
Weak pavement, good surface condition		93-94	136-137
Weak pavement, poor surface condition	55-56	85-86	
Weak Pavement, good drainage condition	67-68	91-92	
Weak Pavement, poor drainage condition	62-63	102-103	

3.5 Preliminary Field Studies, Requirements of HDM-4 and Constraints

Once the above matrix of calibration sections were identified at the desk study level, a preliminary field study was undertaken to see if all the conditions match to the actual condition on the ground. Though the preliminary site investigation shows that the conditions established based on the data collected four years ago in 2008 are generally acceptable, other important factors have to be considered. Some of the important factors considered were

- Availability of a permanent section referencing
- Requirements of HDM-4, specific to each distress type
- Limited time and resources to conduct the field measurement specifically that of deflection measurement
- The need to avoid the town sections and other officially restricted locations
- The need for original pavement surface, as maintenance complicates the estimation of the initiation time of a distress and affects the extent and severity of a distress.

3.6 Availability of a Permanent Referencing

The presence of a permanent referencing is very important while doing the field measurement and for future monitoring of pavement conditions of the calibration sections. For this study the pavement sections are referenced using available kilometer posts.

3.7 Specific HDM-4 Requirements

Table 3-8 shows a summary of specific criteria for identifying calibration sections for each of the deterioration models which is adopted from the HDM-4 calibration manual of Bennett and Paterson (2000).

3.8 Selected Calibration Sections

After scrutinizing and analyzing the historical data and after the initial field study and taking into consideration of the HDM-4 specific requirements, three road segments consisting of two sections of 1-1.2 km length on both lanes of the opposing traffic have been selected. This means that each section consists of

two sections (left side and right side lanes) where measurements are taken on both sides exactly at the same chainage. The evaluation on both lanes of the road was planned to see the effect of the different level of directional traffic loading on the pavement performance.

It should be noted that according to the HDM-4 calibration manual, specific calibration sites meeting the requirements of each distress type is recommended. While this requirement improves the quality of the calibration, it was not possible to include geographically different sites representing the different spectrum of climate, age, strength, environment and pavement conditions. However, the study area is carefully selected so that the sites represent different ages, though of narrow range, different traffic loading, different pavement strengths and different pavement surface conditions.

One of the problems with identifying calibration sections is the requirement to select sites exhibiting a specified extent of distress (example site with area of cracking of less than 5%) or a certain level of pavement strength (strong, medium or weak) pavements, which was not possible to specify before the actual field measurements were made.

It should also be noted that the manual is basically for calibrating the deterioration model for a region or a country, which probably has more than two climatic zones. The sites were carefully selected to meet the requirements of each deterioration model and based on the discussions and analysis running from items 3.4 through 3.7.

Table 3-7 show the selected three pavement segments and the exact chainage of sections.

Table 3-7 Location of Selected Calibration Sites

Name of segment	**Designation**	**Sections(chainage)**	**Referencing**
Addis-Modjo	Segment 1	52+000-53+200(R)	Km post 52
		52+000-53+200(L)	
		55+200-56+200(R)	Km post 55
		55+000-56+200(L)	
		82+000-83+200(R)	Km post 82

Name of segment	Designation	Sections(chainage)	Referencing
Modjo-Meki	Segment 2	82+000-83+200(L)	
		86+800-88+000(R)	Km post 88
		86+800-88+000(L)	
Meki-Zeway	Segment 3	135+000-136+000(R)	Km post 135
		135+000-136+000(L)	
		136+000-137+000(R)	Km post 137
		136+000-137+000(L)	

3.9 **Field Data Collection**

Once the calibration sites were selected the next step was the preparation for field data collection. This required preparation of the methodology for field data collection and discussion with the ERA on the arrangements for the Benkelman beam and the laser based automatic condition survey vehicle, where both equipment were provided to the research for free. After all the necessary preparations, the field data collection was conducted from 8^{th}-10^{th} of September 2012. The month of September, which is the end of the rainy season of the study area, represents the pavement's weakest strength level.

Table 3-8 HDM-4 calibration site selection requirement versus actually adopted

Distress type	HDM-4 Requirement	Peculiar of the Study area
Roughness from Environment	Two to four climatic zones 3 to 10 pavement segments each of 5 km long Pavement age after the last rehabilitation/reconstruction/construction, greater than 10 years Recommended interval of 100m	One climatic zone 3 pavement segments consisting of two sections of 1.2km on both lanes 12 to 14 years Every 10m
Cracking Initiation	Stratification based on climate and pavement type 15 pavement sections of 300m length each with low cracking(<5% area of section area), or medium cracking(between 5 and 30% of section area cracked) Inputs Surfacing age(years), percentage area of all cracking(more than 1mm width), Percentage area of wide cracking, traffic loading, pavement strength, pavement thickness	One climate group The requirements are met, though many of them tend to be medium to high cracking area due old pavement samples All are collected, except the distinction between wide and narrow cracks which is difficult to identify from pavement cameras

Cracking Progression	Stratification based on climate and pavement type 15 pavement sections of 300m length consisting of medium cracking (between 5 and 30% of section area cracked) and high cracking extent (>30%) Inputs Surfacing age(years), percentage area of all cracking(more than 1mm width), Percentage area of wide cracking, traffic loading, pavement strength, pavement thickness	One climate group, AC on GB type of pavement The requirements are met, though many of them tend to be medium to high cracking area due old pavement samples All are collected, except the distinction between wide and narrow cracks which is difficult to identify from pavement cameras
Rut depth Progression	30 pavement sections of about 200 m length each with medium to high mean rut depth(>6 mm).50% of the sections shall be thin surfacing(<50mm) and 50% of them thick(>50mm) Inputs Mean and standard deviation of rut depth, explanatory variables of SNP, YE4, COMP, ACX, HS etc.	All sections are thickness of 100 AC

The data collected during this period include Benkelman Beam defection, laser based roughness and rutting measurements, cracking measurement from automated video recording. A manual condition survey was also conducted as confirmatory to the data collected using the automated condition survey vehicle. The process of data collection was stated as follows

3.9.1 Deflection Measuring Equipment and Procedure

The pavement strength was determined from deflection measurements using Benkelman Beam on the calibration sections established earlier.

The Benkelman Beam is a device that measures the maximum deflection of a road pavement under the dual rear wheels of a slowly moving loaded lorry (TRL ORN 18, 1999). As further explained in the TRL (1999) and Paterson (1987) the maximum deflection (sum of vertical strains) is a good indicator of the overall strength (stiffness) of a pavement and has been shown to correlate well with long term performance of a pavement under traffic. The applied rear axle load varies with different institutions, for example while 63.2KN axle load is recommended by TRL, in the Brazil-UNDP HDM Study 80KN axle load has been adopted. For this study a six wheel loaded truck with the rear axle of 8.16 ton has been used.

The measuring equipment

The following equipment has been used for measuring deflection

- Benkelman beam
- Six wheel truck loaded with crushed stone
- thermometer
- Pick up truck
- Hammer and nails
- Weigh bridge

The Benkelman beam consists of a slender pivoted beam of approximately 3.7m long supported in a low frame which rests on the road. The frame is fitted with dial gauge which register the movement at one end of the pivoted beam.

ERA pavement rehabilitation manual (ERA, 2002) requires that the six wheel lorry have a capacity of at least 4.5 tons and should be fitted with twin rear wheels having a space of 50 mm between the tires. The lorry should be loaded so that the rear axle load measures 8.16 tones (i.e. 4.08 tons on each pair of twin rear wheels). The ERA manual also recommends a tire size of 10 by 20 and the tires should be inflated to a pressure of 552 KPa. The use of tire with tube and ply is recommended.

The pavement and air temperature are measured using a Standard Iron-Constantan thermocouple wire and a temperature potentiometer.

A pickup vehicle was used to cordon the Benkelman Beam and loaded truck from the heavy traffic flow in the direction of measurement. In addition to the pickup, traffic was diverted from the lane under measurement using two persons wearing reflective jackets. Figure 3-6 show the measurement of deflection on the Addis-Modjo segment of the study area.

Figure 3-6 Deflection measurement using Benkelman Beam on Progress

Measurement Procedure

The procedure of measurement is adopted from ERA pavement rehabilitation manual, (2002) and TRL (1999)

- The Six wheel truck is loaded with crushed stone and rear axle load measured at the nearby stationary weighbridge. It involves adjusting the load by adding or removing some of the loaded materials until the rear axle loading reads 8.16 tons on the scale. The truck is then mobilised to the study area. Before commencing the measurement the tire pressure is measured with tire pressure gauge.
- Once mobilised to the study area a point is marked on the outside wheel path at which the deflection is to be measured and the dual wheels of the lorry are positioned at the centre of the marked point. The Points are generally positioned 0.9m from the edge of the pavement which is the recommended offset for lane width of more than 3.35m.
- The deflection beam is inserted between the twin rear wheels until its measuring tip rests on the marked point.
- The foot screws are adjusted to ensure that the frame is level and that the pivoted arm is free to move. The dial gauge is adjusted to zero and the buzzer is turned on.
- The final reading of the dial gauge is recorded after the lorry is driven slowly forward to a point at least 5m in front of the marked point.

The pavements surface temperature is measured using the following procedure

- A small hole of 3 mm depth and 3 mm in diameter is dug using a hammer and nail at a point approximately 254 mm from the edge of the pavement
- The hole is filled with water or asphalt. The thermocouple wire bent at right angles 5 mm from the end is inserted into the 3 mm deep hole filled with the water
- The pavement temperature is then measured using the temperature potentiometer. At this time the air temperature is also recorded.

Figure 3-8 and Figure 3-7 show the traffic management and Benkelman Beam deflection measurement on progress.

Figure 3-8 Traffic management during measurement

Figure 3-7 Adjusting the Benkelman in preparation for measurement

3.9.2 Pavement Condition Data Collection

In addition to traffic, pavement strength and pavement history the condition of the pavement is one of the input parameters for calibrating the HDM-4's pavement deterioration models. As discussed in the literature review cracking, ravelling, potholing, rutting and roughness are the most important distresses modeled in HDM-4 for flexible pavement. All the distresses except ravelling will be considered in this study. Ravelling is not a common distress for asphalt Concrete (AC) surfacing and hence will not be considered in this study.

Two methods were used for collecting pavement condition data.

1. ARRB automated condition survey vehicle
2. Manual condition survey

3.9.2.1 ARRB Automated Survey Vehicle and Data Processing Tool Kit

The ARRB automated survey vehicle of Fig. 3.9, adopted from ARRB Survey Manual (2009), was used to collect pavement condition data on roughness, rutting, cracking and side drainage. The survey vehicle is equipped with data acquisition and processing software packages known as HAWKEYE SERIES 2000 and is developed by the Australian Road Research Board (ARRB).

The measurements were conducted on the 10th of September 2012 on the previously established sections after Benkelman Beam and manual condition surveys were completed.

The data acquisition package consists of hardware units and software modules for capturing and syncronzing data from the various survey packages(ARRB, 2009). The data aquisistion package consists of the following units

- GPS Package for collecting data on the position(coordinates) of the survey vehilce at any location along the survey
- Gipistrac geometry package for collecting road geometry
- Video package for collecting videos of the pavement surface and the road side features.
- Distance package for measuring distance along the survey direction
- Profiler package for collecting road surface profile using light lasers

Figure 3-9: ARRB Automated Survey Vehicle

By a combination of the above survey packages pavement condition data was collected at the specified position when the vehicle is driven at a speed up to 110km/h. The vehicle is also equipped with a computer screen for displaying the position, distance, video, rutting (transverse profile) and roughness (longitudinal profile) of the pavement surface and the road side features while making the survey.

The computer is also equipped with keyboard for recording references, special events and a speech system to warn if the vehicle is operated outside a specified speed range in this case a speed less than 30 km/h and more than 110km/h.

Figure 3-10, adopted from ARRB Hawkeye Survey Manual (2009), provides the main graphical user interface for the Hawkeye 2000 acquisition system. Most acquisition tasks, and some calibration tasks, can be performed from within Onlooker Live (ARRB, 2009).

Figure 3-10 Onlooker Live View

For this study once the data was collected from the field, and then it was processed with its processing toolkit for reporting. The information on rutting and roughness was automatically outputted using algorithms included in the processing toolkit. The data on cracking area and potholes, however, were measured by manually evaluating each photo frame of roughly 2mx2m wide. The following briefly describes the processes of data acquisition and processing for each type of pavement distress.

Roughness

Roughness is calculated from longitudinal profiles measured using two lasers located above the left and right wheel paths. Once the profile is measured it is then processed to IRI through inbuilt software and reported as left wheel path, right wheel path, average IRI and lane IRI. The average IRI is the numerical average of the left and right wheel paths, the lane IRI on the other hand is calculated from the average of the left and right wheel path profiles. Figures Figure 3-11 through Figure 3-13 show measured roughness for the three segments of the study area.

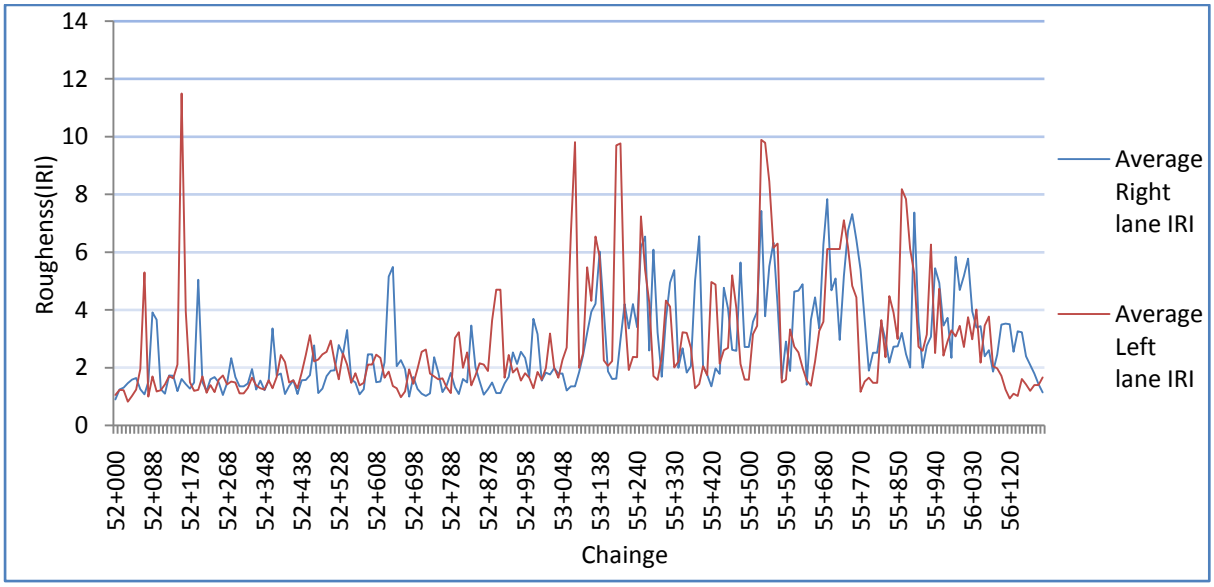

Figure 3-11 Addis-Modjo road segment measured roughness

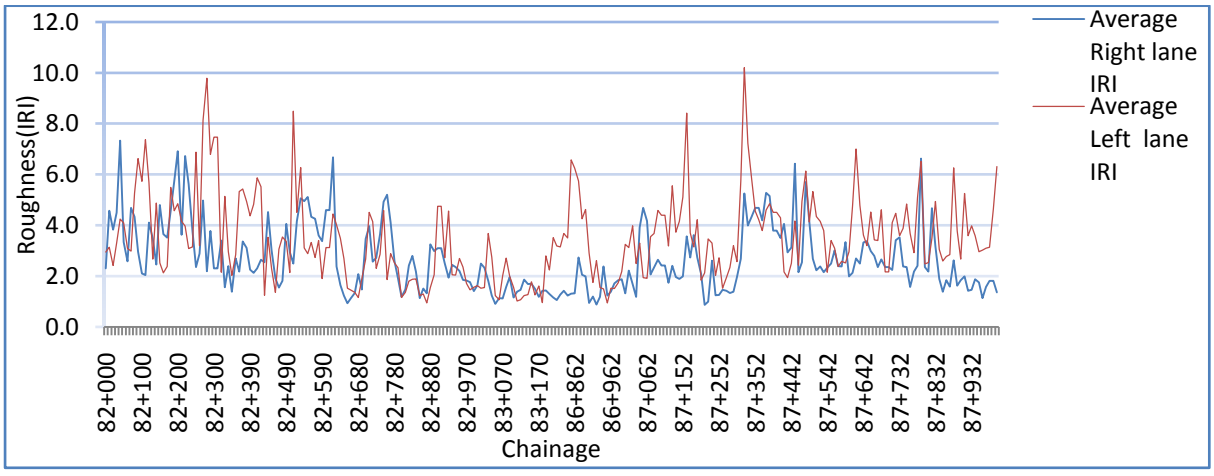

Figure 3-12 Modjo-Meki road segment measured roughness

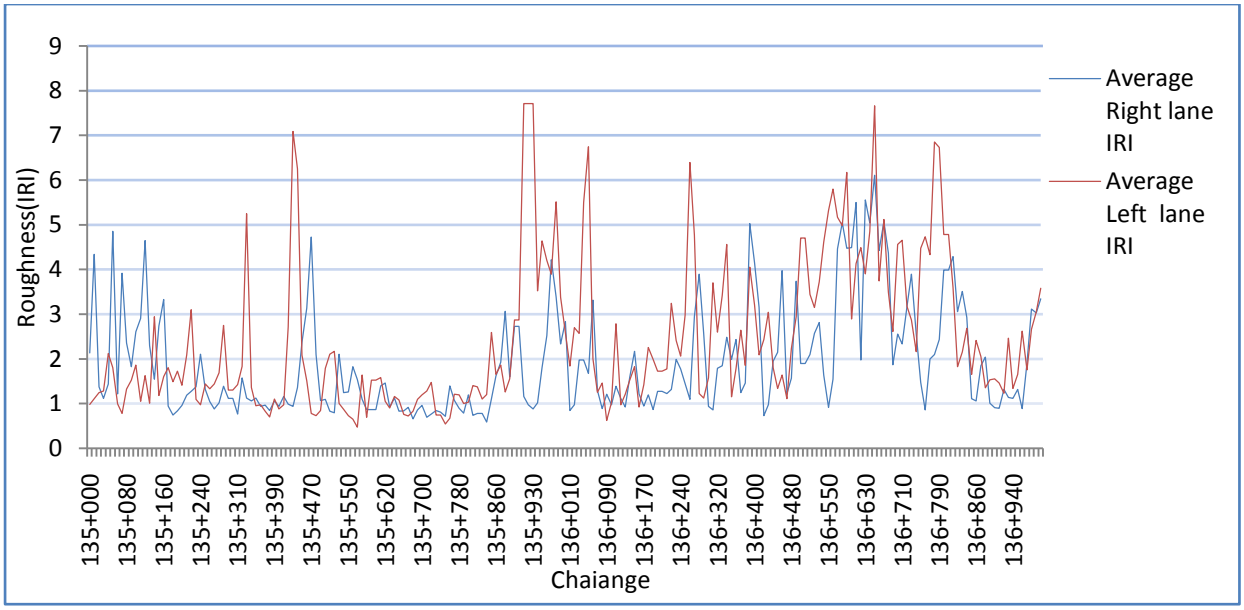

Figure 3-13 Meki-Zeway pavement segment measured roughness

Rutting Measurement

Laser sensors placed under the front body of the vehicle are used to measure road transverse profile from which rutting of left and right wheel paths and the lane rutting which is the maximum rutting of the lane is calculated. While processing the profile data for rutting using the inbuilt software, the simulation for straight edge of length 1.2m, 2m or 3m was selected. The rutting measured under a 1.2m straight edge has been used as input for HDM-III model prediction but for HDM-4 input a 2m straight edge is used and hence the rutting in this study is simulated from a profile using a 2m straight edge. Figure 3-14 to Figure 3-16 show results of the rutting measurement for three road segments considered in the study.

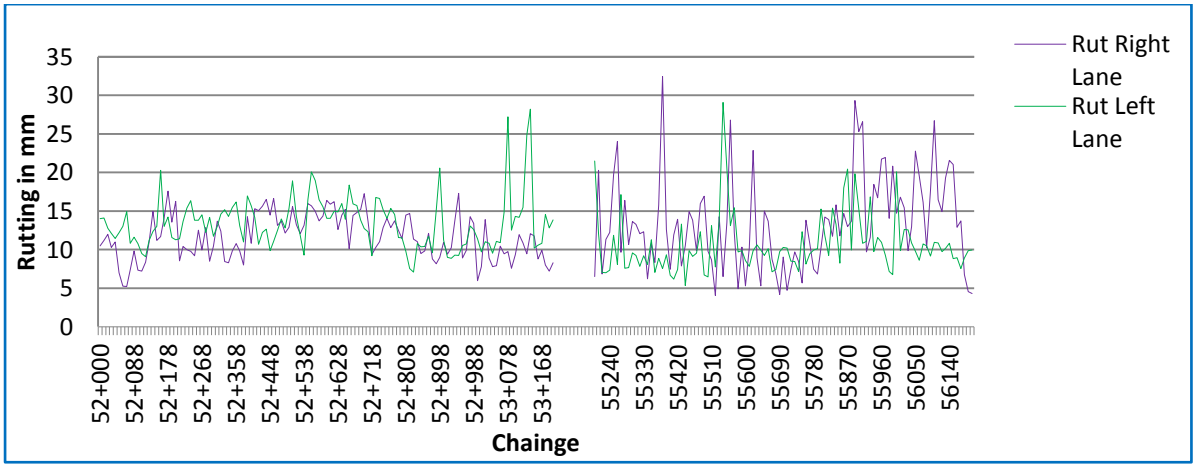

Figure 3-14 Rutting of Addis Ababa-Modjo road segment

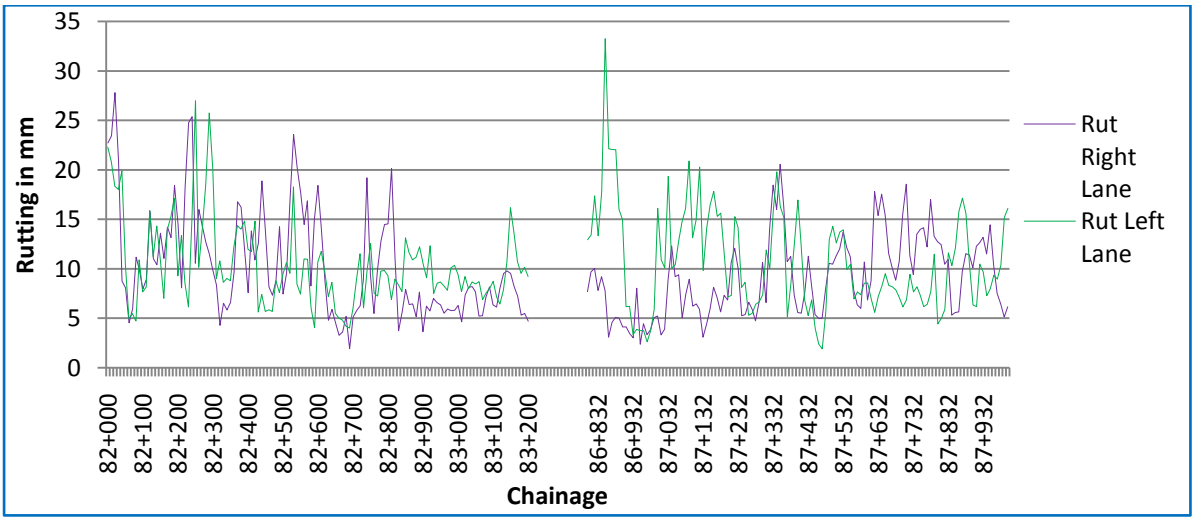

Figure 3-15 Rutting of Modjo-Meki road segment

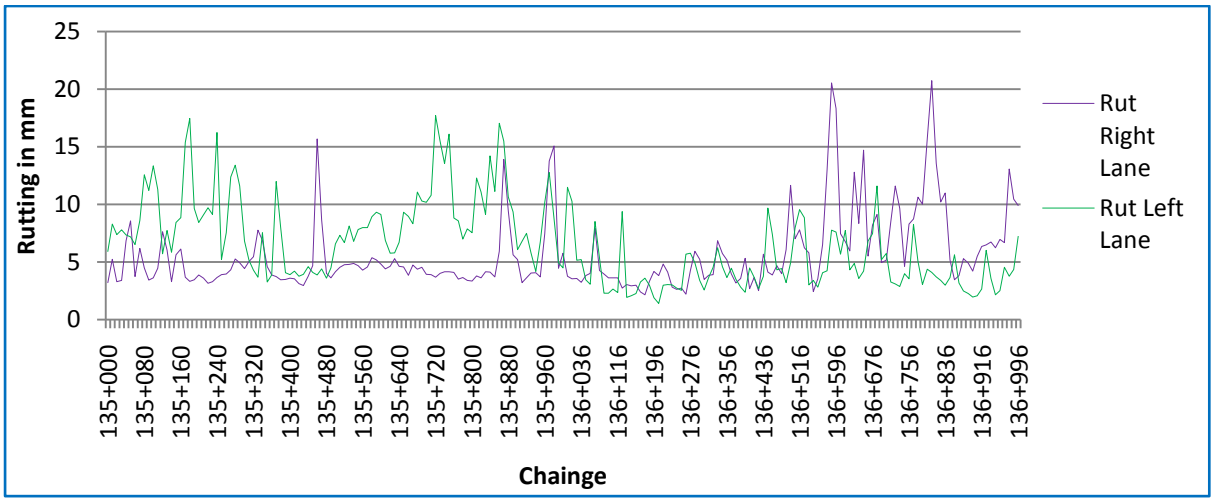

Figure 3-16 Rutting of Meki-Zeway road segment

Cracking Measurement

The video package of the Hawkeye surveying vehicle is equipped with two types of cameras. One set known as asset camera is fixed at the front roof of the vehicle and records what is visible ahead including the road facility and the surrounding environment. The second set known as pavement camera is equipped with two cameras located at the roof of the rear of the vehicle aligned to the left and right wheels of the vehicle. The video data collected from both the left and right pavement cameras is reduced into photo frames of approximately 2m wide and 2m in the direction of the survey. Each photo frame is evaluated

using the processing toolkit for cracking area and potholes and all cracked area is measured manually and saved. When the section being evaluated is completed the measured cracked area and numbers of potholes were exported into a spread sheet to be summed per required section length. The process of measuring cracked area was very tedious involving evaluating about twelve thousand photo frames. Table 3-9 shows a sample of the long spread sheets exported after evaluation of the photo frames.

Table 3-9: Sample spread sheet from HAWKEYE Processing Toolkit

Road Segment: Addis-Modjo					**Direction: Modjo Bound**	
Chainage: 55+000-56+200					**Pavement Camera: Right**	
Section	**Distance from Addis (m)**	**Chainage**	**Photo Frame Number**	**Area of narrow cracking (m^2)**	**Area Wide Cracking (m^2)**	**Area of all cracking (m^2)**
CRACKING SECTION 1	31530	55+200	55077	0	0	0
	31533	55+203	55080	0.4	0	0.4
	31535	55+205	55081	0.4	0	0.4
	31538	55+208	55084	0.15	0	0.15
	31539	55+209	55085	0	1.77	1.77
	31540	55+210	55086	0	2.67	2.67
	31541	55+211	55087	0	2.22	2.22
	31542	55+212	55088	0	1.62	1.62
	31543	55+213	55089	0	2.22	2.22

The percent cracked area is then calculated by dividing the total cracked area in the section by the lane area of the section multiplying by 100.

The video from the asset camera was used for approximately locating the start and end of the section to be evaluated. The exact location was then determined by finding markings placed at the edge of the pavement prior to the start of the survey. Figure 3-17 show a sample photo frame evaluated for area of cracking, which is exported from HAWKEYE processing Toolkit.

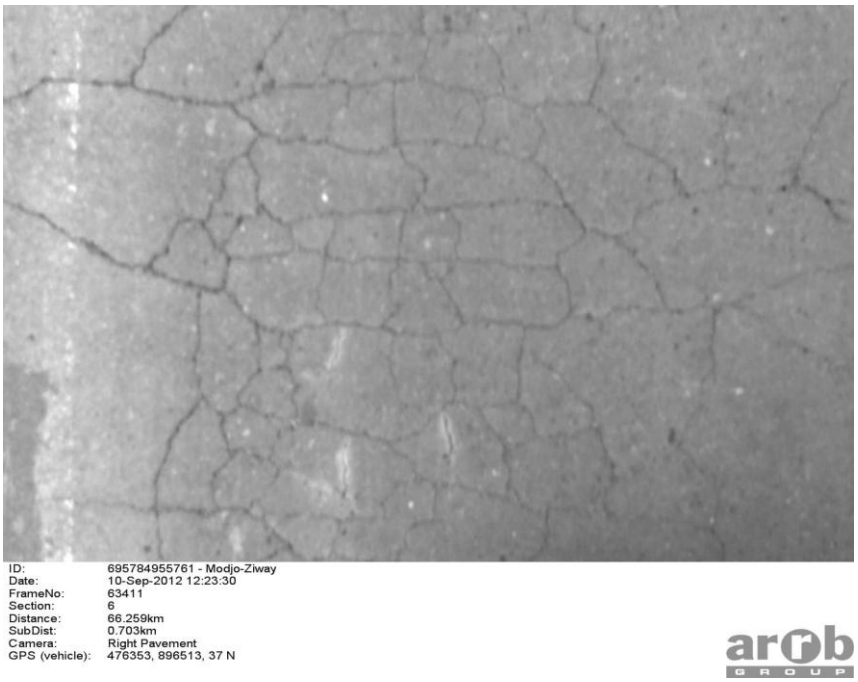

Figure 3-17 Photo frame captured with ARRB Hawkeye survey vehicle

3.9.2.2 Manual Field Condition Survey

While the depth of rutting, area of cracking, number of potholes for this study was basically collected using the Hawkeye equipment, visual condition survey and manual rutting measurement were conducted for confirmatory purposes. One of the basic problems to make detailed measurement of rutting, cracking and potholing was the difficulty of traffic management at the study area, especially that of Addis Ababa-Modjo road is the most heavily trafficked route in Ethiopia, and where it was not possible to close traffic just for few minutes as traffic jam quickly builds up.

- Therefore while it was planned at the beginning to conduct rutting depth measurement on the two wheel paths of a lane at an interval of 10 m as recommended in the HDM calibration manual due to the above difficulty only at 50 m interval on the outside wheel path of the lane was measured.
- The rutting depth was measured using a 2.0 straightedge which is a standard length in the HDM-4 model
- Area of cracking, size and number of potholes were estimated visually while walking by the side of the road.

- Side drain condition was also assessed while walking by the side of the road.

Figure 3-19 and Figure 3-18 show the visual condition survey and Manual rutting measurement on progress.

Figure 3-19 Visual estimation of cracking area

Figure 3-18 Rut depth measurement

3.9.3 **Traffic Study**

The traffic survey after rehabilitation collected from the design consultants and from historical traffic records of ERA was used as the basis for the determining the traffic volume and axle loading. The traffic data has been used to determine the 8th year annual number of all vehicle axles (YAX) and annual number of standard axle load (YE4) which is required inputs for the deterioration models. Detailed calculation for the 8th year traffic loading and the historical traffic volume are contained in Appndex-2

Chapter 4. Data Analysis and Results

4.1 Introduction

With the general objective of calibrating the HDM-4 road deterioration models, data on model inputs and current level of distress has been collected as discussed in chapter three and analyzed in this chapter. Once the data was prepared in the format to be accepted by the model, the output of the model was compared with the actual distress level for a level two calibration of the models. The objective of the level two calibrations is not either to adjust the model parameters or develop a new model, but rather to scale the model predictions to the actual level of deterioration assuming the model prediction is correct.

4.2 Preparation of Model Input Data

In chapter three the analysis of some of the input data like the climatic classification and the traffic loading of the study have been conducted in the process of identifying the calibration sections. The method of analysis for pavement strength classification has also been discussed in the same chapter. In chapter 3, it was necessary to analyze historical data for pavement strength classification of the study area and the process is repeated here because a new deflection data set was collected in this study.

4.2.1 Analysis of Pavement Strength of the Calibration Sections

Once the raw rebound deflection, which is twice the measured deflection is calculated for each data point in the calibration sections then it is adjusted to a deflection at a standard temperature of 21°c by applying temperature adjustment factor (F) read from Figure 3-2. The temperature adjustment factor is a function of the predicted pavement temperature, which is the average of the measured surface temperature, predicted mid depth and bottom temperature of the bituminous layer of the pavement. The 5 day air temperature prior to the deflection survey could not be obtained from the meteorological agency, but from historical records of the study area the average temperature for the month of September, the month of field survey, ranges between 18 and 21°c, where 20°c could be taken as representative.

Figure 4-1, Figure 4-2, Figure 4-3 show plots of the final deflections for the three segments of calibration sections, where each segment consists of two 1-1.2 km long sections. Each section again consists of left and right lanes; purposely set to determine the influence of different traffic loading on level of pavement deterioration of each lane.

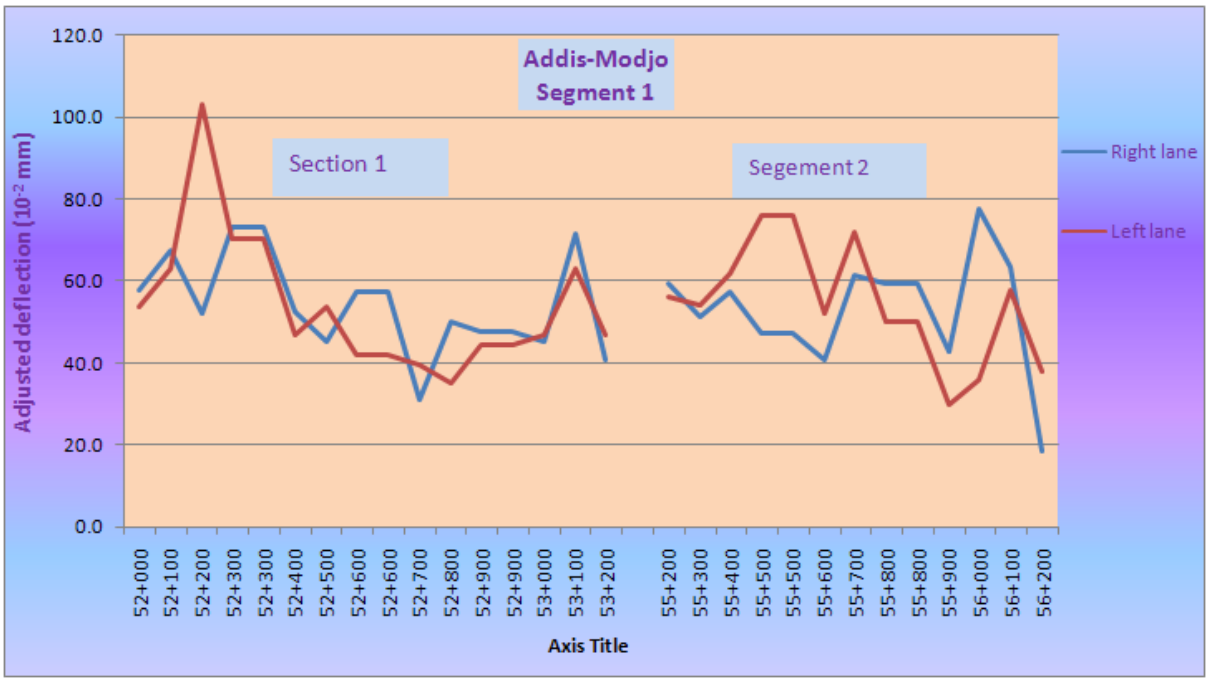

Figure 4-1: Corrected deflection for Addis-Modjo road segment

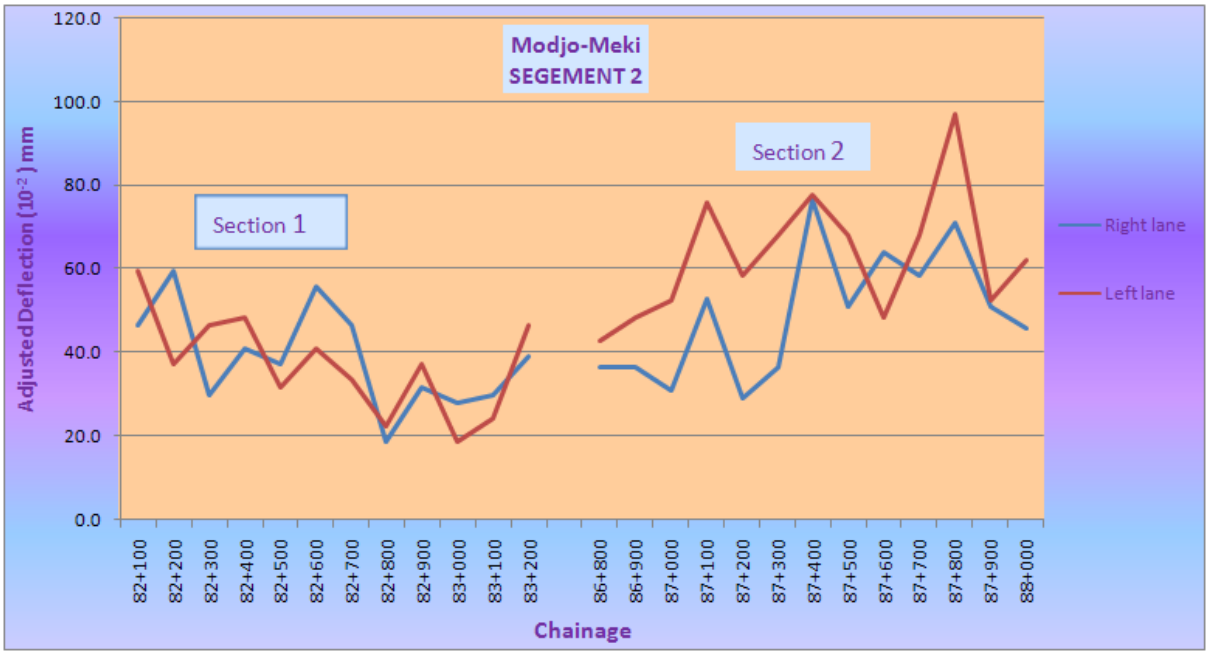

Figure 4-2 Corrected deflection for Modjo-Meki road segment

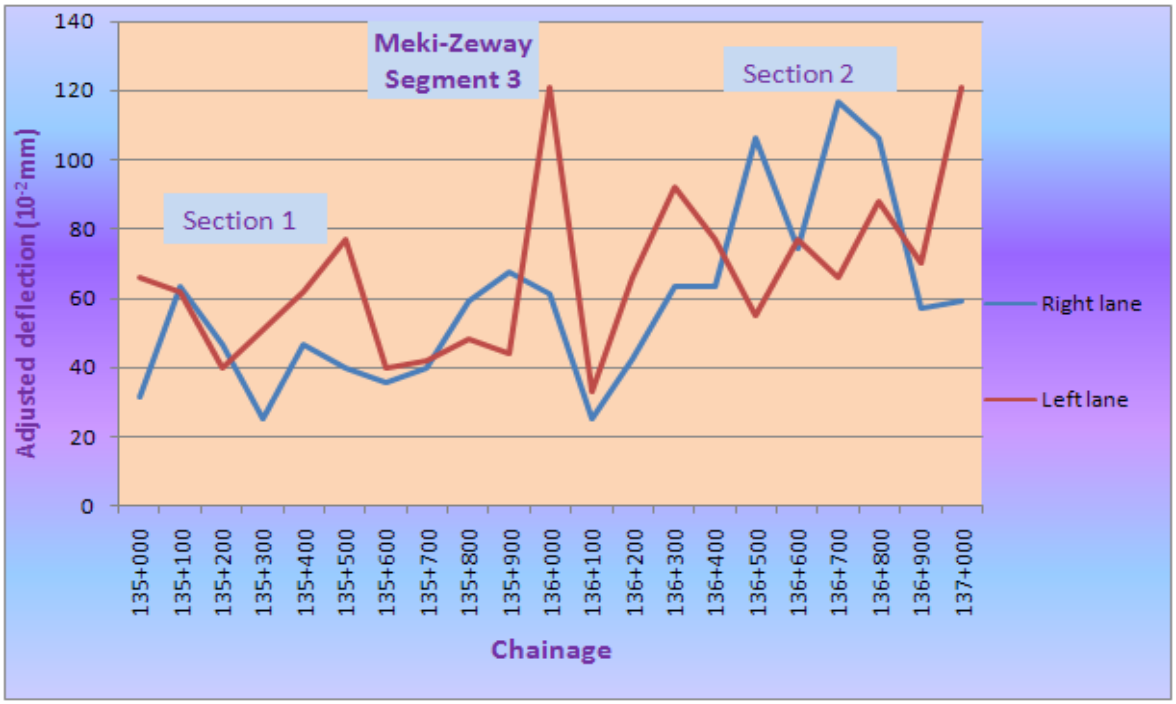

Figure 4-3 Corrected deflection for Meki-Zeway road segment

In the HDM-4 road deterioration models the average annual strength is used, so in this case the deflection was adjusted for seasonal and drainage effects. As explained in chapter three, deflection data was collected at the end of the wet season. Hence to calculate average annual strength, the dry season deflection had to be either measured in the field or estimated using available models. After the deflection data was converted into structural number (SNC) using equation (2-8), equations (2-9) to (2-11) were used to calculate the annual average strength as a function of the wet to dry strength ratio (f) and length of dry season as a fraction of the year (d). In order to calculate the wet to dry strength ratio (f), from a one season structural number, equation (2-11), which is a function of the area of cracking, potholing, the drainage factor and the mean monthly precipitation(MMP) was applied. Table 4-1 shows the mean monthly precipitation (MMP) of three towns located within study road segments.

For the calculation of wet to dry strength ratio (f), the MMP of segment one was taken the same as the records of Debrezeit and for segment two was taken the same as for Modjo and for Segment three the same as Ziway records due to their proximity. Therefore the MMP of segments one, two and three were taken as 71mm/month, 82mm/month, and 61.6mm/month respectively.

Table 4-1 Mean monthly rainfall (mm) records of towns in the study area

Town	Jan	Feb	Mar	Apr	May	Jun	Jul	Aug	Sep	Oct	Nov	Dec	*MMP*
Akaki	34	25	32	97	65	133	254	222	149	15	1	0	*85*
Debrezeit	6	0	0	58	92	77	327	155	123	13	0	0	*71*
Modjo	54	24	84	31	111	130	223	228	91	8	0	0	*82*
Ziway	*16*	*33*	*53*	*85*	*79*	*81*	*151*	*123*	*75*	*36*	*3*	*5*	*62*

Source: Metaferia and Omega, Metaferia and Spice (2009)

Figure 4-4 Side drain Condition on Addis-Modjo Road Segment

It can be seen from equation (2-9) to (2-11), the wet to dry strength ratio (f) also depends on the drainage factor, the area of cracking and the area of potholing. The area of potholing for the study is generally considered as zero and the area of cracking is the measured cracking area expressed as a percentage of the section lane area. The drainage factor depends on the quality of drainage measure provided along the section.

Site investigation of the drainage condition of the study area showed that side drainage (ditch) is not paved but generally the pavement structure is raised above the natural ground level. Figure 4-4 shows the side drainage condition of

Addis-Modjo Road segment, which is representative of the condition of the study area.

From Table C2-10 of the analytical framework of HDM-4 the drainage factor (DF), after interpolation between 1 for excellent and 5 for very poor drainage conditions, is assigned a value of 2. Detailed calculation for the average deflection and the annual average strength is included as shown in Annex 1.

4.2.2 **Traffic Loading**

The analysis of traffic loading has earlier been done in Chapter 3. According to Paterson (1987), the traffic loading rate inputted into the HDM models is the annual number of standard axles (YE4) at the pavement age of 8 years since the road was last rehabilitated/re-constructed. Table 4-2 shows the eighth year equivalent single axle loading (ESAL) rate for both directions of the three road segments selected for the study.

Table 4-2 Eighth year traffic loading for the three segments

Segment	**Traffic Bound**	**Standard axle loading in millions /lane/year (YE4)**
Addis-Modjo	Addis	2.94
	Modjo	1.0
Modjo-Meki	Modjo	0.63
	Meki	0.61
Meki-Zeway	Meki	0.36
	Zeway	0.62

Source: Analysis of data from Metaferia and Omega, Metaferia and Spice (2009)

Detailed calculation of the 8th year equivalent standard axle loading is included as annex 2 of the thesis.

4.2.3 **Materials Quality and Construction Standards of the Roads**

The quality of construction materials used for the different layers of the pavement, the method of construction say the achieved level of compaction in comparison to the nominal level of compaction determines the rate of deterioration throughout its service life. Under this topic first the specification of actual materials used for construction and then the construction standards in

relation to actual compaction achieved was discussed and the values of parameters which were inputted into HDM model were determined. Table 4-3 and Table 4-4 show the design project specification for un-bound and bound pavement layers respectively for the three road segments of the study area.

Table 4-3 Project Specification for Unbound Pavement Layers

Layer	Material Specification							*Field Density Requirements*
	Gradation by weight Passing %				LA	WI	PI	
Subgrade								*≥95%*
Sub-base	Sieve	A	B	C	≤50	≤25	≤6	
	75	100	-	-				
	38	75-85	100	-				
	25	-	-	100				
	4.75	45-65	30-70	40-80				
	0.8	15-40	-	-				*≥95%*
	0.075	0-10	0-15	5-20				
Base	75	100	-	-	≤50	≤25	≤6	*≥98%*
	63	-	100	-				
	50	70-100	80-	100				
	38	60-80	68-88	80-				
	25	50-70	53-73	60-80				
	19	40-60	35-55	50-70				
	9.5	25-45	29-49	30-50				
	4.75	15-35	17-37	20-45				
	2.07	5-25	8-28	10-30				
	0.45	0-15	0-18	5-20				
	0.075	0-10	0-13	0-10				
	Min CBR sub-base 30%, base 80%							

Source: Metaferia and Omega (2009)

In terms of field values of CBR and PI after the roads were constructed, the evaluation of engineering reports of Metaferia & Omega, Metaferia & Spice (2009) shows that the base and sub-base materials meet the minimum requirements of project specification of Table 4-3. The findings and further analysis of the achieved relative compaction and the binder content are discussed as follows.

Compaction

The project specification requirement for field density of base, sub-base and subgrade matches the requirements stated in the specification of the ERA pavement design manual. Moreover the project specification, using the actual pavement thickness of Table 1-1 meets the nominal compaction level calculated using equations (2-39).

Table 4-4 Project Specification of Bituminous Pavement Layer

Layer	Asphalt Components				*Asphalt mixture*				
	Bitumen		Aggregate Grading %Pass		Marshal Stability KN	Flow mm	Void	V.F.B	*I.R.S*
Wearing Course	Type	80/100	37.5	100	Min 6 Max 13	2-5	3-5	Max 80	*Min 75*
			25	90-100					
			12.5	56-80					
			4.75	29-59					
	Content	3.5-7	2.36	19-45					
			0.3	5-17					
			0.075	1-7					
Binder Course	Type	80/100	37.5	100	Min 7- Max 13	2-5	3-8	Max 80	*Min 75*
			25	90-100					
			12.5	56-80					
			4.75	29-59					
	Content	3.5-7	2.36	19-45					
			0.3	5-17					
			0.075	*1-7*					

Source: Metaferia and Omega (2009)

When equation (2-39) is applied at the bottom of the base layer that is Z=0.3 m give a nominal compaction of 0.98 and at the bottom of sub-base Z=0.5 m, it gives a nominal compaction of 0.95, which is exactly similar to the project specification. But the specification alone could not be sufficient and to verify the achieved compaction level data from the Metaferia & Omega (2009) had been

used to calculate the relative compaction using equations (2-39) to (2-42). Details of the calculations are included as annex three.

The calculated weighted average relative compaction (COMP) of all the non-bound layers for the study area becomes 96%. This is due to the fact that all base layer samples meet the nominal compaction, but sub-base and capping layers fall short of meeting the nominal compaction. Therefore the study area's relative compaction (COMP) according to Table C2-12 of the HDM-4 analytical framework manual could be classified as full compliance in some layers, having a value of 95%. It should be noted that the analysis is based only on data from Metaferia & Omega (2009) for the Addis-Modjo segment because the results of compaction for Modjo-Meki and Meki-Zeway segments are not available. Since the same project specification and the same contractor have constructed the three road segments it can be estimated that the same compaction level is achieved for the remaining two segments and hence a minimum relative compaction level of 95% of HDM-4 classification applies.

Construction Defects Indicators

As clearly indicated by Odoki and Kerali (2000) the initiation and in some cases the progression of some distresses are attributed not only on the material quality and compaction index but also to problems in material handling, preparation and construction and hence in HDM-4 two indicators are adopted to account for these defects.

- Construction defects indicator for bituminous surfacing(CDS)
- Construction defects indicator for base(CDB)

Construction defects indicator for bituminous surfacing (CDS)

In order to estimate the CDS value of the study road segments and be inputted into HDM-4 deterioration models, the actual bitumen content is compared with the optimum binder content (OBC). The optimal binder content for densely graded bitumen mixture can be approximately estimated using equation (2-25).The maximum aggregate size (D_{95}) to be inputted into equation (2-25) as read from the project specification is 25 mm. Therefore the OBC for the three

segments is about 5.3%. Table 4-5 show the recovered binder content for Segment one.

Table 4-5 Recovered binder content of Addis Ababa-Modjo road segment

Chainage	52+000	54+000	56+000	58+000
Binder Content %	5.02	5.04	4.84	5.14

Source: Metaferia and Omega (2009)

The average bitumen content of Table 4-5 is about 5.01%, just 5.5% below the optimum. From Table C2-13 of the HDM-4 analytical framework manual it can be concluded that the study area's bituminous binder content is normal having a value of 1.

The Study of Metaferia and Spice (2008) and summarized in Table 4-6 shows that the recovered bitumen content of Modjo-Meki segment is 4.6% which is 13.2% below optimum and that of Meki-Zeway segment is 5.6%, which is 5.6% higher than the optimum.

Table 4-6 Asphalt binder content of Modjo-Meki-Zeway road segments

Chainage		**Asphalt Content (%)**
Start	**End**	
71+000	90+000	4.6
90+000	116+000	4.9
116+000	126+000	5.7
126+000	181+000	5.6
181+000	241+000	5.8
241+000	256+000	5.1
256+000	276+000	5.8

Source: Metaferia and Spice (2009)

From Table C2-13, of HDM-4 analytical framework manual Meki-Modjo will have a CDS value of 0.5, which means it is more susceptible to cracking and Meki-Zeway will have a CDS value of 1, indicative of normal binder content. The high cracking extent of 84% observed for the Modjo-Meki segment is evident of the defects in the binder content of bituminous surfacing.

Construction defects indicator for base (CDB)

The condition survey conducted and tests on the base layer revealed that the base layer for the three segments comply with the gradation, compaction and flakiness index requirements as specified in the project specification. It shall also be noted that during the condition survey the number of potholes per km is found to negligible due to both the maintenance policy and the good material and construction standards adopted. The bituminous surfacing layer is constructed in two layers of 4cm top and 6cm bottom. An observation of the cracking pattern showed that it is confined in the top 4cm layer, reducing the susceptibility of the base to potholing. Therefore, CDB to be used in HDM-4 for the three road segments is zero, meaning no base defects.

4.3 Analysis and Calibration of the HDM-4 Deterioration Models

Once the input data has been collected and analyzed, the result is inputted into each of the deterioration models and through the process of calibration the factors are adjusted to the condition of the study area. The analysis is done using the procedures discussed in the HDM-4's calibration manual prepared by Bennett and Paterson in 2000.

4.3.1 Crack Initiation Adjustment Factor

The models for the prediction of cracking initiation in HDM-4 vary depending on the type of base and whether the pavement surfacing is new or an overlay. Because the pavement structure of the study area is one type, which is asphalt concrete surfacing on crushed aggregate base only models applicable to this type of pavement are evaluated. Though it was in the interest of the researcher to focus only on original pavement surfacings, some overlay sections were not avoided because of the 1km minimum section length requirement for roughness calibration and the need for permanent referencing.

Initiation of All Structural Cracking Adjustment Factor (K_{cia})

Different types of models have been developed as discussed in the literature review but the model used in HDM-III and latter in HDM-4 is the one which is a function of surfacing construction quality represented by CDS, the interactive

effect of traffic loading and pavement strength and the effects of maintenance represented by crack retardation factor (CRT).

Predicted crack initiation time for new asphalt concrete pavements in HDM-4 is represented by the following equation (Odoki and Kerali, 2000)

$$ICA = K_{cia}\left\{CDS^2 a_0 EXP\left[a_1 SNP + a_2\left(\frac{YE4}{SNP^2}\right)\right] + CRT\right\} \quad (4\text{-}1)$$

The model form for crack initiation of an overlaid section is basically the same as the model for new pavement only adjusted for the previous area of wide cracking ($PCRW$) and the thickness of the overlay as represented by the equation (4-2) of Odoki and Kerali (2000)

$$ICA = K_{cia}\left\{CDS^2\left[MAX\left[\begin{array}{l} a_0 exp\left(a_1 SNP + a_2\left(\frac{YE4}{SNP^2}\right)\right) \\ *MAX\left((1-\frac{PCRW}{a_3},0)\right) a_4 HSNEW \end{array}\right]\right] + CRT\right\} \quad (4\text{-}2)$$

Where

ICA = Time to initiation of all structural cracks (years)

CDS = Construction defects indicator for bituminous surfacing

$YE4$ = Annual number of equivalent axle loads (millions/lane)

SNP = Average annual adjusted structural number of the pavement

$PCRW$ = Area of wide cracking before latest reseal or surfacing (% of total carriageway area)

$HSNEW$ =Thickness of the most recent surfacing (mm)

CRT = Crack retardation factor due to maintenance (years)

K_{cia} = Calibration factor for initiation of all structural cracking

a_0, a_1, a_2, a_3, a_4 = Model coefficients, where in the case of AMGB pavements a_0 $=4.21$, $a_1=0.14$, $a_2=-17.1$, $a_3=30$, $a_4=0.025$

In the analysis of cracking initiation, a total of 44 pavement sections each of 300 m long had been evaluated by dividing them based on the extent of observed

cracking. While doing the analysis the observed crack initiation time for the test sections is adjusted to a time when cracking extent is at 0.5% and cracking will progress 10% every year once crack is initiated as recommended in the calibration manual prepared by Bennett and Paterson (2000). Considering the old age of pavements only sections with cracking extent between 0% and 30% have been considered for cracking initiation analysis. Analysis of data above 30% cracking was not reliable because the initiation age is corrected for every 10% cracking area increment in which case the observed initiation age is more skewed towards the predicted age.

Once the predicted crack initiation age is calculated on a spread sheet then the crack initiation adjustment factor (K_{cia}) is calculated as the ratio of the mean observed crack initiation time to the mean predicted crack initiation time as represented by equation (4-3) of Bennett and Paterson, (2000).

$$K_{cia} = \frac{mean\ OTCI}{mean\ PTCI} \tag{4-3}$$

The factor calculated above is then optimized by minimizing the root mean square error (RMSE) between the observed initiation age and predicted initiation ages using equation (2-46). Data points which are far from the general trend of the scatter, the outliers and high leverage points were screened and excluded from the analysis using equations (2-47) to (2-49). Table 4-7 shows the results of the analysis of cracking initiation adjustment factor of the study area.

Table 4-7 Cracking initiation adjustment factor (K_{cia})

Cracking Extent	**Cracking level**	**Number of sections**	**Crack initiation Factor (K_{cia})**
0-5%	Low and medium	27	1.58
>30%	High	11	1.0
Overlaid sections	Medium	5	1.8

Of the 27 sections of low to medium cracking extent four sections had been eliminated as outliers because they unduly affect the slope of the regression line.

Figure 4-5 shows the slopes of the best fitting lines of the data before and after calibrations. According to Bennett and Paterson (2000), the goal of calibration is to reduce any bias of predictions by the model to acceptable level excluding the fundamental lack of fit of the model. It shall be noted that the objective of this research is not to inspect how best the model fits, but assuming that it best fits, minimize the bias between observed and model predictions.

The result of the analysis shows that crack initiation factor varies from 1for high cracking extent to 1.58 for low to medium cracking extent. As discussed above the factor for high cracking extent is rejected because the assumption of 10% annual increment of observed crack initiation age influences the calibration.

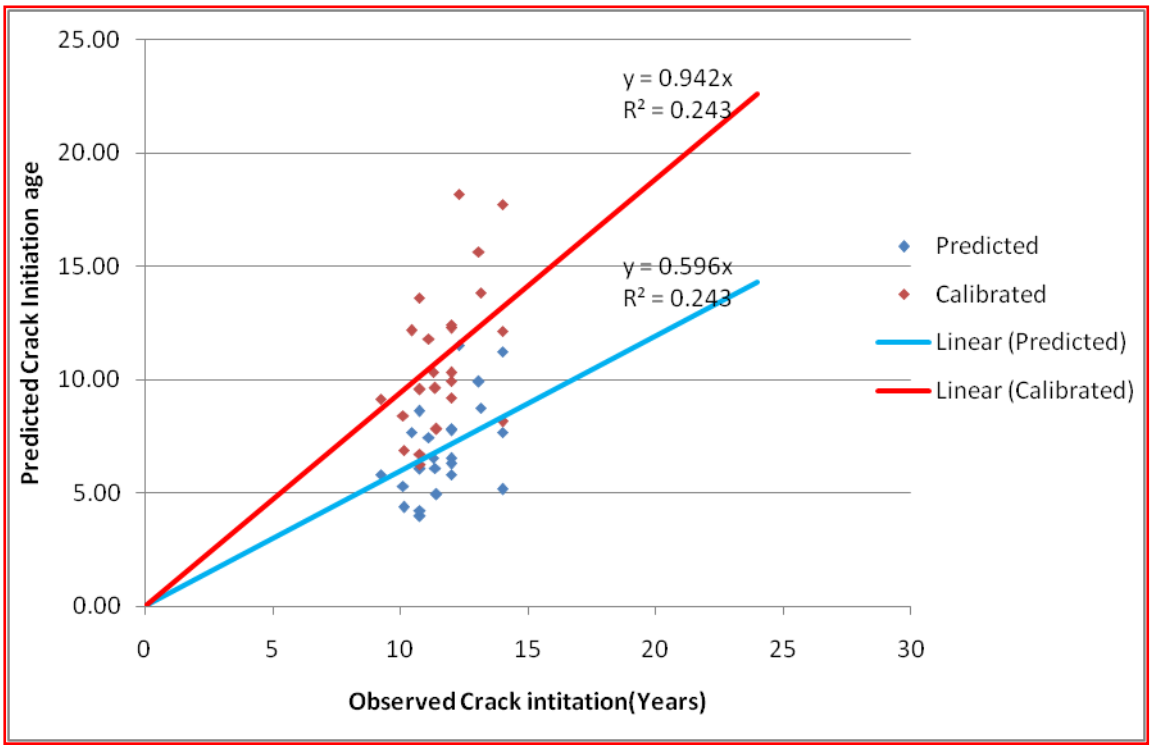

Figure 4-5 Observed versus predicted and calibrated crack initiation ages

The crack initiation factor for overlaid or resealed pavements is higher than for original pavements by a small margin of 0.22. The spread sheet showing the analysis for adjustment factors is included in Annex 4.

Initiation of Wide Structural Cracking adjustment Factor (K_{ciw})

Initiation of wide structural cracking is predicted as a function of initiation age of all structural cracking represented by the following equation of Odoki and Kerali (2000)

$$ICW = K_{ciw} Max\left[\ a_0 + a_1 ICA\ \ , a_2 ICA\ \right] \quad (4\text{-}4)$$

Where

ICA = Time to initiation of all structural cracks (years)

ICW = Time to initiation of wide structural cracks (years)

a_0, a_1, a_2 = Model coefficients, where in the case of AMGB pavements $a_0 = 2.46$, $a_1 = 0.93$, $a_2 = 0$

Similar to the calibration procedure of initiation of all cracking, the sections had been evaluated by classifying based on cracking extents. The wide cracking prediction models show a time lag of nearly 2 years once crack is initiated. The distinction between wide and narrow cracking is generally very difficult and only judgment has been used to classify the data into wide and all cracking severity levels. The results of the analysis for calibration of wide structural cracking factor (K_{ciw}) are given in Table 4-8 and detailed spreadsheet calculations are included in Annex 4.

Table 4-8 Wide cracking initiation calibration factor (K_{ciw})

Cracking Extent	Cracking level	Number of sections	Wide crack initiation adjustment factor (K_{ciw})
0-30%	Low cracking	27	1.4
>30%	High cracking	11	0.85
Overlaid sections	Medium	6	1.6

Source: This Study

4.3.2 **Cracking Progression**

The cracking progression is modeled in HDM-4 as sigmoidal function with the area of cracking and age since crack initiation as explanatory variables.

The following equations represent cracking progression in HDM-4 (Odoki and Kerali, 2000)

All cracking

$$dACA = K_{cpa}\left[\frac{CRP}{CDS}\right]Z_a\left[(Z_a a_0 a_1 \delta t_A + SCA^{a_1})^{1/a_1} - SCA\right] \quad (4\text{-}5)$$

And from Paterson (1987), the time since cracking initiated and reaches cracking extent ACA_a is given as

$$t_{ci} = \frac{\left[1 - Z_a \ 50^{a_1} + Z_a SCA^{a_1} - 0.5^{a_1}\right]}{a_0 a_1} \quad (4\text{-}6)$$

If $ACAa$ >0, δt_A =1 otherwise $\delta t_A = MAX\{0, MIN[(AGE2 - ICA), 1]\}$ (4-7)

If $ACAa \geq 50$ then $Z_a = -1$ otherwise $Z_a = 1$ (4-8)

$$ACAa = \mathrm{MAX}(ACA_a, 0.5) \quad (4\text{-}9)$$

$$\mathrm{SCA} = \mathrm{MIN}[ACA_a, (100 - ACA_a)] \quad (4\text{-}10)$$

$$Y = [Z_a a_0 a_1 \delta t_A + SCA^{a_1}] \quad (4\text{-}11)$$

If $\mathrm{Y}<0$, then $dACA = \mathrm{K_{cpa}}\left[\frac{\mathrm{CRP}}{\mathrm{CDS}}\right](100 - \mathrm{ACA_a})$ (4-12)

If $\mathrm{Y} \geq 0$, then $dACA = \mathrm{K_{cpa}}\left[\frac{\mathrm{CRP}}{\mathrm{CDS}}\right]\mathrm{Z_a}(\mathrm{Y}^{a_1} - \mathrm{SCA})$ (4-13)

If $\mathrm{ACA_a} \leq 50$ and $\mathrm{ACA_a} + \mathrm{dACA} > 50$, then $\mathrm{dACA} = \mathrm{K_{cpa}}\left[\frac{\mathrm{CRP}}{\mathrm{CDS}}\right]\left(100 - \mathrm{c}_1^{\frac{1}{a1}} - \right.$ (4-14)

ACAa

Where $\mathrm{C1} = \mathrm{MAX}\{[2(50^{a1}) - \mathrm{SCA}^{a1} - \mathrm{a_0 a_1 \delta t_A}], 0\}$ (4-15)

$dACA$ = Incremental change in area of all structural cracking during the analysis year(% of total carriageway area)

ACA_a = Area of all structural cracking at the start of the analysis year (% of total carriageway area)

δt_A = Fraction of analysis year in which all structural cracking progression

$\mathrm{AGE2}$ = Pavement surface age since last reseal, overlay, reconstruction or new construction (years)

K_{cpa} = Calibration factor for progression of all structural cracking

CRP = Retardation of cracking progression due to preventive treatment, given by $CRP=1\text{-}0.12CRT$

a_0, a_1 = Model coefficients, where in the case of AMGB pavements $a_0=1.84$, $a_1=0.45$

The above models predict the annual or fraction of the annual incremental change of cracking area and are applied for calibration when time series data are available. For the level two calibration of the cracking progression model Bennett and Paterson (2000) have proposed two methods. The first method is to estimate directly from an inverse of the crack initiation factor as follows.

$$K_{cpa} = \frac{1}{K_{cia}} \tag{4-16}$$

In the second method the factor is estimated by analyzing field data collected from pavement samples having medium (5-30%) and high (>30%) cracking extents.

According to Bennett and Paterson (2000) the progression factor is then estimated first by plotting the time since cracking initiation versus the percent observed cracking area and fit a sigmoidal curve. The observed time to progress to 30% cracking denoted as ET30 in the calibration manual is then estimated from the graph by either interpolation or extrapolation. The predicted time to 30% cracking (PT30) is estimated from the model relationships above and then the cracking progression factor is estimated as follows

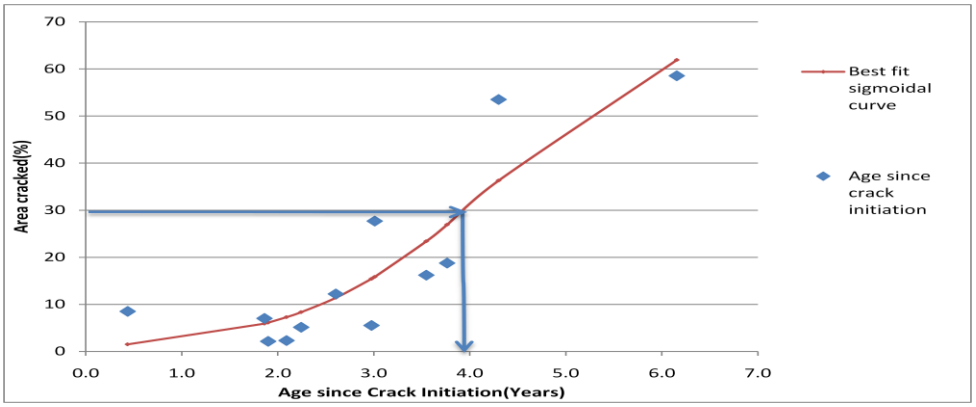

Figure 4-6 Sigmoid curve fitting for determining time to 30% cracking

$$K_{cp} = \frac{MeanPT_{30}}{MeanET_{30}} \quad (4\text{-}17)$$

From the analysis of field data and fitting of a sigmoid curve, Figure 4-6, the observed time to 30% of cracking area is 4 years and from the model relationship of Paterson (1987) and presented here as equation (4-6), the predicted time to 30% of cracking gives 4.7 years. Therefore the calibration factor calculated using equation (4-17) for study area is 1.175, which is rounded to 1.2

As expected and explained by Bennett and Paterson (2000), the data for cracking progression shows a significant scatter and some sections were screened and removed from the analysis as outliers.

4.3.3 Rutting Progression

While in HDM–III all the explanatory variables are contained in one summary progression model in HDM-4 four separate models are developed each with its own calibration factor. The model coefficients used in HDM-4 are also different to that of HDM-III to account for the different length of straight edge used for measuring rutting. In HDM-4 a 2m straight edge and in HDM-III a 1.2m straight edge are adopted as a standard. In the following sections first the four model components used in HDM-4 will be discussed and then the method of calibration for the three models will be discussed. One of the models, which is the contribution of rutting due to surface wear resulting from use of studded tire is not applicable for Ethiopian condition and hence it is not considered in this study.

Rutting due Initial Densification

This component of rutting applicable to the first year of the pavement life is dependent on the traffic loading, pavement structural strength and compaction index which is a summarized index of the thickness and achieved level of compaction of base, sub-base and selected subgrade.

The following equation represents the contribution of rutting due to initial densification (Odoki and Kerali, 2000).

$$RDO = K_{rid}\left[a_0 \;\; YE_4 10^6 \;\;^{a_1+a_2 DEF} \;\; SNP^{a3} COMP^{a_4} \right] \quad (4\text{-}18)$$

Where

RDO = Rutting due to initial densification (mm)

COMP = Relative compaction (%)

K_{rid} = Calibration factor for initial densification

a_0, a_1, a_2, a_3, a_4 = Model coefficients where for AMGB pavements $a_0 = 51740$, $a_1 = 0.09$, $a_2 = 0.0384$, $a_3 = 30$, $a_4 = 0.025$

Rutting due Structural Deformation

This component is the contribution of rutting due to shear stress imposed by traffic loading and is a function of pavement strength, traffic loading and the compaction index. The contribution is divided for the time before start of cracking and after cracking.

Structural deformation without cracking is given as

$$\Delta RDST_{uc} = K_{rst} \;\; a_0 SNP^{a_1} YE_4^{\;a_2} COMP^{a_3} \quad (4\text{-}19)$$

And structural deformation with cracking is given

$$\Delta RDST_{crk} = K_{rst} \;\; a_0 SNP^{a_1} YE_4^{\;a_2} COMP^{a_3} CRX_a^{\;a_4} \quad (4\text{-}20)$$

Where

$\Delta RDST_{uc}$ = Incremental rutting due to structural deformation without cracking in the analysis year (mm)

$\Delta RDST_{crk}$ = Incremental rutting due to structural deformation after cracking in the analysis year

K_{rst} = Calibration factor due to structural deformation

a_0, a_1, a_2, a_3, a_4 = Model coefficients where for uncracked AMGB pavements $a_0 = 44950$, $a_1 = -1.14$, $a_2 = 0.11$, $a_3 = -2.3$, $a_4 = 0$ and for cracked pavements $a_0 = 0.0000248$, $a_1 = -0.84$, $a_2 = 0.14$, $a_3 = -1.07$, $a_4 = 1.11$

Rutting due to Plastic Deformation

This component of rutting is the result of the deformation of bituminous surfacing and is applicable for thickness of more than 100mm.The component depends on the construction standard of the asphalt layer, the traffic loading, speed of the heavy vehicles and thickness of the asphalt surfacing as presented by Odoki and Kerali (2000)

$$\Delta RDPD = K_{rpd} CDS^3 a_0 YE_4 Sh^{a_1} HS^{a_2} \quad (4\text{-}21)$$

Where

$\Delta RDPD$ = Incremental increase in plastic deformation in the analysis year (mm)

CDS = Construction defects indicator for bituminous surfacing

Sh = Speed of heavy vehicles in km/h

HS = Total thickness of bituminous surfacing

K_{rpd} = Calibration factor for plastic deformation

a_0, a_1, a_2 = Model coefficients where for asphalt concrete pavements $a_0 = 2.46$, $a_1 = -0.78$, $a_2 = 0.71$

Once the individual components are calculated the total rut depth is given as follows (Odoki and Kerali 2000)

If $AGE4 \leq 1$, then

$$\Delta RDM = RDO + \Delta RDPD + \Delta RDW \quad (4\text{-}22)$$

Otherwise

$$\Delta RDM = \Delta RDST + \Delta RDPD + \Delta RDW \quad (4\text{-}23)$$

Where

ΔRDM = Incremental increase in total mean rut depth in both wheels in the analysis year (mm)

To calibrate the HDM-4 rutting model components individually one needs to have annually recorded data starting from the date of rehabilitation or reconstruction.

The methodology adopted for this study is to calculate the cumulative rutting from the three components considering unity for each calibration factor and then adjust with a single factor by comparing with the observed depth of rutting. Similar to the other deterioration models, the procedure of calibration is based on the recommendations of the HDM-4's calibration manual prepared by Bennett and Paterson (2000)

A total of 44 pavement sections, just similar to the cracking calibration had been evaluated and calculations made on a spread sheet for each of the three model components. The prediction of rutting due to initial densification is applied for the first year after pavement reconstruction (Odoki and Kerali, 2000). For structural deformation before cracking, the model is of incremental type and hence the calculated rutting has to be multiplied by the observed crack initiation year less one year of initial densification. On the other hand for rutting after cracking, the incremental rutting calculated is the sum of the rutting if pavement is not cracked and when pavement cracked multiplied by the years since cracking initiation. For the calculation of rutting due to plastic deformation of the asphalt layer, the speed of the heavy truck is assumed to be 60 km/h.

Once the components of predicted rutting are calculated using the methods discussed above the calibration factor is determined using any of the following three procedures as recommended by Bennett and Paterson (2000).

1) As a ratio of the geometric mean of the observed rutting to the geometric mean of the predicted rutting represented in equation form as

$$K_{rp} = \frac{\text{Geometric Mean}\left[\text{ORDM}_j\right]}{\text{Geomtric Mean}\left[\text{PRDM}_j\right]} \quad (4\text{-}24)$$

2) As a ratio of sum of the log of the observed to the sum log of predicted rut depth

$$K_{rp} = \frac{SUM\left[log\ ORDM_j\right]}{SUM\left[\log\log PRDM_j\right]} \quad (4\text{-}25)$$

3) From linear regression of the $log\ ORDM_j$ versus $log\ PRDM_j$

Where $ORDM_j$ = Observed mean rut depth for each calibration section j

$PRDM_j$ =Predicted mean rut depth for each calibration section j

The analysis for the calibration using the first method results in a calibration factor of 1.13 and the second method results a calibration factor of 1.06. The plot of linear regression of the data is shown in Figure 4-7. The slope of the line is now the calibration factor, which in this case is 1. From the analysis of the data using the three methods the calibration factor varies between 1 and 1.13, therefore it can be concluded that the prediction factor for asphalt concrete pavement in Ethiopia is 1.06, which is the average of the three methods.

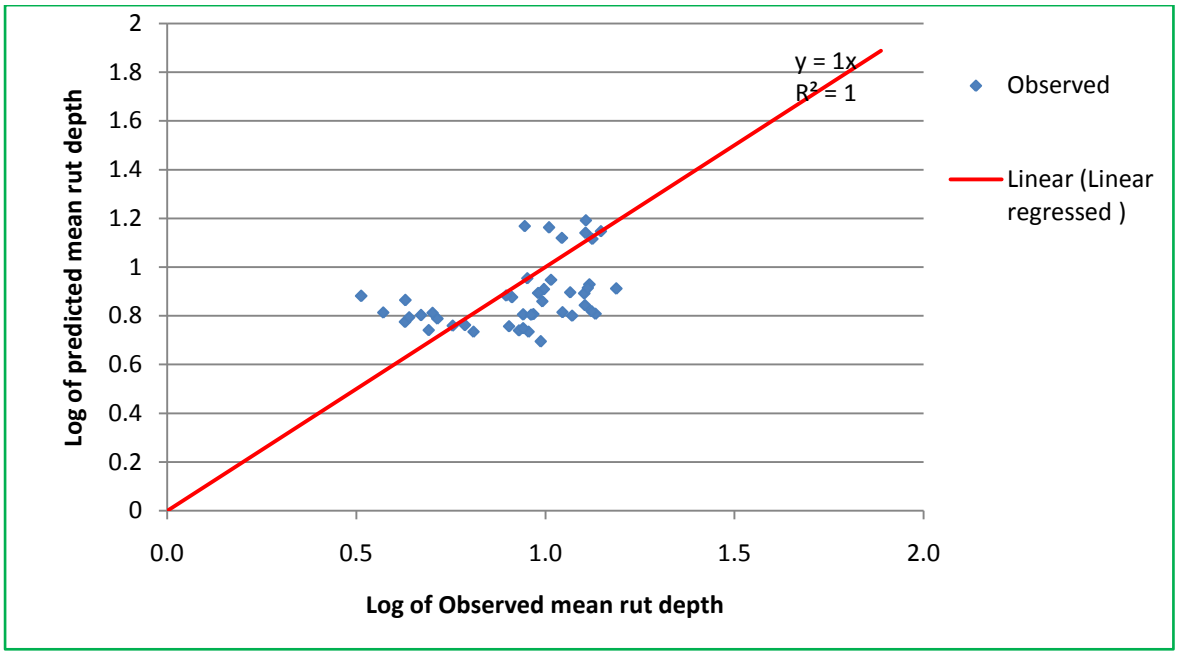

Figure 4-7 Linear regression of predicted versus observed mean rut depths

4.3.4 **Roughness Progression**

Roughness is a distress, which in addition to the structural and environmental effects, is the end product of the other pavement distresses. Therefore in HDM-4, roughness is predicted as a function of traffic loading, pavement strength, environment, cracking, rutting, potholing and maintenance effects such as patching. In HDM III and HDM-4 roughness was modeled in two ways

- Incremental model
- Summary model

The incremental model predicts the change in pavement roughness for each year of pavement analysis. According to Bennett and Paterson (2000), to

calibrate such a model requires input data on roughness, traffic loading and other pavement distresses to be collected for a minimum of four years.

The roughness incremental models in HDM-4 are developed for each causative factor and are briefly discussed below.

Structural

This is due to the shear stress imposed by traffic loading on the pavement structure and in HDM-4 it is modeled as follows(Odoki and Kerali, 2000)

$$\Delta Rl_s = a_0 \exp\ mk_{gm} AGE3\quad 1 + SNPK_b\ ^{-5} YE_4 \tag{4-26}$$

$$SNPK_b = MAX\left[\ SNP_a - dSNPK\ ,1.5\right] \tag{4-27}$$

$$dSNPK = K_{snpk} a_0 \left\{ \begin{array}{l} MIN\ \ a_1, ACX_a\ \ HSNEW + \\ MAX\left[\ MIN\ \ ACX_a - PACX, a_2\ \ ,0\right] HSOLD \end{array} \right\} \tag{4-28}$$

Where

ΔRl_s = Incremental change in roughness due to structural deterioration during the analysis year (IRI m/km)

$dSNPK$ = Reduction in adjusted structural number of pavement due to cracking

$SNPK_b$ = Adjusted structural number of pavement due to cracking at the end of the analysis year

SNP_a = Adjusted structural number of pavement at the start of the analysis year

ACX_a = Area of indexed cracking at the at the start of the analysis year (% of total carriageway area)

$PACX$ = Area of previous indexed cracking in the old surfacing (% of total carriageway area)

$HSNEW$ = Thickness of the most recent surfacing

$HSOLD$ = Total thickness of the previous underlying surfacing layers (mm)

$AGE3$ = Pavement age since the last overlay, reconstruction or new construction (years)

$YE4$ = Annual number of equivalent standard axles (millions/lane)

m = Environmental coefficient, given in the model

k_{gm} = Calibration coefficient for environment

K_{snpk} = Calibration factor for SNPK

Roughness due to cracking

$$\Delta RI_c = a_0 \Delta ACRA \quad (4\text{-}29)$$

Where

ΔRI_c = Incremental change in roughness due to cracking during the analysis year

$\Delta ACRA$ = Incremental change in area of total cracking during the analysis year (% of total carriageway area)

Roughness due to Rutting

$$\Delta RI_r = a_0 \Delta RDS \quad (4\text{-}30)$$

Where

ΔRI_r = Incremental change in roughness due to rutting during the analysis year (m/km IRI)

ΔRDS = Incremental change in standard deviation of rut depth during the analysis year (mm) (RDS_b - RDS_a)

Roughness due to Potholing

The component of roughness due to potholing will not be discussed here due to the fact that no significant potholing has been observed in the study area.

Roughness due to Environment-ageing

This is the most influential component of roughness resulted from the environmental effects of moisture and temperature fluctuations.

$$\Delta RI_e = m * kg_m * RI_a \quad (4\text{-}31)$$

Where

ΔRI_e= Incremental change in roughness due to the environment during the analysis year

RI_a= Roughness at the start of the analysis year (IRI m/km)

m = Environmental coefficient

kg_m= Calibration factor of the environmental component

The total change of roughness is then the sum of the structural, cracking, rutting, potholing and environmental components, written as follows.

$$\Delta RI = kg_p\left[\Delta RI_s + \Delta RI_c + \Delta RI_r + \Delta RI_t\right] + \Delta RI_e \quad (4\text{-}32)$$

Where,

ΔRI= Total incremental change in roughness during the analysis year (IRI m/km)

kg_p = Calibration factor for roughness progression

ΔRI_t= Roughness contribution from potholing

$\Delta RI_s, \Delta RI_c, \Delta RI_r$ = Are as defined above.

The values of model coefficients for the different roughness component models are summarized in Table 4-9

Table 4-9 Model Coefficients for the different roughness components

Pavement Type	Roughness component	a_0	a_1	a_2
All pavement types	Structural	134		
	dSNPK	0.0000758	63	40
	Cracking	0.0066		
	Rutting	0.088		
	Potholing	0.00019	2.0	1.5

Source: Odoki and Kerali (2000)

Roughness Summary Model

The integration of the incremental roughness model with respect to time results in a summary roughness model, where in order to estimate the environmental coefficient (m) is re-written as follows (Bennett and Paterson, 2000)

$$m = \frac{\ln\left[1.02RI_t - 0.143RDS + 0.0068ACRX + 0.056APAT\right] - \ln\left[RI_0 + 263NE\ 1 + SNP^{-5}\right]}{AGE3} \quad (4\text{-}33)$$

The observed environmental coefficient (m) has to be calculated first using the observed values of roughness, standard deviation of rut depth, cracking index, age and an estimate of the initial roughness using relationship (4-33). The calculated value of environmental factor then has to be adjusted to account for the observed drainage and construction standards of the study area, by referring to Table 7.4 of HDM-4 calibration manual.

Once the adjusted observed environmental coefficient is calculated, the calibration factor for the environmental component of roughness (k_{gm}) will be calculated using the recommendation of Bennett and Paterson (2000) as

$$k_{gm} = \frac{m_{adjusted}}{0.023} \quad (4\text{-}34)$$

A total of 44 pavement sections of 300m long and as an alternative a total of 12 pavements sections of 1.0-1.2 km long, as recommended by Bennett and Paterson(2000), had been evaluated for calibration purposes. From the analysis for the environmental coefficient (m) the longer sections of 1-1.2km long give reasonable results. The adjustment factor for drainage and construction standards of the study area as read from Table 7.4 of the calibration manual will be unity. The adjusted environmental coefficient will then be 0.032. The environmental calibration factor calculated using equation (4-34) will then be 1.41. This means that the environment of the study area fastens the deterioration of the road in terms of environment related roughness.

For the calibration of the general roughness progression model the summary model of equation (4-35), re-written from equation (4-33) of Bennett and Paterson, has been used to predict the current level of absolute roughness.

$$RI_t = 0.98\left[e^{AGE3*m}\ RI_o + 263NE\ 1+SNP^{\ -5}\ + 0.143RDS + 0.0068ACRX + 0.056APAT \right] \quad (4\text{-}35)$$

The comparison of average observed roughness to the predicted roughness shows that the observed roughness is 15% higher than predicted by the model. As can be seen from Figure 4-8 the slope of the predicted versus observed roughness for the 12 pavement sections of the study area is not very far from unity, indicating that the model's prediction represents the actual situation.

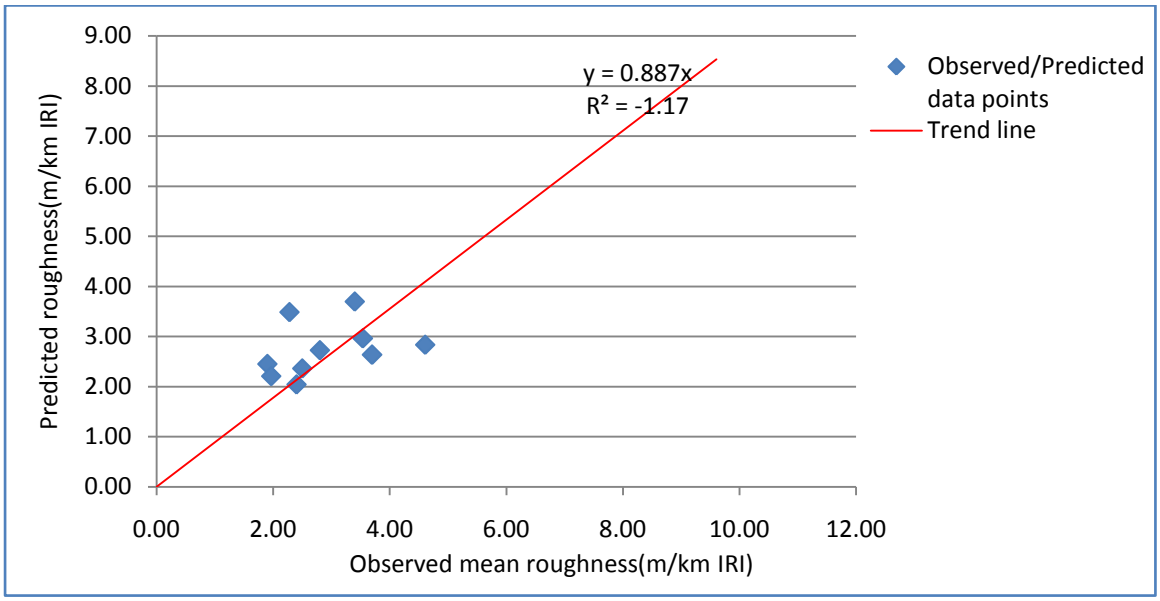

Figure 4-8 Predicted versus observed roughness of the study area

Chapter 5. Discussion of Results

In chapter three input data to the HDM-4 models were collected. The data was analyzed, inputted, and calibration of prediction factors was conducted in chapter four. In this chapter the findings of the study will be discussed.

5.1 Discussion on Analysis of Input Data

The process for the calibration of the HDM-4 road deterioration models show that much of the work involves with the identification of suitable calibration sections, and collection and analysis of the input data in a format suitable to each of the deterioration models.

5.1.1 Climatic Classification

Since the objective of calibration is to adjust the model predictions to the observed deterioration in each climatic zone, the first and most important process in the calibration of the HDM-4 model predictions is the classification of the study area into homogenous climatic zones. This requires calculation of not only the mean annual rainfall and temperature but also the Thornthwaite Moisture Index. Paterson (1987) clearly outlined that the Thornthwaite moisture index is a better quantifier of moisture content than precipitation because for example two areas of similar precipitation will have different moisture content due to variation in temperature, evapotranspiration and the water holding capacity of the soil. Fortunately for this study, the climatic zone classification based on the calculated Thornthwaite Moisture Index matches the classification based on the amount of rainfall. As has been discussed in chapter three and shown in Table 3-1, Table 3-2 and Table 3-3 the calculation for Thornthwaite Moisture Index involves determination of the net available moisture (water balance) of the study area. The analysis shows that the climate of the study area falls into the sub-humid/Tropical zone. A further study on the calibration of the HDM-4 models representing Ethiopia should be based on climatic classification of the study area after developing a Thornthwaite moisture index contour map.

5.1.2 **Traffic Loading**

While designing the calibration sections, consideration has been given to capture the different levels of traffic loading across lanes and across road links. The different traffic loading across lanes is designed to see its effect on road deterioration across a nominally homogenous road cross section. The different traffic loading across road links is planned to show the effect of traffic on pavements of different strengths and ages. A total of six different traffic levels, in each direction of three pavement segments were evaluated, detailed calculations are contained in Annex 2.

From Table 5-1, the traffic loading varies from 2.94 million ESAL/year on the Addis bound lane of Addis-Modjo Road to 0.36 million ESAL/year on Meki bound lane of Meki-Zeway Road. However, the big difference of traffic loading is not correspondingly translated into equivalent road deteriorations. Cracking area of the heavily loaded lane is less than its adjacent lane of traffic loading of 1million ESAL/year and the other road segments of even less level of traffic loading. Modjo-Meki Road, for example, which is younger in terms of pavement age and which carries much less traffic loading has more cracked area. This implies that traffic loading alone is not a very strong indicator of structural deterioration as far as cracking is concerned. On the other hand, average observed roughness correlates with traffic loading, although the correlation is still weak. The mean observed rut depth also shows similar trend as roughness but not very consistently correlated with traffic. The case with rutting is also influenced by other factors such as drainage and road longitudinal gradient. It has been observed from practice that rutting increases with poor drainage and with rising longitudinal gradient.

Table 5-1 Observed Deterioration versus Traffic Loading and Deflection

Seg.	Chaiange		Traffic loading MSAL /lane/year		Deflection (10^-2) mm		Roughness (IRI)		Rutting (mm)		Cracking (% area)	
			R	L	R	L	R	L	R	L	R	L
1	52+000-53+200	Mean	2.94	1.0	53.1	54.5	1.9	2.3	11.6	13.4	5.8	6.3
		Max			73.0	103.0	6.0	11.5	17.6	28.2	9.2	11.6

Seg.	Chaiange		Traffic loading MSAL /lane/year		Deflection (10^-2) mm		Roughness (IRI)		Rutting (mm)		Cracking (% area)	
			R	L	R	L	R	L	R	L	R	L
		Min			30.9	35.1	0.9	0.8	5.2	7.1	2.3	1.3
	55+200-56+200	Mean			52.5	53.1	3.7	3.4	13.4	10.7	31.4	19.2
		Max			77.5	76.0	7.8	9.9	32.4	29.1	44.3	38.8
		Min			18.4	30.0	1.1	0.9	4.1	5.3	17.8	12.3
2	82+000-83+200	Mean	0.61	0.63	38.6	37.2	2.9	3.2	10.3	10.4	59.4	53.5
		Max			59.5	59.5	7.3	9.8	27.8	27.0	84.1	79.8
		Min			18.6	18.6	0.9	0.9	1.9	4.0	25.5	22.6
	86+800-88+000	Mean			49.1	63.0	2.5	3.7	9.0	10.7	17.4	56.0
		Max			76.4	97.0	6.6	10.2	20.5	33.2	18.7	58.6
		Min			29.1	42.7	0.9	0.9	2.4	1.9	16.2	53.5
3	135+000-136+000	Mean	0.62	0.36	47.2	59.2	1.6	1.9	4.9	8.5	5.6	2.9
		Max			67.8	121.0	4.9	7.7	15.7	17.7	7.0	5.1
		Min			25.4	39.6	0.6	0.5	3.0	3.3	4.4	1.5
	136+000-137+000	Mean			70.5	78.8	2.3	3.0	6.3	4.5	19.3	32.8
		Max			116.6	121.0	6.1	7.7	20.7	11.6	34.1	72.6
		Min			25.4	33.0	0.7	0.6	2.2	1.4	12.2	12.3

5.1.3 **Pavement Strength**

As can be seen from Table 5-1 and Figure 5-1, one thing which is consistently correlated is the effect of cracking on pavement strength, roughness and rutting. With an increase of cracked area pavement strength decreases, rutting and roughness increases. The observed deflection ranges between a minimum of 0.184mm (a very strong) pavement and a maximum of 1.21mm (a weak pavement). As can be seen from Figure 5-2 to Figure 5-7, the deflection generally follows the general trend of the area of cracking when compared locally. As can be seen from Table 5-1, when deflection is compared with area of cracking in different segments it does not correlate very well, meaning higher deflection of one segment does not necessarily give rise to higher area of cracking. Similar explanation holds true for the observed rutting depth and roughness.

The pavement structural number (SNC) calculated with the three methods of equations (2-1), (2-3), and (2-7) give slightly different results. Generally equation

(2-7), which is based on deflection measurements, gives higher structural number than equation (2-1) or (2-3). Annex 3-3 contains such calculations. Moreover the higher structural number obtained using equation (2-7) give a reasonable prediction when inputted into the HDM-4 deterioration models.

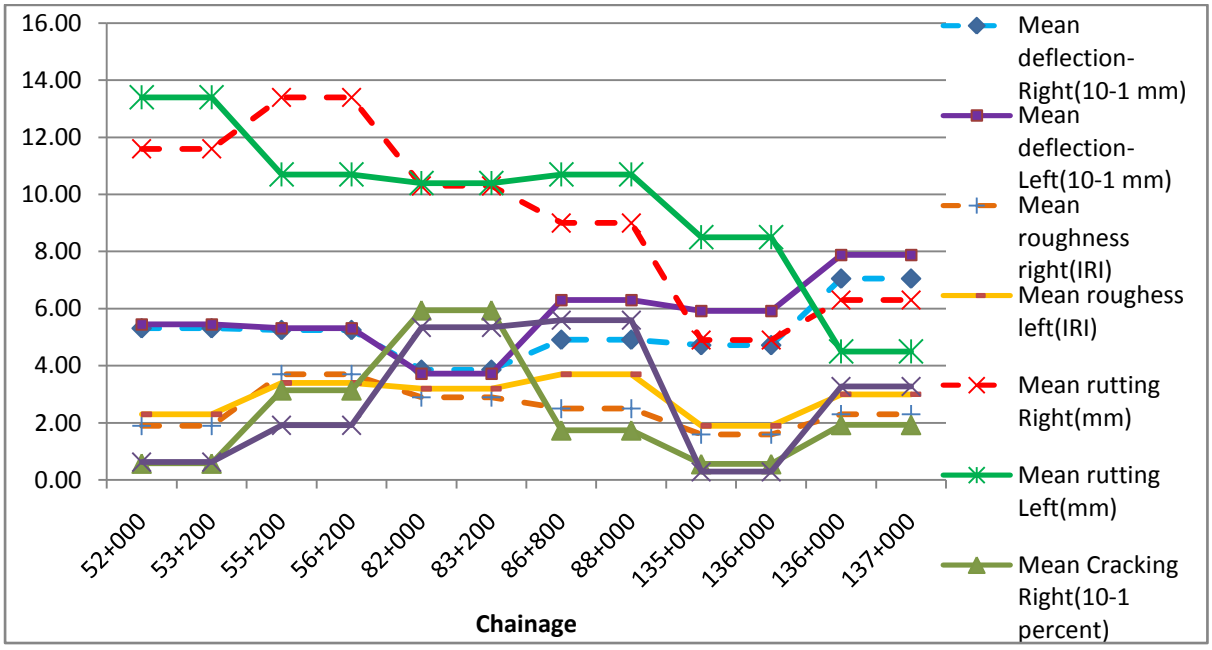

Figure 5-1 Plot of mean pavement condition versus chainage

5.1.4 Quality of Construction and Quality of Drainage

These two factors are found to greatly influence the rate of deterioration. As discussed in chapter 4 the binder content of Modjo-Meki road segment, is less than the optimum, which explains the highest observed area of cracking in that segment. Rutting and roughness are also found to be highly affected by the effect of road surface and side drainage. The higher level of rutting and roughness in the first section of Addis-Modjo road segment and the last section of Meki-Zeway segment are explained by differences in the quality of drainage.

5.2 Interaction of Pavement Strength, Traffic Loading and Road Deteriorations

The objective of this comparison is to see the effect of traffic loading, pavement strength, maintenance and environment on the level of deterioration. The comparison is done after plotting on a scatter diagram of pavement strength,

cracking, rutting and roughness against chainage for each different level of traffic loading.

5.2.1 Addis Ababa-Modjo Pavement Segment

Figure 5-2 and Figure 5-3 are plots of the pavement deflection and pavement conditions against chainage for the right and left lanes of the Addis Ababa-Modjo pavement segment. Generally both left and right side lanes show similar trends indicating that the pavement strength across the pavement is similar. The graphs also show that pavement strength, rutting and roughness follow the general trend of the extent of cracking.

The traffic loading of the left lane is nearly three times greater than the right lane, but in terms of average deterioration there is no significant difference between the heavily loaded left lane and lightly loaded right lane. However, the highest deflection and roughness are observed on the heavily loaded lanes indicating the effect of traffic loading. In terms of the deterioration level of the two sections, section two is highly deteriorated as a result of the high cracking extent. Though the deflection follows the general trend of cracking, the amount of deflection between the two sections is not significantly different, indicative of the fact that deflection is not only affected by the amount of cracking but also by the environmental effect of precipitation.

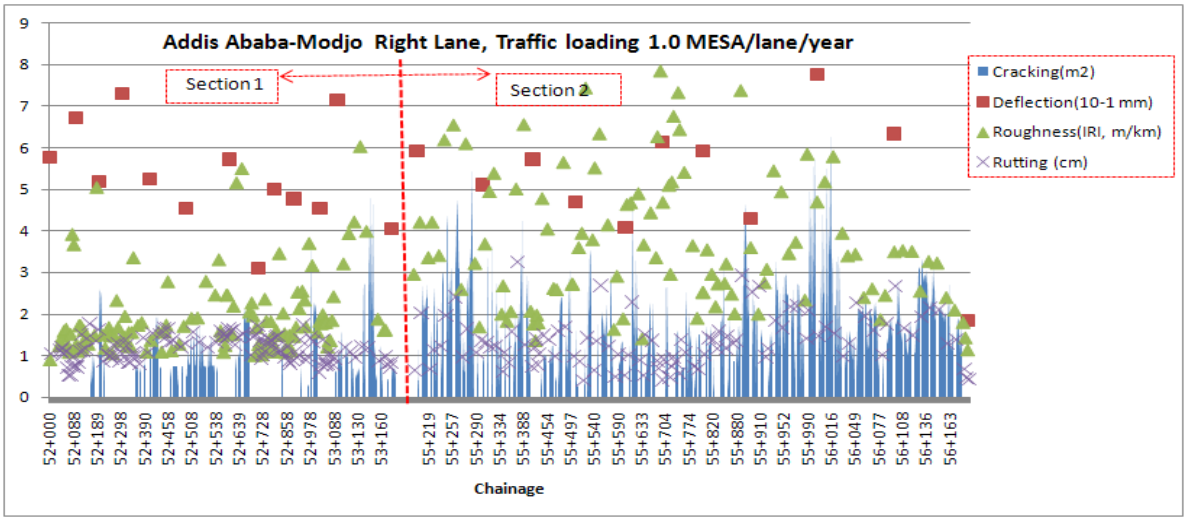

Figure 5-2 Addis Ababa-Modjo right lane Pavement condition versus chainage

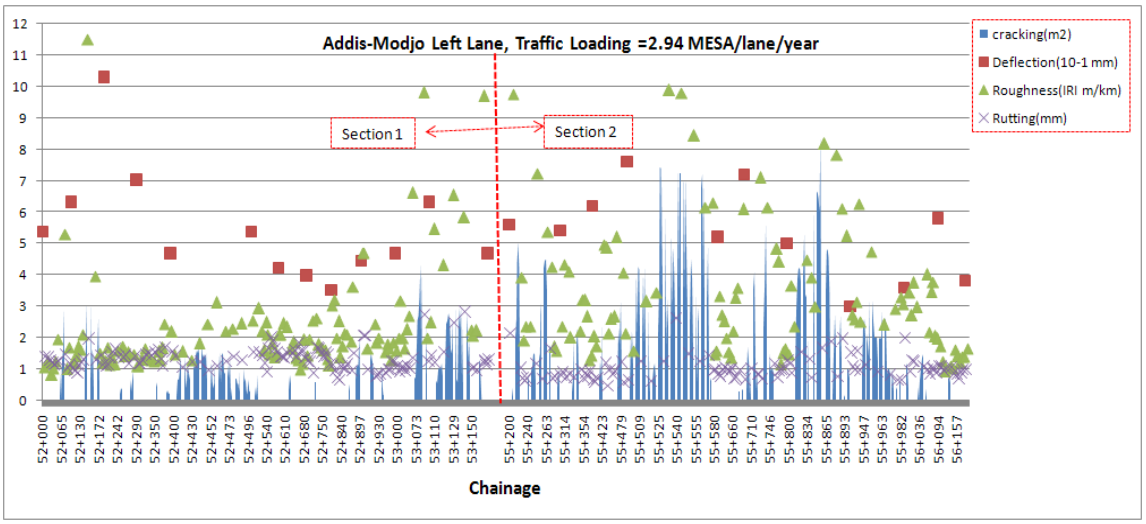

Figure 5-3 Addis Ababa-Modjo left lane pavement condition versus chainage

5.2.2 **Modjo-Meki Pavement Segment**

As can be seen from Figure 5-4 and Figure 5-5, in the section where high cracking extent is observed the pavement strength is reduced, roughness and rutting increased similar to the trends of the Addis Ababa-Modjo road segment. In the first section the right lane is more cracked than the left lane and in the second section the left lane is more cracked than the right lane. Interestingly, though the pavement is younger and lightly loaded, the level of cracking for this segment of road is higher than the Addis-Modjo road segment. In terms of pavement deflection the segment is experiencing less deflection than Addis-Ababa-Modjo road. Therefore the high cracking observed in this segment is attributed mainly either due to a poor handling or poor quality of binder used for surfacing. Due to the prevailing high level of cracking, some sections in this segment have been overlaid. The overlay has increased the strength for some of the sections and reduced distresses like cracking, rutting and roughness, for example for chainage 82+700-83+200. However in the other overlaid sections the strength is still weak and the roughness is high (section 87+300-87+800). The traffic loading on the left lane is slightly higher than the right lane and the effect is observed by an increase of observed roughness.

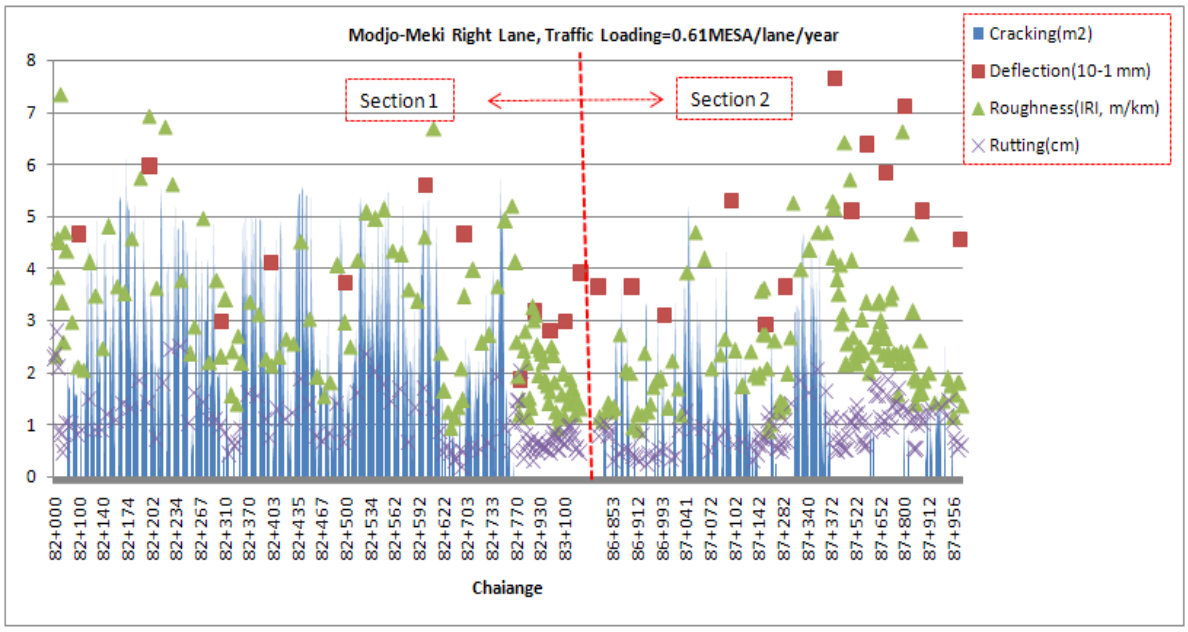

Figure 5-4 Modjo-Meki right lane pavement conditions versus chainage

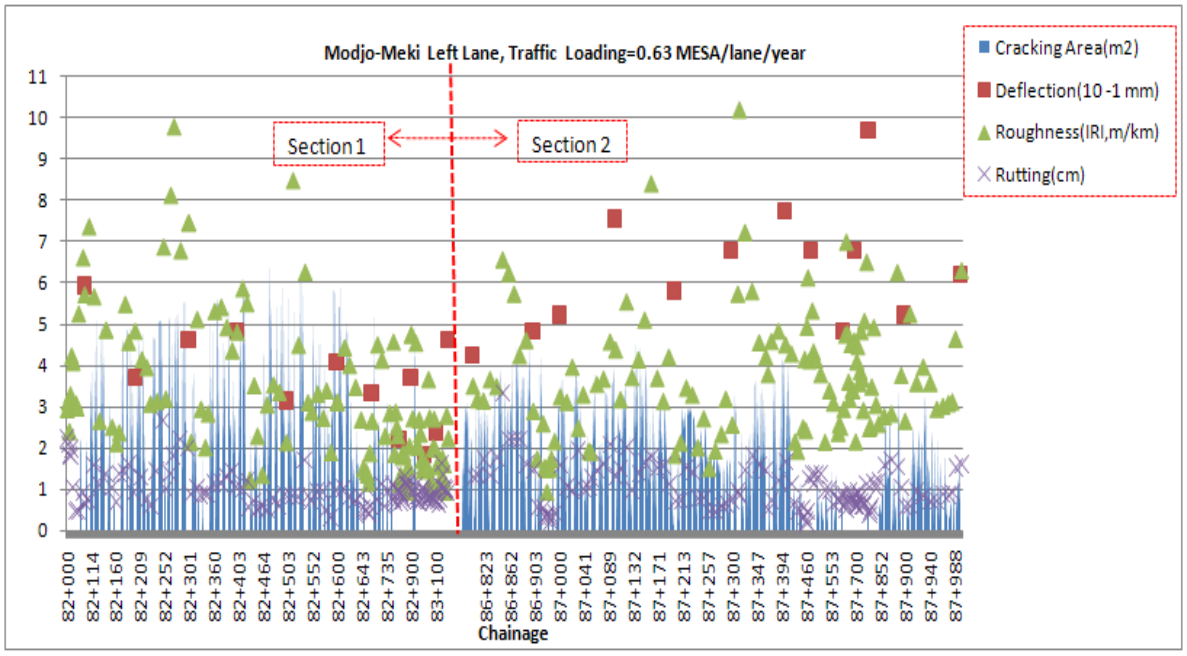

Figure 5-5 Modjo-Meki left lane pavement conditions versus chainage

5.2.3 **Meki-Zeway Pavement Segment**

Figure 5-6 and Figure 5-7 show the pavement conditions versus chainage for the right lane and left lanes of the Modjo-Meki road segment.

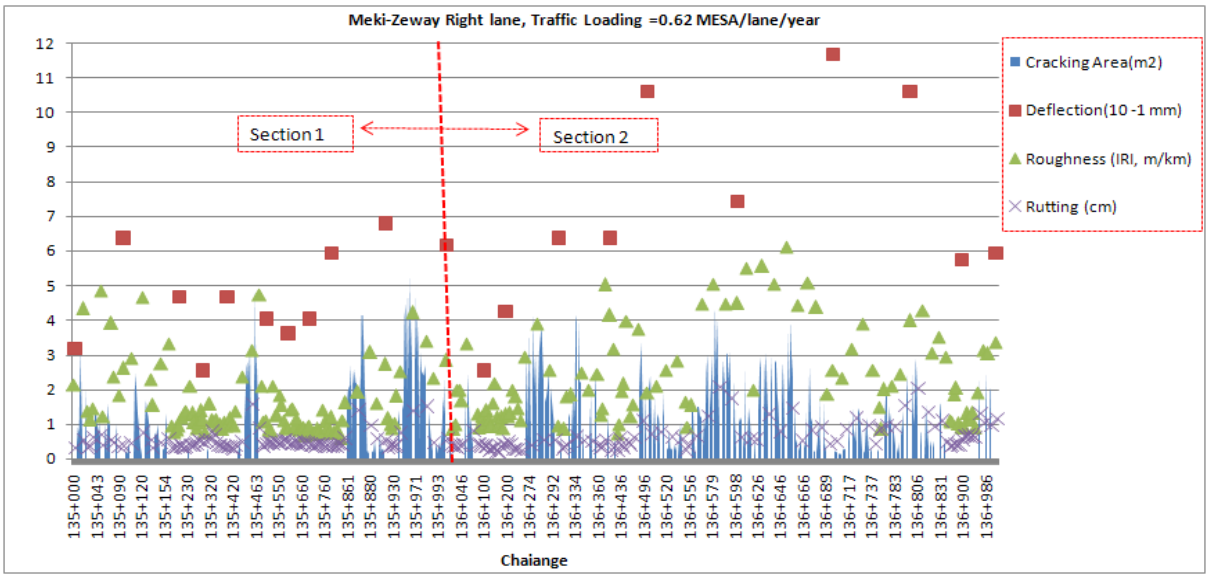

Figure 5-6 Meki-Zeway left lane pavement conditions versus chainage

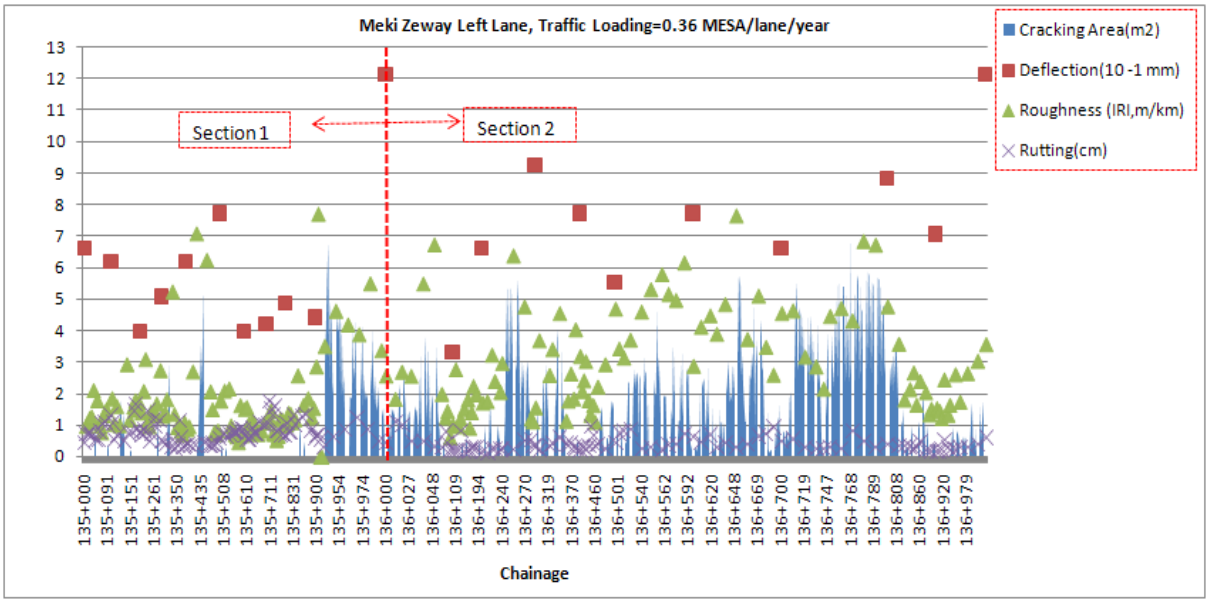

Figure 5-7 Meki-Zeway left lane pavement conditions versus chainage

In this segment, the observed rutting and roughness on the left side is higher for the first section due to weaker pavement strength, the effect of rising longitudinal slope and poor drainage. The rutting and roughness for the second section is higher on the right lane due to drainage problems and higher cracking extent. For this segment, the pattern of cracking is dominantly transverse, indicative of failure due to ageing. Section 2, however is more distressed than section 1 primarily due to drainage problem and the deflection is large conforming the effect of drainage.

5.3 Discussion of Results of HDM-4 Models Calibration

The analysis for the calibration of the HDM-4 models show that the HDM-4 road deterioration models for asphalt concrete surfacing on granular base are generally applicable to the study area in Ethiopia. This is because the calibration factors found after the analysis of this research are within the limits set out in the calibration manual of HDM-4 and included in this report in Table 2-6. Annex 4 contains detailed calculation of the calibration processes.

5.3.1 Cracking Initiation Model and Calibration Factor

The model for prediction of cracking initiation time generally gives good prediction for traffic loading of low to medium range, with an average of 6 years before calibration. For the higher traffic range, in the case of Addis bound traffic with annual loading of 2.94 million ESAL, even with the highest construction quality and pavement strength the prediction of cracking initiation age is very short in the order of less than 2 years. Annex 4-1 contains detailed calculation of cracking calibration. The observed crack initiation ages show that the pavements perform quite well with an average crack initiation age of 10.8 years. This might be due to the lower temperatures and rainfall compared to the condition in Brazil, where the data for model development is drawn from. The rainfall in Brazil is between 1200-2000mm per year compared to the study area which is generally less than 1200mm per year. The crack initiation adjustment factor which gives the least prediction error is 1.58, which means that cracking initiation is delayed by 58% in the study area compared to the default value which is representative of the Brazil condition. The crack initiation for an overlaid section is delayed by another 22%, which is equivalent to an additional of 2 more years.

Any future work in updating the cracking initiation age shall include selection of calibration sites which are representative of a wider spectrum of pavement age, geographical and environmental regions of Ethiopia.

5.3.2 Cracking Progression Model and Calibration Factor

The cracking progression model developed and included in HDM-4 is of an incremental type, and therefore for full calibration of the HDM-4 crack progression model a time series data of inputs and pavement conditions is required. The plot

of the crack initiation since initiation versus the area of cracking shows a wide scatter and therefore a filtering of the data using the statistical techniques of outliers and high leverage points have been adopted. The detailed calculation for calibration of cracking progression factor is contained in Annex 4-2. The observed time to progress to 30% cracking is 4 years compared to the 4.7 years of the model predictions. This shows that even though the crack initiation age is late in the study area, once initiated it progresses at a faster rate than the model predictions. Probably it is due to the contribution of ageing as a result of harsh tropical climate. A cracking progression factor of 1.2 adopted for the study area means that cracking in the study area progresses 20% faster than predicted by the model probably due to ageing.

5.3.3 Rut Depth Progression Calibration Factor

The prediction factor for rutting progression calculated with the three methods discussed under sub title 4.3.3 of this thesis vary between 1 and 1.1, which means that rutting progress from 0 to 10% faster than the default value of 1, which is representative of the Brazil condition. An average of the three methods which is 1.06 is adopted for the study area. This means that the observed rate of rutting in Ethiopia is 6% faster than predicted by the model. Detailed analysis of the calibration process of rut depth progression is contained in Annex 4-3 of the thesis.

5.3.4 Roughness Progression Calibration Factor

The calibration of the roughness progression factor involves first the calibration of the environmental coefficient (m). The environmental coefficient calculated for the study area is 0.032, which when calibrated for the default value of 0.023, results in calibration factor of 1.41. This indicates that the environmental component of roughness for the study area progresses at a rate 41% faster than the default value. Once the environmental coefficient is calculated then the general roughness progression predicted using equation (4-35) results an average roughness of 2.52 IRI (m/km) compared to the observed average roughness of 2.9 IRI (m/km). The results show that the observed roughness is 15% higher than predicted by the model due to mainly the environmental effects as reflected in the higher environmental coefficient (m) for the study area. The detailed calculation

for the calibration of the environmental coefficient (m) and the general roughness progression factor is contained in Annex 4-4 of the thesis.

5.4 Comparison of Calibration Factors in the Region

The study resulted calibration factors summarized in Table 5-2 for the condition of the study area. Generally it is difficult to compare the calibration factor of one country with another due to variation in climate, quality of construction materials, construction standards and the level of traffic loading. Even results of calibration factor within one country vary from region to region mainly due to change of climate. Most studies conducted are also not comprehensive. In some countries studies focused say on surface treatments, or base of either cemented or granular pavements. In other countries the studies focused either on new or overlaid pavements. Calibration factors found are also not very clear on what level of calibration the studies had been conducted. A calibration factor based on a level three data collection gives more reasonable estimates than of level two or level one. The factors determined from this study are within the range of calibration factors included in the HDM-4 calibration manual prepared by Bennett and Paterson (2000).

Table 5-2 Comparison of calibration factor of the study area versus typical range

Model	**Calibration Factor**	**Typical value of factor**
All cracking initiation adjustment factor(K_{cia})	1.58	0.5-2.0
Wide cracking initiation adjustment factor (K_{ciw})	1.4	0.5-2.0
All cracking initiation adjustment factor for overlaid section (K_{cia})	1.78	0.5-2.0
All cracking progression adjustment factor(K_{cpa})	1.2	0.5-2.0
Rutting progression adjustment factor(K_{rp})	1.06	0.5-2.0
Environmental coefficient adjustment factor(K_{gm})	1.42	0.2-5.0
General roughness progression adjustment factor(K_{gp})	1.15	0.8-1.2

A comprehensive study, at least at a level two calibration, could not be found in Ethiopia and in the region. An initial HDM-4 setup study for Kenya by Carl Bro, Grontmij and Gath Consultants in 2008, however suggested the factors in Table 5-3.

Table 5-3: HDM-4 Calibration Factors used in Kenya

Model	Calibration Factor
All cracking initiation adjustment factor(K_{cia})	0.9
Wide cracking initiation adjustment factor (K_{ciw})	0.9
All cracking initiation adjustment factor for overlaid section (K_{cia})	0.9
All cracking progression adjustment factor(K_{cpa})	1.1
Rutting progression adjustment factor(K_{rp})	1
Environmental coefficient adjustment factor(K_{gm})	0.3-1.2
General roughness progression adjustment factor(K_{gp})	1

Source: Carl Bro, Grontmij & Gath (2008)

As can been from Table 5-3, the calibration factor for cracking initiation for Kenyan Roads is 0.9. Hence cracking starts earlier than predicted by the model, which is quite different to the observation in Ethiopia. In terms of cracking progression the value used is 1.1, while the research in Ethiopia shows this to be 1.2, which is more or less similar. Rutting and roughness progression factors are also not very far from the result of research in Ethiopia, with values of 1.06 and 1.15 respectively. The environmental adjustment factor for Kenya varies from 0.3-1.2, while in the case of Ethiopia it is 1.42. The finding of the research in Ethiopia is higher than the upper limit of Kenya, indicating that the condition in Ethiopia is more favorable for roughness arising from the environment. It shall be noted that the Kenyan study is based on a level one calibration, which is not supported by any form of field data and it is difficult to make conclusive comparison with this study.

5.5 **Summary Key Findings**

- The crack initiation adjustment factor which gives the least prediction error is 1.58, which means that cracking initiation is delayed by 58% in the study area compared to the default value of 1 representative of the Brazil condition.

- The observed time to progress to 30% cracking is 4 years compared to the 4.7 years of the model predictions, resulting in a cracking progression factor of 1.2 for the study area.
- Rut depth progression factor is 1.06 for the study area. This means that the observed rate of rutting in Ethiopia is 6% faster than predicted by the model.
- The environmental coefficient calculated for the study area is 0.032, which when calibrated for the default value of 0.023, results in a calibration factor of 1.41. This indicates that the environmental component of roughness for the study area progresses 41% faster than the default value.
- General roughness progression factor for the study area is 1.15, indicating that roughness of the study area progresses 15% faster than predicted by the model.

Chapter 6. Conclusions and Recommendations

6.1 Conclusions

This study tested the applicability of the HDM-4 road deterioration models for the condition of the study area in Ethiopia. The study shows that HDM-4 road deterioration models are generally applicable to the Ethiopian conditions. It tried to calibrate the adjustment factors for a level two calibration, thereby assessing the performance of the Ethiopian Roads.

The preferred method of data collection for this type of exercise is one based on long-term pavement performance studies where data on both the factors of pavement deterioration and the pavement conditions have to be collected for years. Due to the unavailability of such recorded data, the method used for this study is slice in time, which is normally less accurate due to the natural variability of construction materials and workmanship. This variability was clearly observed during the analysis of the data collected from the three different road segments sampled in the study.

The study shows that pavement strength is contributing more to road deterioration than the effect of traffic loading. The local effects of materials quality, workmanship and environment are more significant in influencing pavement performance than traffic loading.

From the study, HDM-4 cracking initiation model is found to be more sensitive to higher range of traffic loading even for strong pavements. In such cases, the predicted life before cracking initiation is very short, in contrary to the performance in the field. Generally, the field data shows a wider dispersion in the extent and severity of cracking. Data from some pavement section, which exhibit very small deflection (strong pavement), is found to have very high cracking severity and extent. In this case, the structural number calculation from deflection measurements has shortcomings. The performance of the roads of the study area is good in terms of cracking initiation when compared with the model predictions using a default value of one. This might be due to less aggressive rainfall compared to the Brazil condition, where the model was developed. In

terms of cracking progression, however, the observed condition is a little faster than predicted by the model. This is probably due to ageing but there is a need of further study to confirm the hypothesis.

The environmental contribution of roughness progression is higher than expected for the volume of rainfall and temperature. This could be due to poor drainage resulting in soaked subgrade and pavement layers, which in turn results to variation in longitudinal profile expressed in the form of roughness. The natural sub-grade of the study pavement segments is also predominantly expansive, which in the presence of water will result in variable volume change affecting the pavement structure. Another reason could be due to long hours of sunshine or less cloud cover, which fastens the oxidation of the binder material making it susceptible cracking and hence roughness.

In terms of rutting and general roughness progression factors, the model prediction is stable and good, requiring only minor adjustment of 6% in the case of rutting and 15% in the case of roughness.

6.2 **Recommendations**

As has been discussed in the conclusion, the methodology of data collection is less accurate for good calibration of the HDM-4 models. However, it is the belief of the researcher that this study can be used as initial HDM-4 setup in Ethiopia and a basis of future study on the topic of road deterioration. To improve the quality of calibration factors future studies should focus on

- Collection of a time series data for at least four years and based on the data apply a level three calibration of the models.
- The data for this study is from a climatically and geographically limited area of Ethiopia, applicable for Sub-humid/Tropical climate only. A future research on calibration of the models should focus on low and high altitude regions of Ethiopia.
- The effect of maintenance on the rate of pavement deterioration should be evaluated by recording the type of maintenance applied and the age of pavement at maintenance. In this research, it was not possible to identify the effect, as most sections used were original pavements.

Although the recommendations of this study are focused on improving the quality of HDM-4 models calibration applicable to asphalt concrete surfacing on granular base pavements, for a complete HDM-4 road deterioration models calibration a future study should focus on models of surface treatments, concrete and gravel surfaced roads.

References

AASHTO (1993). AASHTO Guide for Design of Pavement structures. American Association of State Highway and Transportation Officials, Washington D.C.

Africon (2009).Technical Assistance to Strengthen ERA's Pavement Management System: Tasks 1.6.1/1.6.2/1.6.3 The Calibration of HDM-4 Pavement Performance Models, Final

Alebachew, F. (2005).Pavement Distresses on Addis Ababa City Arterial Roads, causes and maintenance options. A thesis in partial fulfillment of the Master of Science in Civil Engineering, Addis Ababa University

ARRB (2010), User Manual for HAWKEYE 2000 Series, Part No HKE-2000-ACQ-UM, ARRB Group Ltd.

Bezabeh, G.B. (1992).Ageing of Bitumen in Tropical Conditions. Thesis for fulfillment of Master of Science in Civil Engineering, University of Nairobi

Carl Bro, Grontmij, Gath (2008). Consultancy Services for the Development of a Road Sector Investment Program (RSIP): HDM-4 Workspace Calibration Report and Guideline. Ministry of Roads and Public Works, Northern Corridor Transport Improvement Project, Republic of Kenya

COTO (2007). Guidelines for Network Level Measurement of Road Roughness, Version 1.0, Committee of Transport Officials, South Africa.

Dickson, E.J. (1984).Bituminous Roads in Australia, Australian Road Research Board, Melbourne

ERA (2002). Pavement Rehabilitation and Overlay Design Manual. Ethiopian Roads Authority, Federal Democratic Republic of Ethiopia

FHWA (2003). Distress Identification Manual for the Long-Term Pavement Performance Program, Publication Number FHWA-RD-03-31, US Department of Transportation of the Federal Highway Administration

Ethiopian reporter (7th January, 2012).Interview with Zaid Woldegebriel, Director General, Ethiopian Roads Authority

Gichaga, F.J. (1971). A study of Deflection Characteristics and Elastic Response of Flexible Pavements in Kenya. Thesis for the fulfillment of Master of Science in Civil Engineering, University of Nairobi

Hide, H., Abaynayaka, S.W, Sayer, I., and Wyatt, R.J (1975). The Kenya Road Transport Cost Study: Research on Vehicle Operating Costs. TRRL Laboratory Report 672, overseas unit of TRRL, Crowthorne, Berkshire

Hodges, J.W., Rolt, J., Jones, T.E.(1975). The Kenya Road Transport Cost Study: Research on Road Deterioration. Department of the Environment, Transport and Road Research Laboratory Report LR 673, Crowthorne, UK

Kyendo, M., (1991).Flexible Road Pavement Performance and Maintenance Studies. Thesis for fulfillment of Master of Science in Civil Engineering, University of Nairobi

Metaferia & Omega (2009).Final Pavement Evaluation Report. Addis Ababa-Modjo Road Maintenance Project

Metaferia & Spice (2009).Soils, Materials and Pavement Design Report (Final). Detailed Engineering Design and Tender Document Preparation for Modjo – Awasa Periodic Maintenance Project

Mrawira D.M. (1995). A study to calibrate HDM-III for Tanzania Conditions. Agricultural Transport Assistance Program (ATAP), Project No 631-0166, Final Report

Moavenzadeh F. J.H., Stafford, J.H., Suhrbier, J. Alexander (1971). Highway Design Standards Study Phase I: The Model. World Bank Staff Working Paper no 96, Washington D.C., World Bank

Murunga, P.A. (1983). A performance Study of Flexible Pavements in Kenya. Thesis for fulfillment of Master of Science in Civil Engineering, University of Nairobi

NASA (2012).NASA Surface Meteorology and Solar Energy. Atmospheric Data Centre, http://eosweb.larc.nasa.gov/cgi-bin/sse/sse.cgi?+s01#s01

NDLI (1995b).Modeling Road Deterioration and Maintenance Effects in HDM-4. Report to the Asian Development Bank, N.D. Lea International Ltd., B.C., Canada

NMA (2008).National Meteorological Agency Weather Records, Addis Ababa, Ethiopia

Odoki, J.B., Kerali H.G.R (2000). Highway Development and Management Series: Volume 4-Analytical Framework and Model Description. World Roads Association (PIARC), Paris and the World Bank, Washington DC.

Parsley, L.L., and Robinson R., (1982).The TRRL Road Investment Model for Developing Countries (RTIM2). TRRL Laboratory Report 1057, Overseas Unit of Transport and Road Research Laboratory, Crowthorne, Berkshire, UK

Paterson, W.D.0. (1987). Road Deterioration and Maintenance Effects: Models for Planning and Management, the Highway Design and Maintenance Standards Series. Published for World Bank, the Johns and Hopkins University Press, Balitimore and London

Paterson, W.D.O, Attoh-okine, B. (1992).Simplified Models of Paved Road Deterioration Based on HDM-III, Paper for Annual Meeting of Transportation Research Board

Pell,S.P.(1978).Developments in Highway Pavement Engineering-1. Applied Science Publishers LTD,London

Rao,Tangella,S.C.S., Craus, J., Deacon, J.A., Monismith, C.L. (1990).Summary Report on Fatigue Response of Asphalt Mixtures. TM-UCB-A-003A-89-3, Prepared for Strategic Highway Research Program, Project A-003-A, Institute of Transportation Studies, University of California, Berkeley, California

Sayers, M.W., Gillespie, T.D., Quiroz, C.A.V. (1986).The International Roughness Experiment: Establishing and Calibration Standard for Measurements. World Bank Technical Paper Number 45, World Bank, Washington DC, U.S.A

Sayers, M.W., Gillespie, T.D., Paterson, W.D.O. (1986).Guidelines for Conducting and Calibrating Road Roughness Measurements. World Bank Technical Paper Number 46, World Bank, Washington DC, U.S.A

Sayers, M.W., Karamihas, S.W. (1998). The Little Book of Profiling; Basic Information about Measuring and Interpreting Road Profiles. The University of Michigan

TRB (2007).Pavement Lessons learned from the AASHO Road Test and Performance of the Interstate Highway System. Transportation Research Circular E-C118, Pavement Management section of Transportation Research Board, www.TRB.org

TRL(1999). A guide to Pavement Evaluation and maintenance of bitumen surfaced roads in Tropical and Sub-Tropical countries. Overseas Road Note 18, overseas centre of, Transport Research Laboratory, Crowthorne, Berkshire, UK

Thornwaite, C.W., and J.R. Mather (1957). Instructions and Tables for Computing Potential Evapotranspiration and the Water Balance. Drexel Institute of Technology, Laboratory of Climatology, Publications in Climatology

Thornthwaite,C.W., and J.R. Mather (1955). The Water Balance. Laboratory of Climatology, Publ. 8, Centerton, N.J.

Watanatada, T., Harral, C.G., Paterson, W.D.O., Dhareshwar, A.M., Bhandari, A., and F.Tsunokawa (1987a). The Highway Design and Maintenance Standards Model: Volume 1-Description of HDM-III Model. World Bank Publications, Washington D.C

APPENDECES

ANNEX 1-PAVEMENT STRENGTH CALCULATION

Calcualtion for average section deflection and average annual pavement strength																
Segement one-Section 0ne																
Chaiange	52+000	52+100	52+200	52+300	52+300	52+400	52+500	52+600	52+600	52+700	52+800	52+900	52+900	53+000	53+100	53+200
Section	Section 1				Section 2				Section 3				Section 4			
Right lane																
Right lane deflection(10^{-2} mm)	57.6	67.2	51.8	73.0	73.0	52.4	45.2	57.1	57.1	30.9	50.0	47.6	47.6	45.2	71.4	40.5
Average right lane deflection(10^{-2} mm)	62.4	62.4	62.4	62.4	56.9	56.9	56.9	56.9	46.4	46.4	46.4	46.4	51.8	51.8	51.8	51.8
SNP_{wet}=(Equation 2-7)	4.3	4.3	4.3	4.3	4.6	4.6	4.6	4.6	5.2	5.2	5.2	5.2	4.8	4.8	4.8	4.8
$ACRA_a$(%)	2.3	2.3	2.3	2.3	8.5	8.5	8.5	8.5	3.0	3.0	3.0	3.0	9.2	9.2	9.2	9.2
MMP(mm)	71.0	71.0	71.0	71.0	71.0	71.0	71.0	71.0	71.0	71.0	71.0	71.0	71.0	71.0	71.0	71.0
Drainage factor (DF)	2.0	2.0	2.0	2.0	2.0	2.0	2.0	2.0	2.0	2.0	2.0	2.0	2.0	2.0	2.0	2.0
SNP_{wet}/SNP_{dry} ratio(f)-Equation (2-11)	0.9	0.9	0.9	0.9	0.9	0.9	0.9	0.9	0.9	0.9	0.9	0.9	0.9	0.9	0.9	0.9
$SNPdry=SNP_w/f$	4.7	4.7	4.7	4.7	4.9	4.9	4.9	4.9	5.6	5.6	5.6	5.6	5.2	5.2	5.2	5.2
Fraction of dry season(d)- 7 month of dry	0.6	0.9	0.6	0.6	0.6	0.6	0.6	0.6	0.6	0.6	0.6	0.6	0.6	0.6	0.6	0.6
f_s =Equation (2-10)	1.0	1.0	1.0	1.0	1.0	1.0	1.0	1.0	1.0	1.0	1.0	1.0	1.0	1.0	1.0	1.0
Average Annual Strength(SNP)=$fs*SNP_d$	4.5	4.5	4.5	4.5	4.8	4.8	4.8	4.8	5.4	5.4	5.4	5.4	5.1	5.1	5.1	5.1
Average annual deflection in(10^{-2} mm)	58.4	58.4	58.4	58.4	53.2	53.2	53.2	53.2	43.3	43.3	43.3	43.3	48.4	48.4	48.4	48.4
Left lane																
Left lane deflection(10^{-2} mm)	53.8	63.2	103.0	70.2	70.2	46.8	53.8	42.1	42.1	39.8	35.1	44.5	44.5	46.8	63.2	46.8
Average left deflection(10^{-2} mm)	72.5	72.5	72.5	72.5	53.2	53.2	53.2	53.2	40.4	40.4	40.4	40.4	50.3	50.3	50.3	50.3
SNP_{wet}=(Equation 2-7)	3.9	3.9	3.9	3.9	4.8	4.8	4.8	4.8	5.7	5.7	5.7	5.7	4.9	4.9	4.9	4.9
$ACRA_a$(%)	3.9	3.9	3.9	3.9	8.5	8.5	8.5	8.5	1.3	1.3	1.3	1.3	11.6	11.6	11.6	11.6
MMP(mm)	71.0	71.0	71.0	71.0	71.0	71.0	71.0	71.0	71.0	71.0	71.0	71.0	71.0	71.0	71.0	71.0
Drainage factor (DF)	2.0	2.0	2.0	2.0	2.0	2.0	2.0	2.0	2.0	2.0	2.0	2.0	2.0	2.0	2.0	2.0
SNP_{wet}/SNP_{dry} ratio(f)-Equation (2-11)	0.9	0.9	0.9	0.9	0.9	0.9	0.9	0.9	0.9	0.9	0.9	0.9	0.9	0.9	0.9	0.9
$SNPdry=SNP_w/f$	4.3	4.3	4.3	4.3	5.2	5.2	5.2	5.2	6.1	6.1	6.1	6.1	5.4	5.4	5.4	5.4
d-(7 dry months)/12months	0.6	0.6	0.6	0.6	0.6	0.6	0.6	0.6	0.6	0.6	0.6	0.6	0.6	0.6	0.6	0.6
f_s =Equation (2-10)	1.0	1.0	1.0	1.0	1.0	1.0	1.0	1.0	1.0	1.0	1.0	1.0	1.0	1.0	1.0	1.0
Average Annual Strength(SNP)=$fs*SNP_d$	4.1	4.1	4.1	4.1	5.0	5.0	5.0	5.0	5.9	5.9	5.9	5.9	5.2	5.2	5.2	5.2
Average annual deflection in(10^{-2} mm)	67.9	67.9	67.9	67.9	49.4	49.4	49.4	49.4	37.7	37.7	37.7	37.7	46.4	46.4	46.4	46.4

ANNEX 1-PAVEMENT STRENGTH CALCULATION

Calcualtion for average section deflection and average annual pavement strength													
Segement one-Section two													
Chaiange	55+200	55+300	55+400	55+500	55+500	55+600	55+700	55+800	55+800	55+900	56+000	56+100	56+200
Section	Section 1				Section 2				Section 3				
Right lane													
Right lane deflection(10^{-2} mm)	59.2	51.0	57.1	46.9	46.9	40.8	61.2	59.2	59.2	42.8	77.5	63.2	18.4
Average right lane deflection(10^{-2} mm)	53.6	53.6	53.6	53.6	52.0	52.0	52.0	52.0	52.2	52.2	52.2	52.2	52.2
SNPwet=(Equation 2-7)	4.7	4.7	4.7	4.7	4.8	4.8	4.8	4.8	4.8	4.8	4.8	4.8	4.8
ACRAa(%)	32.3	32.3	32.3	32.3	17.7	17.7	17.7	17.7	44.3	44.3	44.3	44.3	44.3
MMP(mm)	71.0	71.0	71.0	71.0	71.0	71.0	71.0	71.0	71.0	71.0	71.0	71.0	71.0
Drainage factor (DF)	2.0	2.0	2.0	2.0	2.0	2.0	2.0	2.0	2.0	2.0	2.0	2.0	2.0
SNPwet/SNPdry ratio(f)-Equation (2-11)	0.9	0.9	0.9	0.9	0.9	0.9	0.9	0.9	0.9	0.9	0.9	0.9	0.9
SNPdry=SNPw/f	5.4	5.4	5.4	5.4	5.4	5.4	5.4	5.4	5.6	5.6	5.6	5.6	5.6
Fraction of dry season(d)- 7 month of dry	0.6	0.6	0.6	0.6	0.6	0.6	0.6	0.6	0.6	0.6	0.6	0.6	0.6
fs =Equation (2-10)	0.9	0.9	0.9	0.9	1.0	1.0	1.0	1.0	0.9	0.9	0.9	0.9	0.9
Average Annual Strength(SNP)=fs*SNPd	5.1	5.1	5.1	5.1	5.1	5.1	5.1	5.1	5.2	5.2	5.2	5.2	5.2
Average annual deflection in(10^{-2} mm)	47.9	47.9	47.9	47.9	47.5	47.5	47.5	47.5	45.9	45.9	45.9	45.9	45.9
Left lane deflection													
Left lane deflection(10^{-2} mm)	56.0	54.0	62.0	76.0	76.0	52.0	72.0	50.0	50.0	30.0	36.0	58.0	38.0
Average left deflection(10^{-2} mm)	62.0	62.0	62.0	62.0	62.5	62.5	62.5	62.5	42.4	42.4	42.4	42.4	42.4
	4.3	4.3	4.3	4.3	4.3	4.3	4.3	4.3	5.5	5.5	5.5	5.5	5.5
$ACRA_a$(%)	12.1	12.1	12.1	12.1	38.8	38.8	38.8	38.8	25.8	25.8	25.8	25.8	25.8
MMP(mm)	71.0	71.0	71.0	71.0	71.0	71.0	71.0	71.0	71.0	71.0	71.0	71.0	71.0
Drainage factor (DF)	2.0	2.0	2.0	2.0	2.0	2.0	2.0	2.0	2.0	2.0	2.0	2.0	2.0
SNP_{wet}/SNP_{dry} ratio(f)-Equation (2-11)	0.9	0.9	0.9	0.9	0.9	0.9	0.9	0.9	0.9	0.9	0.9	0.9	0.9
$SNPdry=SNP_w/f$	4.8	4.8	4.8	4.8	5.0	5.0	5.0	5.0	6.2	6.2	6.2	6.2	6.2
d-(7 dry months)/12months	0.6	0.6	0.6	0.6	0.6	0.6	0.6	0.6	0.6	0.6	0.6	0.6	0.6
f_s =Equation (2-10)	1.0	1.0	1.0	1.0	0.9	0.9	0.9	0.9	0.9	0.9	0.9	0.9	0.9
Average Annual Strength(SNP)=fs*SNP_d	4.6	4.6	4.6	4.6	4.6	4.6	4.6	4.6	5.9	5.9	5.9	5.9	5.9
Average annual deflection in(10^{-2} mm)	57.3	57.3	57.3	57.3	55.6	55.6	55.6	55.6	38.3	38.3	38.3	38.3	38.3

ANNEX 1-PAVEMENT STRENGTH CALCULATION

Calcualtion for average section deflection and average annual pavement strength															
Segement two-Section 0ne															
Chaiange	**82+100**	**82+200**	**82+300**	**82+300**	**82+400**	**82+500**	**82+600**	**82+600**	**82+700**	**82+800**	**82+900**	**82+900**	**83+000**	**83+100**	**83+200**
Section	**Section 1**			**Section 2**				**Section 3**				**Section 4**			
Right lane															
Right lane deflection(10^{-2} mm)	46.5	59.5	29.8	29.8	40.9	37.2	55.8	55.8	46.5	18.6	31.6	31.6	27.9	29.8	39.1
Average right lane deflection(10^{-2} mm)	45.3	45.3	45.3	40.9	40.9	40.9	40.9	38.1	38.1	38.1	38.1	32.1	32.1	32.1	32.1
SNP_{wet}=(Equation 2-7)	5.3	5.3	5.3	5.6	5.6	5.6	5.6	5.9	5.9	5.9	5.9	6.5	6.5	6.5	6.5
$ACRA_a$(%)	73.4	73.4	73.4	88.0	88.0	88.0	88.0	25.5	25.5	25.5	25.5	0.0	0.0	0.0	0.0
MMP(mm)	82.0	82.0	82.0	82.0	82.0	82.0	82.0	82.0	82.0	82.0	82.0	82.0	82.0	82.0	82.0
Drainage factor (DF)	2.0	2.0	2.0	2.0	2.0	2.0	2.0	2.0	2.0	2.0	2.0	2.0	2.0	2.0	2.0
SNP_{wet}/SNP_{dry} ratio(f)-Equation (2-11)	0.8	0.8	0.8	0.8	0.8	0.8	0.8	0.9	0.9	0.9	0.9	0.9	0.9	0.9	0.9
$SNPdry=SNP_w/f$	6.3	6.3	6.3	6.9	6.9	6.9	6.9	6.5	6.5	6.5	6.5	7.0	7.0	7.0	7.0
Fraction of dry season(d)- 7 month of dry	0.6	0.6	0.6	0.6	0.6	0.6	0.6	0.6	0.6	0.6	0.6	0.6	0.6	0.6	0.6
f_s =Equation (2-10)	0.9	0.9	0.9	0.9	0.9	0.9	0.9	1.0	1.0	1.0	1.0	1.0	1.0	1.0	1.0
Average Annual Strength(SNP)=fs*SNP_d	5.8	6.0	5.8	6.3	6.3	6.3	6.3	6.2	6.2	6.2	6.2	6.8	6.8	6.8	6.8
Average annual deflection in(10^{-2} mm)	39.0	37.4	39.0	34.6	34.6	34.6	34.6	34.8	34.8	34.8	34.8	30.2	30.2	30.2	30.2
left lane															
Left lane deflection(10^{-2} mm)	59.5	37.2	46.5	46.5	48.4	31.6	40.9	40.9	33.5	22.3	37.2	37.2	18.6	24.2	46.5
Average left deflection(10^{-2} mm)	47.7	47.7	47.7	41.9	41.9	41.9	41.9	33.5	33.5	33.5	33.5	31.6	31.6	31.6	31.6
SNP_{wet}=(Equation 2-7)	5.1	5.1	5.1	5.5	5.5	5.5	5.5	6.4	6.4	6.4	6.4	6.6	6.6	6.6	6.6
$ACRA_a$(%)	62.2	62.2	62.2	79.3	79.3	79.3	79.3	22.1	22.1	22.1	22.1	1.1	1.1	1.1	1.1
MMP(mm)	82.0	82.0	82.0	82.0	82.0	82.0	82.0	82.0	82.0	82.0	82.0	82.0	82.0	82.0	82.0
Drainage factor (DF)	2.0	2.0	2.0	2.0	2.0	2.0	2.0	2.0	2.0	2.0	2.0	2.0	2.0	2.0	2.0
SNP_{wet}/SNP_{dry} ratio(f)-Equation (2-11)	0.9	0.9	0.9	0.8	0.8	0.8	0.8	0.9	0.9	0.9	0.9	0.9	0.9	0.9	0.9
$SNPdry=SNP_w/f$	6.0	6.0	6.0	6.7	6.7	6.7	6.7	7.0	7.0	7.0	7.0	7.1	7.1	7.1	7.1
d-(7 dry months)/12months	0.6	0.6	0.6	0.6	0.6	0.6	0.6	0.6	0.6	0.6	0.6	0.6	0.6	0.6	0.6
f_s =Equation (2-10)	0.9	0.9	0.9	0.9	0.9	0.9	0.9	1.0	1.0	1.0	1.0	1.0	1.0	1.0	1.0
Average Annual Strength(SNP)=fs*SNP_d	5.6	5.6	5.6	6.1	6.1	6.1	6.1	6.7	6.7	6.7	6.7	6.9	6.9	6.9	6.9
Average annual deflection in(10^{-2} mm)	41.7	41.7	41.7	35.8	35.8	35.8	35.8	30.7	30.7	30.7	30.7	29.7	29.7	29.7	29.7

Calcualtion for average section deflection and average annual pavement strength																
Section	**Section 1**				**Section 2**				**Section 3**				**ection 4**			
Right lane																
Right lane deflection(10^{-2} mm)	36.4	36.4	30.9	52.8	52.8	29.1	36.4	76.4	76.4	51.0	63.7	58.2	58.2	71.0	51.0	45.5
Average right lane deflection(10^{-2} mm)	39.1	39.1	39.1	39.1	48.7	48.7	48.7	48.7	62.3	62.3	62.3	62.3	56.4	56.4	56.4	56.4
SNP_{wet}=(Equation 2-7)	5.8	5.8	5.8	5.8	5.0	5.0	5.0	5.0	4.3	4.3	4.3	4.3	4.6	4.6	4.6	4.6
$ACRA_a$(%)	16.2	16.2	16.2	16.2	14.8	14.8	14.8	14.8	0.6	0.6	0.6	0.6	3.4	3.4	3.4	3.4
MMP(mm)	82.0	82.0	82.0	82.0	82.0	82.0	82.0	82.0	82.0	82.0	82.0	82.0	82.0	82.0	82.0	82.0
Drainage factor (DF)	2.0	2.0	2.0	2.0	2.0	2.0	2.0	2.0	2.0	2.0	2.0	2.0	2.0	2.0	2.0	2.0
SNP_{wet}/SNP_{dry} ratio(f)-Equation (2-11)	0.9	0.9	0.9	0.9	0.9	0.9	0.9	0.9	0.9	0.9	0.9	0.9	0.9	0.9	0.9	0.9
SNPdry=SNP_w/f	6.3	6.3	6.3	6.3	5.5	5.5	5.5	5.5	4.6	4.6	4.6	4.6	4.9	4.9	4.9	4.9
Fraction of dry season(d)- 7 month of dry	0.6	0.6	0.6	0.6	0.6	0.6	0.6	0.6	0.6	0.6	0.6	0.6	0.6	0.6	0.6	0.6
f_s =Equation (2-10)	1.0	1.0	1.0	1.0	1.0	1.0	1.0	1.0	1.0	1.0	1.0	1.0	1.0	1.0	1.0	1.0
Average Annual Strength(SNP)=fs*SNP_d	6.1	6.1	6.1	6.1	5.3	5.3	5.3	5.3	4.5	4.5	4.5	4.5	4.8	4.8	4.8	4.8
Average annual deflection in(10^{-2} mm)	36.2	36.2	36.2	36.2	45.1	45.1	45.1	45.1	59.0	59.0	59.0	59.0	53.1	53.1	53.1	53.1
left lane																
Left lane deflection(10^{-2} mm)	42.7	48.5	52.4	75.7	75.7	58.2	67.9	77.6	77.6	67.9	48.5	67.9	67.9	97.0	52.4	62.1
Average left deflection(10^{-2} mm)	54.8	54.8	54.8	54.8	69.8	69.8	69.8	69.8	65.5	65.5	65.5	65.5	69.8	69.8	69.8	69.8
SNP_{wet}=(Equation 2-7)	4.7	4.7	4.7	4.7	4.0	4.0	4.0	4.0	4.2	4.2	4.2	4.2	4.0	4.0	4.0	4.0
$ACRA_a$(%)	53.2	53.2	53.2	53.2	58.5	58.5	58.5	58.5	7.9	7.9	7.9	7.9	19.0	19.0	19.0	19.0
MMP(mm)	82.0	82.0	82.0	82.0	82.0	82.0	82.0	82.0	82.0	82.0	82.0	82.0	82.0	82.0	82.0	82.0
	2.0	2.0	2.0	2.0	2.0	2.0	2.0	2.0	2.0	2.0	2.0	2.0	2.0	2.0	2.0	2.0
SNP_{wet}/SNP_{dry} ratio(f)-Equation (2-11)	0.9	0.9	0.9	0.9	0.9	0.9	0.9	0.9	0.9	0.9	0.9	0.9	0.9	0.9	0.9	0.9
SNPdry=SNP_w/f	5.4	5.4	5.4	5.4	4.7	4.7	4.7	4.7	4.5	4.5	4.5	4.5	4.4	4.4	4.4	4.4
d-(7 dry months)/12months	0.6	0.6	0.6	0.6	0.6	0.6	0.6	0.6	0.6	0.6	0.6	0.6	0.6	0.6	0.6	0.6
f_s =Equation (2-10)	0.9	0.9	0.9	0.9	0.9	0.9	0.9	0.9	1.0	1.0	1.0	1.0	1.0	1.0	1.0	1.0
Average Annual Strength(SNP)=fs*SNP_d	5.1	5.1	5.1	5.1	4.4	4.4	4.4	4.4	4.4	4.4	4.4	4.4	4.2	4.2	4.2	4.2
Average annual deflection in(10^{-2} mm)	48.5	48.5	48.5	48.5	61.5	61.5	61.5	61.5	61.4	61.4	61.4	61.4	64.6	64.6	64.6	64.6

ANNEX 1-PAVEMENT STRENGTH CALCULATION

Calcualtion for average section deflection and average annual pavement strength												
Segement three-Section 0ne and two												
Chaiange	**135+000**	**MM**	**135+200**	**135+300**	**135+300**	**135+400**	**135+500**	**135+600**	**135+600**	**135+700**	**135+800**	**135+900**
Section	**Section 1**				**Section 2**				**Section 3**			
Right lane												
Right lane deflection(10^{-2} mm)	31.8	63.6	46.6	25.4	25.4	46.6	40.3	36.0	36.0	40.3	59.4	67.8
Average right lane deflection	41.9	41.9	41.9	41.9	37.1	37.1	37.1	37.1	50.9	50.9	50.9	50.9
SNP_{wet}=(Equation 2-7)	5.5	5.5	5.5	5.5	6.0	6.0	6.0	6.0	4.9	4.9	4.9	4.9
$ACRA_a$(%)	7.0	7.0	7.0	7.0	4.4	4.4	4.4	4.4	5.5	5.5	5.5	5.5
MMP(mm)	61.6	61.6	61.6	61.6	61.6	61.6	61.6	61.6	61.6	61.6	61.6	61.6
Drainage factor (DF)	2.0	2.0	2.0	2.0	2.0	2.0	2.0	2.0	2.0	2.0	2.0	2.0
SNP_{wet}/SNP_{dry} ratio(f)-Equation (2-11)	0.9	0.9	0.9	0.9	0.9	0.9	0.9	0.9	0.9	0.9	0.9	0.9
$SNPdry=SNP_w/f$	6.1	6.1	6.1	6.1	6.6	6.6	6.6	6.6	5.4	5.4	5.4	5.4
Fraction of dry season(d)- 7 month of dry	0.6	0.6	0.6	0.6	0.6	0.6	0.6	0.6	0.6	0.6	0.6	0.6
f_s =Equation (2-10)	1.0	0.9	1.0	1.0	1.0	1.0	1.0	1.0	1.0	1.0	1.0	1.0
Average Annual Strength(SNP)=$fs*SNP_d$	5.8	5.8	5.8	5.8	6.3	6.3	6.3	6.3	5.2	5.2	5.2	5.2
Average annual deflection in(10-2 mm)	38.5	39.4	38.5	38.5	34.2	34.2	34.2	34.2	47.0	47.0	47.0	47.0
Left lane												
Left lane deflection(10-2 mm)	66.0	61.6	39.6	50.6	50.6	61.6	77.0	39.6	39.6	41.8	48.4	44.0
Average left deflection(10-2 mm)	54.5	54.5	54.5	54.5	57.2	57.2	57.2	57.2	43.5	43.5	43.5	43.5
SNP_{wet}=(Equation 2-7)	4.7	4.7	4.7	4.7	4.5	4.5	4.5	4.5	5.4	5.4	5.4	5.4
$ACRA_a$(%)	2.1	2.1	2.1	2.1	5.1	5.1	5.1	5.1	1.4	1.4	1.4	1.4
MMP(mm)	61.6	61.6	61.6	61.6	61.6	61.6	61.6	61.6	61.6	61.6	61.6	61.6
Drainage factor (DF)	2.0	2.0	2.0	2.0	2.0	2.0	2.0	2.0	2.0	2.0	2.0	2.0
SNP_{wet}/SNP_{dry} ratio(f)-Equation (2-11)	0.9	0.9	0.9	0.9	0.9	0.9	0.9	0.9	0.9	0.9	0.9	0.9
$SNPdry=SNP_w/f$	5.1	5.1	5.1	5.1	5.0	5.0	5.0	5.0	5.9	5.9	5.9	5.9
d-(7 dry months)/12months	0.6	0.6	0.6	0.6	0.6	0.6	0.6	0.6	0.6	0.6	0.6	0.6
f_s =Equation (2-10)	1.0	1.0	1.0	1.0	1.0	1.0	1.0	1.0	1.0	1.0	1.0	1.0
Average Annual Strength(SNP)=$fs*SNP_d$	4.9	4.9	4.9	4.9	4.8	4.8	4.8	4.8	5.7	5.7	5.7	5.7
Average annual deflection in(10-2 mm)	50.6	50.6	50.6	50.6	52.9	52.9	52.9	52.9	40.3	40.3	40.3	40.3

Calcualtion for average section deflection and average annual pavement strength
Segement three-Section 0ne and two

Chaiange	135+900	136+000	136+100	136+200	136+200	136+300	136+400	136+500	136+500	136+600	136+700	136+800	136+800	136+900	137+000
Section	Section 4				Section 5				Section 6				Section 7		
Right lane															
Right lane deflection(10^{-2} mm)	67.8	61.5	25.4	42.4	42.4	63.6	63.6	106.0	106.0	74.2	116.6	106.0	106.0	57.2	59.4
Average right lane deflection(10^{-2} mm)	49.3	49.3	49.3	49.3	68.9	68.9	68.9	68.9	100.7	100.7	100.7	100.7	74.2	74.2	74.2
SNP_{wet}=(Equation 2-7)	5.0	5.0	5.0	5.0	4.0	4.0	4.0	4.0	3.2	3.2	3.2	3.2	3.9	3.9	3.9
$ACRA_a$(%)	12.2	12.2	12.2	12.2	18.4	18.4	18.4	18.4	34.1	34.1	34.1	34.1	12.3	12.3	12.3
MMP(mm)	61.6	61.6	61.6	61.6	61.6	61.6	61.6	61.6	61.6	61.6	61.6	61.6	61.6	61.6	61.6
Drainage factor (DF)	2.00	2.00	2.00	2.00	2.00	2.00	2.00	2.00	2.00	2.00	2.00	2.00	2.00	2.00	2.00
SNP_{wet}/SNP_{dry} ratio(f)-Equation (2-11)	0.90	0.90	0.90	0.90	0.89	0.89	0.89	0.89	0.86	0.86	0.86	0.86	0.90	0.90	0.90
$SNPdry=SNP_w/f$	5.56	5.56	5.56	5.56	4.55	4.55	4.55	4.55	3.69	3.69	3.69	3.69	4.30	4.30	4.30
Fraction of dry season(d)- 7 month of dry	0.58	0.58	0.58	0.58	0.58	0.58	0.58	0.58	0.58	0.58	0.58	0.58	0.58	0.58	0.58
f_s =Equation (2-10)	0.95	0.95	0.95	0.95	0.95	0.95	0.95	0.95	0.94	0.94	0.94	0.94	0.95	0.95	0.95
	5.30	5.30	5.30	5.30	4.32	4.32	4.32	4.32	3.45	3.45	3.45	3.45	4.10	4.10	4.10
Average annual deflection in(10^{-2} mm)	45.1	45.1	45.1	45.1	62.6	62.6	62.6	62.6	89.5	89.5	89.5	89.5	68.1	68.1	68.1
Left lane															
Left lane deflection(10-2 mm)	44.0	121.0	33.0	66.0	66.0	92.4	77.0	55.0	55.0	77.0	66.0	88.0	88.0	70.4	121.0
Average left deflection(10^{-2} mm)	66.0	66.0	66.0	66.0	72.6	72.6	72.6	72.6	71.5	71.5	71.5	71.5	93.1	93.1	93.1
SNP_{wet}=(Equation 2-7)	4.2	4.2	4.2	4.2	3.9	3.9	3.9	3.9	4.0	4.0	4.0	4.0	3.3	3.3	3.3
$ACRA_a$(%)	27.7	27.7	27.7	27.7	18.8	18.8	18.8	18.8	72.5	72.5	72.5	72.5	12.3	12.3	12.3
MMP(mm)	61.6	61.6	61.6	61.6	61.6	61.6	61.6	61.6	61.6	61.6	61.6	61.6	61.6	61.6	61.6
Drainage factor (DF)	2.0	2.0	2.0	2.0	2.0	2.0	2.0	2.0	2.0	2.0	2.0	2.0	2.0	2.0	2.0
SNP_{wet}/SNP_{dry} ratio(f)-Equation (2-11)	0.9	0.9	0.9	0.9	0.9	0.9	0.9	0.9	0.8	0.8	0.8	0.8	0.9	0.9	0.9
$SNPdry=SNP_w/f$	4.8	4.8	4.8	4.8	4.4	4.4	4.4	4.4	4.9	4.9	4.9	4.9	3.7	3.7	3.7
d-(7 dry months)/12months	0.6	0.6	0.6	0.6	0.6	0.6	0.6	0.6	0.6	0.6	0.6	0.6	0.6	0.6	0.6
f_s =Equation (2-10)	0.9	0.9	0.9	0.9	0.9	0.9	0.9	0.9	0.9	0.9	0.9	0.9	1.0	1.0	1.0
Average Annual Strength(SNP)=$fs*SNP_d$	4.5	4.5	4.5	4.5	4.2	4.2	4.2	4.2	4.4	4.4	4.4	4.4	3.6	3.6	3.6
Average annual deflection in(10^{-2} mm)	59.1	59.1	59.1	59.1	65.9	65.9	65.9	65.9	59.8	59.8	59.8	59.8	85.6	85.6	85.6

ANNEX 1-PAVEMENT STRENGTH CALCULATION

Pavement Strength Calculations using Equation 2-1

Pavement Layer	a_i				
	Table 4.7 of Paterson(1987)			**Based on equation, Paterson(1987)**	
GCS Base	0.12 for Axle load of 8t			0.129632	$(29.14\ CBR - 0.1977\ CBR^2 + 0.00045\ CBR^3)\ 10^{-4}$
Sub-base	0.12 for CBR greater than 50			0.120433	0.01 + 0.065LOG10(CBR)
Capping if any	0.1 for CBR greater than 25			0.100866	0.01 + 0.065LOG10(CBR)
Sub-grade				-0.13783	3.51 log10 CBR - 0.85 (log1o CBR)2 - 1.4
				5.141767	**SNC from Equation 2-1**

Pavement Strength Calculations using Equation 2-3					
sub-base	bo	1.6		0.994757	SNBUSAs using equation (2-5)
Capping	b1	0.6		0.655263	SNBUSAs using equation (2-5)
base	b2	0.008		1.63116	SNBASUs using equation (2-4)
AC surfacing	b3	0.00207		1.576	SNBASUs using equation (2-4)
		0.94514		-0.0778	SNSUBGs using equation (2-6)
				4.779379	SNPs using equation (2-3)

ANNEX 2: Traffic Volume, Composition and Traffic Loading

AKAKI - DEBRE ZEIT

Year	Car	L/Rover	S/Bus	L/Bus	S/Truck	M/Truck	H/Truck	Truck & Trailer	Total	H/Truck TT as % of AADT
1998	593	727	426	430	542	474	463	574	4229	25
1999	721	1086	858	705	729	756	852	890	6597	26
2000	721	1086	858	705	729	756	852	890	6597	26
2001	792	1134	518	519	421	667	998	666	5715	29
2002	979	1349	714	643	547	1067	1283	930	7512	29
2003	1310	1733	991	770	498	1374	1339	987	9002	26
2004	1418	1849	1122	791	485	1531	1413	1156	9765	26
2005	1384	0.945136	1338	1149	1081	1847	1665	1737	10201.95	33
2006	1223	1464	1592	995	1367	1480	1344	1340	10805	25
2007	1964	2262	2159	1511	964	2184	1644	2583	15271	28
2008	1982	2185	2377	1654	1911	2043	1908	2298	16358	26
2009	2181	2505	2671	1680	2266	2337	2153	2434	18227	25
2010	2279	2601	2687	1834	2591	2524	2339	2603	19458	25
									Average	27

DEBRE ZEIT - MOJDO

Year	Car	L/Rover	S/Bus	L/Bus	S/Truck	M/Truck	H/Truck	Truck & Trailer	Total	H/Truck TT as % of AADT
1998	420	640	523	253	355	358	413	465	3427	26
1999	368	673	550	343	292	598	546	713	4083	31
2000	544	712	759	581	771	723	707	771	5568	27
2001	440	663	531	474	601	729	787	711	4936	30
2002	919	1269	1120	949	1067	1401	1501	1419	9645	30
2003	701	1193	827	679	881	981	970	1098	7330	28
2004	629	1165	715	538	720	829	837	824	6257	27
2007	1251	1599	1587	1141	1160	1748	1791	1905	12182	30
2008	1109	1268	1560	999	1009	1282	897	1885	10009	28
2009	786	885	1189	708	831	1245	998	1403	8045	30
2010	1217	1613	1735	1343	1549	1837	1864	1982	13140	29
									Average	29

MOJO - SHASHEMENE

Year	Car	L/Rover	S/Bus	L/Bus	S/Truck	M/Truck	H/Truck	Truck & Trailer	Total	H/Truck TT as % of AADT
2001	57	275	224	104	135	178	242	151	1366	29
2002	75	250	233	125	192	249	203	138	1465	23
2003	74	283	237	121	211	216	245	141	1528	25
2004	100	364	291	155	357	234	187	172	1860	19
2005	103	298	321	140	299	265	176	166	1768	19
2006	131	324	328	186	247	365	231	189	2001	21
2007	131	352	381	200	333	346	272	228	2243	22
2008	194	427	543	213	389	357	296	298	2717	22
2009	241	540	642	222	510	276	298	336	3065	21
2010	240	486	561	236	488	278	280	366	2935	22
									Average	22

SHASHEMENE - AWASA

Year	Car	L/Rover	S/Bus	L/Bus	S/Truck	M/Truck	H/Truck	Truck & Trailer	Total	H/Truck TT as % of AADT
2001	38	314	265	101	121	142	223	70	1274	23
2002	59	318	305	92	149	126	157	44	1250	16
2003	73	373	306	92	193	94	143	40	1314	14
2004	74	238	267	100	161	278	125	57	1300	14
2005	92	333	350	152	295	227	144	67	1660	13
2006	120	305	321	173	252	297	122	57	1647	11
2007	192	411	444	172	470	285	144	92	2210	11
2008	206	448	533	258	464	558	326	163	2956	17
2009	255	583	583	296	564	517	448	286	3532	21
2010	234	436	529	217	299	457	203	103	2478	12
									Average	15

ANNEX 2: Traffic Volume, Composition and Traffic Loading

ESAL (Addis Ababa-Modjo)-Based on Consultants 2008 count and projections									
Growth rate	7.40%	7%	7.40%	9.50%	6.60%	6.60%	7.40%		
	AADT							ESAL/year	
Year	S/Bus	M/Bus	L/Bus	S/Truck	M/Truck	H/Truck	Truck-Trailer		
1998	94	47	22	290	60	199	275	721458.45	
1999	101	50	24	318	64	212	295	773784.02	
2000	109	54	26	348	68	226	317	829924.92	
2001	117	58	28	381	73	241	340	890161.02	
2002	125	62	30	417	78	257	365	954792.85	
2003	135	66	32	457	83	274	392	1024143.1	
2004	145	71	34	500	88	292	421	1098558.5	
2005	155	76	37	548	94	311	452	1178411.2	
2006	167	81	39	600	100	332	486	1264100.9	1001735
2007	179	86	42	657	107	353	522	1356057.1	
2008	192	1	46	719	114	377	561	1454741	
2009	207	99	49	772	122	405	602	1562391.8	
2010	222	107	52	829	131	435	647	1678008.8	
2011	238	115	56	891	141	467	694	1802181.5	
2012	256	123	61	957	151	501	746	1935542.9	
								18524258	17750474

8th year AADT and ESAL/year
Actual AADT from counted traffic
Cumulative traffic to date

ESAL (Modjo-Addis Ababa)-Based on Consultant's 2008 count and projections									
Growth rate	7.40%	7%	7.40%	9.50%	6.60%	6.60%	7.40%		
	AADT							ESAL/year	
Year	S/Bus	M/Bus	L/Bus	S/Truck	M/Truck	H/Truck	Truck-Trailer		
1998	102	46	22	254	71	260	295	2123536.6	
1999	110	50	24	278	76	278	317	2275777.2	
2000	118	53	26	305	81	296	340	2438971.8	
2001	127	57	28	334	86	315	365	2613911.6	
2002	136	61	30	365	92	336	393	2801445	
2005	168	75	37	480	112	407	486	3449042.5	
2006	181	80	39	525	119	434	522	3696735.6	2937046
2007	194	85	42	575	127	463	561	3962282.7	
2008	209	91	46	630	135	493	602	4246975.8	
2009	224	98	49	677	145	530	647	4561252	
2010	241	105	52	727	156	569	695	4898784.6	
2011	258	113	56	780	167	611	746	5261294.7	
2012	277	122	61	838	180	656	802	5650630.5	
								54201122	51925345

8th year AADT and ESAL/year
Actual AADT from counted traffic
Cumulative traffic to date

ESAL (Modjo-Meki)-Based on a Consultant's 2008 count and projections									
Growth rate	5.00%	5%	5.00%	9.00%	9.00%	9.00%	7.00%		
	AADT							ESAL/year	
Year	S/Bus	M/Bus	L/Bus	S/Truck	M/Truck	H/Truck	Truck & Trailer		
1998	60	38	20	147	42	93	47	403472.1	
1999	63	40	21	160	46	101	51	433476.43	
	66	42	22	175	50	110	54	465760.49	
2001	70	44	23	190	55	120	58	500501.03	
2002	73	46	25	208	60	131	62	537888.82	
2003	77	49	26	226	65	142	66	578129.7	
2004	81	51	27	247	71	155	71	621445.82	
2005	85	54	29	269	77	169	76	668076.98	
2006	89	56	30	293	84	184	81	718282.03	
2007	93	59	31	319	92	201	87	772340.42	607803.2
2008	98	62	33	348	100	219	93	830553.85	
2009	103	65	35	379	109	236	100	891278.51	
2010	108	68	36	413	119	255	106	956502.95	
2011	113	72	38	451	130	275	114	1026564.9	
2012	119	75	40	491	141	297	122	1101827.6	
								9669153.1	9203393

8th year AADT and ESAL/year
Actual AADT from counted traffic
Cumulative traffic to date

ESAL (Meki-Modjo)-Based on a Consultant's 2008 count and projections									
Growth rate	5.00%	5%	5.00%	9.00%	9.00%	9.00%	7.00%		
	AADT							ESAL/year	
Year	S/Bus	M/Bus	L/Bus	S/Truck	M/Truck	H/Truck	Truck & Trailer		
1998	56	50	23	183	33	92	57	376155.14	
1999	59	53	25	200	36	101	61	411048.27	
2000	62	56	26	218	39	111	66	449247.95	
2001	65	58	27	237	43	122	70	491071.82	
2002	69	61	29	259	48	135	75	536868.29	
2003	72	64	30	282	52	148	81	587019.55	
2004	76	67	32	307	57	162	86	641944.89	
2005	79	71	34	335	63	179	92	702104.26	
2006	83	74	35	365	69	196	99	768002.27	
2007	88	78	37	398	76	216	106	840192.57	627056.4
2008	92	82	39	434	83	235	113	913075.97	
2009	97	86	41	473	90	254	121	984488.51	
2010	101	90	43	516	99	274	129	1061535.4	
2011	107	95	45	562	107	295	138	1144664.1	
2012	112	100	47	613	117	319	148	1234358.1	
								10354574	9905326

8th year AADT and ESAL/year
Actual AADT from counted traffic
Cumulative traffic to date

ESAL (Meki-Zeway)-Based on a Consultant's 2008 count and projections									
Growth rate	5.00%	5%	5.00%	9.00%	9.00%	9.00%	7.00%	ESAL	
	AADT								
Year	S/Bus	M/Bus	L/Bus	S/Truck	M/Truck	H/Truck	Truck & Trailer		
1998	58	21	17	162	40	61	55	411887.6	
1999	61	23	17	176	43	66	59	442081.71	
2000	64	24	18	192	47	72	63	474527.27	
2001	67	25	19	210	51	79	67	509395.03	
2002	70	26	20	228	56	86	72	546868.97	
2003	74	27	21	249	61	94	77	587147.22	
2004	77	29	22	271	67	102	82	630443.3	
2005	81	30	23	296	73	111	88	676987.21	
2006	85	32	24	322	79	121	94	727026.83	
2007	90	33	26	351	86	132	101	780829.27	616653.1
2008	94	35	27	383	94	144	108	838682.4	
2009	99	37	28	417	102	155	116	899601.43	
2010	104	39	30	455	112	168	124	964997.02	
2011	109	41	31	496	122	181	132	1035202	
2012	114	43	33	541	133	195	142	1110574.1	
								9307754.8	8798360

8th year AADT and ESAL/year
Actual AADT from counted traffic
Cumulative traffic to date

ESAL (Zeway-Meki)-Based on a Consultant's 2008 count and projections									
Growth rate	5.00%	5%	5.00%	9.00%	9.00%	9.00%	7.00%	ESAL	
	AADT								
Year	S/Bus	M/Bus	L/Bus	S/Truck	M/Truck	H/Truck	Truck-Trailer		
1998	50	17	17	178	33	48	50	225144.62	
1999	52	18	17	194	36	52	53	244297.34	
2000	55	19	18	211	40	57	57	265106.66	
2001	58	20	19	230	43	62	61	287717.49	
2002	60	21	20	251	47	67	65	312287.54	
2003	63	22	21	274	51	73	70	338988.41	
2004	67	23	22	298	56	80	75	368006.85	
2005	70	24	23	325	61	87	80	399546.1	
2006	73	25	24	354	66	95	86	433827.35	
2007	77	27	26	386	72	104	92	471091.34	359571.5
2008	81	28	27	421	79	113	98	511600.06	
2009	85	29	28	459	86	122	105	551854.88	
2010	89	31	30	500	94	132	112	595310.55	
2011	94	32	31	545	102	142	120	642223.78	
2012	98	34	33	594	112	153	128	692871.99	
								5605326.4	5317609

8th year AADT and ESAL/year
Actual AADT from counted traffic
Cumulative traffic to date

ANNEX 3-COMPACTION INDEX COMPUTATION

Addis-Modjo Base Layer Laboratory Test Result and Relative Compaction calculations

Chainage	ACV %	TFV KN	PI %	CBR at 98 % of MDD	Specific gravity	MDD gm/cm^3	OMC(%)	NMC(%)	Insitu density FDD	Insitu CBR	Relative compaction c_i -	Thickness of AC	thicness(cm)	Z_i	$C_{nom,i}$ (1.02-0.14*Zi)	Rc_i min(1,c_i/c_{no}
23	11.3		8	89	2.827	2.2	7.6	4.9	2.139	85	0.97	10	20	30	0.98	0.99
27	19.9		10	82	2.597	2.132	8.4	5.4	2.141	89	1.00	10	20	30	0.98	1.00
31	16		8	91	2.817	2.21	7	3	2.257	97.5	1.02	10	20	30	0.98	1.00
41	13.7		8	89		2.2	7.4	6	2.345	95	1.07	11	22	33	0.97	1.00
51	21		10	87		2.162	8.8					9	20	29	0.98	
59		242	8	84	2.621	2.096	7.8	3.6	2.057	83.5	0.98	10	19	29	0.98	1.00
66		230	10	83		2.06	8.8	4.9	2	80	0.97	10	21	31	0.98	0.99
71		265	9	84		2.084	10					10	20	30	0.98	0.00
									Average		1.0027	10	20.25	30.25	0.98	1.00

Addis-Modjo Sub-base Layer Laboratory Test Results and Relative Compaction Calcualtion

Chainage	Material Description	ACV %	PI %	CBR at 95 % of MDD	Specificgravity	MDD(gm/cm3)	OMC %	NMC %	Insitu density FDD Gm/Cm^3	Initu CBR	Relative compaction ci -FDD/MDD	Thickness of AC	thicness base(	thicness sub-b	Z_i	$C_{nom,i}$ (1.02-0.1	Rc_i min(1,c_i/c_{no}
23	Cinder /Re	18	NP	56	2.8	2.148	8.6	3.7	1.838	28	0.86	10	20	18	48	0.95	0.90
25	Milled		11	83	2.571	2.207	7.6					10	20	20	50	0.95	
31	Cinder	17	15	25	2.687	1.996	12.2	8.3	1.752	11	0.88	10	20	20	50	0.95	0.92
37	Cinder		NP	85								12	18	20	50	0.95	
41	Milled		14	64	2.77	2.168	9.4	6	2.345	82	1.08	11	22	20	53	0.95	1.00
51	Milled		11	50								9	20	20	49	0.95	0.00
57	Milled		11	66.8	2.281	2.168	9.4					9.5	20	20	49.5	0.95	0.00
63	Milled		11	41	2.625	2.108	8					12	20	20	52	0.95	0.00
69.5	Cinder		9	66	2.568	2.019	8.4	6.7	1.567	18	0.78	11	18		29		
									Average		**0.90**	**10.50**	**19.78**	**19.75**	**47.83**	**0.95**	**0.94**

ANNEX 3-COMPACTION INDEX COMPUTATION

Addis-Modjo Sub-grade Layer Laboratory Test Result and Relative Compaction Calcualtion

Chainage	Material Description	LL	PI %	CBR at 95 % of MDD	Swell at 100%	Linear Shrinkage %	MDDGm/cm3	OMC %	NMC %	Insitu density FDD Gm/Cm^3	Initu CBR	Relative(Density %)	Thickness of AC	thicness base(cm)	thicness sub-base(cm)	Thickness capping(cm)	Z_i	$C_{nom,i}$ (1.02-0.14*Zi)	Rc_i min(1,c_i/c_{nom})
23	Capping/ Cinder	15	3	48.5	0.1	2	2.019	8.2	7.6	1.754	19.5	0.87	10	20	20	30	80	0.91	0.96
27	Capping/ Cinder	38	18	27.7	0.65	3	1.952	14.6	1.1	1.674	14	0.86	10	20	20	30	80	0.91	0.94
29	Cinder		NP	54.8	0.09	2	2.059	7.4					10	20	20	15	65	0.93	
31	Dark Brown Silty Clay	86	39	1.9	10.8	15	1.516	26.2					10	20	20	20	70	0.92	
33	Dark Brown Silty Clay	77	35	2	10.3	13	1.576	26.8					10	19	20	30	79	0.91	
41	Dark Brown Silty Clay	46	22	5.6	2.1	15	1.595	20					11	22	20	15	68	0.92	
55	Dark Brown Silty Clay	61	31	2.5	6.87	15	1.58	21					10	20	20	0	50	0.95	
57	Dark Brown Silty Clay	57	27	2.6	5.1	15	1.577	21.4					9.5	20	20	30	79.5	0.91	

Addis-Modjo Sub-grade Layer Laboratory Test Result and Relative Compaction Calcualtion

Chainage	Material Description	LL	PI %	CBR at 95 % of MDD	Swell at 100%	Linear Shrinkage %	MDDGm/cm3	OMC %	NMC %	Insitu density FDD Gm/Cm^3	Initu CBR	Relative(Density %)	Thickness of AC	thicness base(cm)	thicness sub-base(cm)	Thickness capping(cm)	Z_i	$C_{nom,i}$ (1.02-0.14*Zi)	Rc_i min(1,c_i/c_{nom})
59	Dark Brown Silty Clay	50	24	4.5	2.94	15	1.583	22.2	10.3	1.345	2	0.85	10	18	20	30	78	0.91	0.93
63	Dark Brown Silty Clay	64	32	3.1	4.99	15	1.535	25.2					12	20	20	20	72	0.92	
66	Dark Brown Silty Clay	0.945	27	3.5	4.1	16	1.584	23.4	11.4	1.367	2	0.86	10	21		20	51	0.95	0.91
69.5	Cinder	27	10	33	0.13	3	1.878	10.8					11	18			29	0.98	
71.5	Yellowish Silty Clay	54	25	3.6	4.38	15	1.59	19					10	20	20	0	50	0.95	
									Average			0.86	10.27	19.85	16.92	18.46	65.50	0.93	0.93

	RC_I	thickness		$COMP = \sum_{i=2,n} RC_i \left(\frac{H_i}{\sum_{i=2,n} H_i} \right)$		
Base	1	0.2		0.957		
Sub-Ba	0.94	0.2				
Sub-Gr	0.93	0.2				

ANNEX 4- CALIBRATION OF HDM 4 ROAD DETERIORATION MODELS

Prediction and calibration of cracking initiation for cracking area less than 30%

$$ICA = K_{cia}\left\{CDS^2 a_0 EXP\left[a_1 SNP + a_2\left(\frac{YE4}{SNP^2}\right) + CRT\right]\right\}$$

Lane	Cracking Section	YE4	SNP	a0	a1	a2	CDS	Predicted (years)		Observed cracked(%)	surfacing age	Observed	(pr-obs)^2	
Left	3(52+600-52+900)	2.94	5.92	4.21	0.14	-17.1	1.5	5.169	8.167	0.6	14	13.9	33.36	
Left	3(135+600-135+900)	0.36	5.78	4.21	0.14	-17.1	1	7.865	12.43	1.4	12	11.9	0.326	
Left	1(135+000-135+300)	0.36	4.93	4.21	0.14	-17.1	1	6.517	10.3	2.1	12	11.8	2.218	
Right	1(52+000-52+300)	1	4.51	4.21	0.14	-17.1	1.5	7.684	12.14	2.3	14	13.8	2.653	
Right	3(52+600-52+900)	1	5.4	4.21	0.14	-17.1	1.5	11.22	17.73	3.0	14	13.7	16.29	
Left	1(52+000-52+300)	2.94	4.1	4.21	0.14	-17.1	1.5	0.845	1.335	3.5	14	13.6	151.6	
Right	2(135+300-135+600)	0.62	6.29	4.21	0.14	-17.1	1	7.769	12.27	4.4	12	11.6	0.515	
Left	2(135+300-135+600)	0.36	4.79	4.21	0.14	-17.1	1	6.295	9.946	5.1	12	11.5	2.373	
Right	3(135+600-135+900)	0.62	5.16	4.21	0.14	-17.1	1	5.822	9.199	5.5	12	11.4	5.058	
Right	1(135+000-135+300)	0.945	5.58	4.21	0.14	-17.1	1	5.472	8.645	7.0	12	11.3	7.039	
Left	2(52+300-52+600)	2.94	5.01	4.21	0.14	-17.1	1.5	2.578	4.073	7.1	14	13.3	84.97	
Right	2(52+300-52+600)	1	4.78	4.21	0.14	-17.1	1.5	8.751	13.83	8.5	14	13.1	0.459	
Right	4(52+900-53+200)	1	5.07	4.21	0.14	-17.1	1.5	9.904	15.65	9.2	14	13.1	6.601	
Left	4(52+900-53+200)	2.94	5.2	4.21	0.14	-17.1	1.5	3.056	4.829	11.5	14	12.9	64.37	
Left	1(55+200-55+500)	2.94	4.54	4.21	0.14	-17.1	1.5	1.56	2.465	12.2	14	12.8	106.4	
Right	4(135+900-136+200)	0.62	5.3	4.21	0.14	-17.1	1	6.062	9.578	12.2	12	10.8	1.442	
Right	7(136+800-137+000)	0.62	4.1	4.21	0.14	-17.1	1	3.978	6.285	12.3	12	10.8	20.15	
Left	7(136+800-137+000)	0.36	3.55	4.21	0.14	-17.1	1	4.246	6.709	12.3	12	10.8	16.52	
Right	2(87+100-87+400)	0.61	5.3	4.21	0.14	-17.1	1	6.099	9.636	16.2	13	11.4	3.039	
Right	2(55+500-55+800)	1	5.47	4.21	0.14	-17.1	1.5	11.5	18.18	17.0	14	12.3	34.51	
Right	5(136+200-136+500)	0.62	4.32	4.21	0.14	-17.1	1	4.367	6.9	18.4	12	10.2	10.6	
Right	1(86+800-87+100)	0.61	6.1	4.21	0.14	-17.1	1	7.472	11.81	18.7	13	11.1	0.454	
Left	5(136+200-136+500)	0.36	4.18	4.21	0.14	-17.1	1	5.314	8.396	18.8	12	10.1	2.985	
Left	3(82+600-82+900)	0.63	6.78	4.21	0.14	-17.1	1	8.605	13.6	22.6	13	10.7	8.136	
Right	3(82+600-82+900)	0.61	6.23	4.21	0.14	-17.1	1	7.698	12.16	25.5	13	10.5	2.93	
Left	3(55+800-56+200)	2.94	5.85	4.21	0.14	-17.1	1.5	4.945	7.813	25.7	14	11.4	13.09	
Left	4(135+900-136+200)	0.36	4.48	4.21	0.14	-17.1	1	5.8	9.165	27.7	12	9.2	0.004	
			Sum					**166.6**	**263.2**			**318.9**	**598.1**	
			Mean					**6.17**	**9.749**			**11.8**	**22.15**	**MSE**
			K_{cia} before djusted					**1.914**			**RMSE**	**4.707**		
			K_{cia} after djusted					**1.58**						

ANNEX 4- CALIBRATION OF HDM 4 ROAD DETERIORATION MODELS

Prediction and calibration of cracking initiation for cracking area greater 30%

$$ICA = K_{cia}\left\{CDS^2 a_0 EXP\left[a_1 SNP + a_2\left(\frac{YE4}{SNP^2}\right) + CRT\right]\right\}$$

Lane	Cracking Section	YE4	SNP	a0	a1	a2	CDS	Predicted Initiation		Observed cracked(%)	surfacing age	Observed	
Right	1(55+200-55+500)	1.00	5.09	4.21	0.14	-17.10	1.50	9.98	9.98	31.19	14.00	10.88	0.80
Right	3(55+800-56+200)	1.00	5.23	4.21	0.14	-17.10	1.50	10.54	10.54	44.27	14.00	9.57	0.94
Left	2(55+500-55+800)	2.94	4.81	4.21	0.14	-17.10	1.50	2.11	2.11	38.76	14.00	10.12	64.15
Right	1(82+000-82+300)	0.61	5.80	4.21	0.14	-17.10	1.00	6.95	6.95	73.44	13.00	5.66	1.69
Right	2(82+300-82+600)	0.61	6.26	4.21	0.14	-17.10	1.00	7.75	7.75	87.98	13.00	4.20	12.59
Left	1(82+000-82+300)	0.63	5.56	4.21	0.14	-17.10	1.00	6.47	6.47	62.20	13.00	6.78	0.10
Left	2(82+300-82+600)	0.63	6.13	4.21	0.14	-17.10	1.00	7.46	7.46	79.81	13.00	5.02	5.94
Left	1(86+800-87+100)	0.63	5.06	4.21	0.14	-17.10	1.00	5.61	5.61	53.51	13.00	7.65	4.15
Left	2(87+100-87+400)	0.63	4.37	4.21	0.14	-17.10	1.00	4.42	4.42	58.55	13.00	7.15	7.45
Right	6(136+500-136+800)	0.95	3.45	4.21	0.14	-17.10	1.00	1.76	1.76	34.14	12.00	8.59	46.66
Left	6(136+500-136+800)	0.36	4.44	4.21	0.14	-17.10	1.00	5.74	5.74	72.55	12.00	4.75	0.98
			Sum					**68.79**	**68.79**			**80.36**	**145.44**
			Mean					**6.25**	**6.25**			**7.31**	**13.22**
			K_{cia} before djusted					**1.17**			**RMSE**	**3.64**	**MSE**
			K_{cia} after djusted					**1**					

ANNEX 4- CALIBRATION OF HDM 4 ROAD DETERIORATION MODELS

Prediction and calibration of cracking initiation for overlaid Sections

$$ICA = K_{cia}\left\{CDS^2\left[MAX\left[a_0 exp\left[a_1 SNP + a_2\left(\frac{YE4}{SNP^2}\right)\right] MAX\left(1 - \frac{PCRW}{a_3}, 0\right) a_4 HSNEW\right]\right] + CRT\right\}$$

Lane	Cracking Section	YE4	SNP	a0	a1	a2	a3	a4	HSNEW(mm)	PCRW(%)	CDS	Predicted (years)		Observed cracked(%)	surfacing age	Observed	
Right	4(82+900-83+200)	0.61	6.61	4.21	0.14	-17.1	30	0.025	20	30	1	0.5	0.9	0.0	13	13.0	146.4
Left	4(82+900-83+200)	0.63	6.81	4.21	0.14	-17.1	30	0.025	20	30	1	8.659	15.59	1.1	13	12.9	7.3
Right	3(87+400-87+700)	0.61	4.5	4.21	0.14	-17.1	30	0.025	20	30	1	4.723	8.501	0.6	13	12.9	19.8
Right	4(87+700-88+000)	0.61	5.23	4.21	0.14	-17.1	30	0.025	20	30	1	5.979	10.76	3.4	13	12.7	3.6
Left	4(87+700-88+000)	0.63	5.85	4.21	0.14	-17.1	30	0.025	20	30	1	6.97	12.55	19.0	13	11.1	2.1
							Sum					**26.83**				**62.6**	**179.1**
							Mean					**5.366**				**12.52**	**35.8**
							K_{cia} before djusted					**2.333**			**RMSE**	**5.985**	
							K_{cia} after djusted					**1.8**					

0.945

ANNEX 4- CALIBRATION OF HDM 4 ROAD DETERIORATION MODELS

Prediction and calibration of wide cracking initiation for cracking area less than 30%

$$ICW = K_{ciw}\, Max[(a_0 + a_1 ICA), a_2 ICA]$$

Lane	Cracking Section	All cracking coeff.					Wide cracking coeff.			CDS	Predicted all cracking initiation age(years)	Predicted wide cracking initiation age(years)	Wide cracking prediction adjusted by factor	Observed all cracking(%)	Observed wide cracking	surfacing age	Observed all intiation	Observed wide intiation	
		YE4	SNP	a0	a1	a2	a0	a1	a2										
Right	2(52+300-52+600)	1	4.78	4.21	0.14	-17.1	2.46	0.93	0	1.5	8.75	10.60	14.84	8.51	0.95	14.00	13.15	13.90	0.87
Right	4(52+900-53+200)	1	5.07	4.21	0.14	-17.1	2.46	0.93	0	1.5	9.90	11.67	16.34	9.21	8.82	14.00	13.08	13.12	10.37
Left	2(52+300-52+600)	2.94	5.01	4.21	0.14	-17.1	2.46	0.93	0	1.5	2.58	4.86	6.80	8.46	8.46	14.00	13.15	13.15	40.38
Left	4(52+900-53+200)	2.94	5.2	4.21	0.14	-17.1	2.46	0.93	0	1.5	3.06	5.30	7.42	11.58	11.58	14.00	12.84	12.84	29.36
Right	2(55+500-55+800)	1	5.47	4.21	0.14	-17.1	2.46	0.93	0	1.5	11.50	13.16	18.42	17.68	16.26	14.00	12.23	12.37	36.58
Left	1(55+200-55+500)	2.94	4.54	4.21	0.14	-17.1	2.46	0.93	0	1.5	1.56	3.91	5.48	12.18	12.06	14.00	12.78	12.79	53.55
Left	3(55+800-56+200)	2.94	5.85	4.21	0.14	-17.1	2.46	0.93	0	1.5	4.94	7.06	9.88	25.69	25.80	14.00	11.43	11.42	2.37
Right	3(82+600-82+900)	0.61	6.23	4.21	0.14	-17.1	2.46	0.93	0	1	7.70	9.62	13.47	25.49	25.05	13.00	10.45	10.50	8.83
Left	3(82+600-82+900)	0.945	6.78	4.21	0.14	-17.1	2.46	0.93	0	1	7.65	9.58	13.41	22.57	22.08	13.00	10.74	10.79	6.84
Right	1(86+800-87+100)	0.61	6.1	4.21	0.14	-17.1	2.46	0.93	0	1	7.47	9.41	13.17	18.69	16.25	13.00	11.13	11.38	3.23
Right	2(87+100-87+400)	0.61	5.3	4.21	0.14	-17.1	2.46	0.93	0	1	6.10	8.13	11.38	16.20	14.84	13.00	11.38	11.52	0.02
Right	1(135+000-135+30	0.62	5.58	4.21	0.14	-17.1	2.46	0.93	0	1	6.54	8.54	11.96	7.01	2.49	12.00	11.30	11.75	0.04
Right	4(135+900-136+20	0.62	5.3	4.21	0.14	-17.1	2.46	0.93	0	1	6.06	8.10	11.34	12.21	3.30	12.00	10.78	11.67	0.11
Right	5(136+200-136+50	0.62	4.32	4.21	0.14	-17.1	2.46	0.93	0	1	4.37	6.52	9.13	18.44	7.41	12.00	10.16	11.26	4.53
Right	7(136+800-137+00	0.62	4.1	4.21	0.14	-17.1	2.46	0.93	0	1	3.98	6.16	8.62	12.26	0.76	12.00	10.77	11.92	10.89
Left	4(135+900-136+20	0.36	4.48	4.21	0.14	-17.1	2.46	0.93	0	1	5.80	7.85	11.00	27.69	21.81	12.00	9.23	9.82	1.39
Left	5(136+200-136+50	0.36	4.18	4.21	0.14	-17.1	2.46	0.93	0	1	5.31	7.40	10.36	18.76	16.61	12.00	10.12	10.34	0.00
Left	7(136+800-137+00	0.36	3.55	4.21	0.14	-17.1	2.46	0.93	0	1	4.25	6.41	8.97	12.27	5.11	12.00	10.77	11.49	6.34
Right	1(52+000-52+300)	1	4.51	4.21	0.14	-17.1	2.46	0.93	0	1.5	7.68	9.61	13.45	2.31	1.15	14.00	13.77	13.88	0.19
Right	3(52+600-52+900)	1	5.4	4.21	0.14	-17.1	2.46	0.93	0	1.5	11.22	12.90	18.06	3.04	3.04	14.00	13.70	13.70	19.01
Left	1(52+000-52+300)	2.94	4.1	4.21	0.14	-17.1	2.46	0.93	0	1.5	0.85	3.25	4.54	3.86	3.86	14.00	13.65	13.61	82.26
Left	3(52+600-52+900)	2.94	5.92	4.21	0.14	-17.1	2.46	0.93	0	1.5	5.17	7.27	10.17	1.28	1.28	14.00	13.94	13.87	13.68
Right	2(135+300-135+60	0.62	6.29	4.21	0.14	-17.1	2.46	0.93	0	1	7.77	9.68	13.56	4.43	1.34	12.00	11.56	11.87	2.87
Right	3(135+600-135+90	0.62	5.16	4.21	0.14	-17.1	2.46	0.93	0	1	5.82	7.87	11.02	5.52	0.55	12.00	11.45	11.94	0.85
Left	3(135+600-135+90	0.36	5.78	4.21	0.14	-17.1	2.46	0.93	0	1	7.86	9.77	13.68	1.45	1.41	12.00	11.86	11.86	3.33
						Sum					**153.9**	**204.6**	**286.5**				**295.4**	**302.8**	**337.9**
						Mean					**5.70**	**7.58**					**10.94**	**11.21**	**12.51**
						K_{ciw} before djusted						**1.48**				**RMSE**	**3.54**		
						K_{ciw} after djusted						**1.4**							

ANNEX 4- CALIBRATION OF HDM 4 ROAD DETERIORATION MODELS

Prediction and calibration of wide cracking initiation for cracking area greater than 30%

$$ICW = K_{ciw}\, Max[(a_0 + a_1 ICA), a_2 ICA]$$

Lane	Cracking Section			All cracking coeff.			Wide cracking coeff.			CDS	Predicted all cracking initiation age(years)	Predicted wide cracking initiation age(years)	Wide cracking prediction adjusted by factor	Observed all cracking(%)	Observed wide cracking	surfacing age	Observed all intiation	Observed wide intiation	
		YE4	SNP	a0	a1	a2	a0	a1	a2										
Right	1(55+200-55+500)	1	5.1	4.2	0.1	-17.1	2.5	0.9	0.0	1.5	10.0	11.7	10.0	32.3	30.0	14.0	10.8	11.0	1.0
Right	3(55+800-56+200)	1	5.2	4.2	0.1	-17.1	2.5	0.9	0.0	1.5	10.5	12.3	10.4	44.3	43.5	14.0	9.6	9.6	0.6
Left	2(55+500-55+800)	2.94	4.8	4.2	0.1	-17.1	2.5	0.9	0.0	1.5	2.1	4.4	3.8	38.8	38.8	14.0	10.1	10.1	40.4
Right	1(82+000-82+300)	0.61	5.8	4.2	0.1	-17.1	2.5	0.9	0.0	1.0	7.0	8.9	7.6	68.7	68.7	13.0	6.1	6.1	2.1
Right	2(82+300-82+600)	0.61	6.3	4.2	0.1	-17.1	2.5	0.9	0.0	1.0	7.7	9.7	8.2	84.1	83.2	13.0	4.6	4.7	12.5
Left	1(82+000-82+300)	0.63	5.6	4.2	0.1	-17.1	2.5	0.9	0.0	1.0	6.5	8.5	7.2	58.2	58.2	13.0	7.2	7.2	0.0
Left	2(82+300-82+600)	0.63	6.1	4.2	0.1	-17.1	2.5	0.9	0.0	1.0	7.5	9.4	8.0	79.8	79.3	13.0	5.0	5.1	8.5
Left	1(86+800-87+100)	0.63	5.1	4.2	0.1	-17.1	2.5	0.9	0.0	1.0	5.6	7.7	6.5	53.5	53.2	13.0	7.6	7.7	1.3
Left	2(87+100-87+400)	0.95	4.4	4.2	0.1	-17.1	2.5	0.9	0.0	1.0	3.3	5.6	4.7	58.5	47.4	13.0	7.1	8.3	12.5
Right	6(136+500-136+800	0.62	3.5	4.2	0.1	-17.1	2.5	0.9	0.0	1.0	2.8	5.1	4.3	34.1	8.5	12.0	8.6	11.2	46.9
Left	6(136+500-136+800	0.36	4.4	4.2	0.1	-17.1	2.5	0.9	0.0	1.0	5.7	7.8	6.6	72.5	53.4	12.0	4.7	6.7	0.0
						Sum					**68.8**	**91.0**	**77.3**				**81.5**	**87.6**	**125.9**
						Mean					**6.3**	**8.3**					**7.4**	**8.0**	**11.4**
						K_{ciw} before djusted						**1.0**				**RMSE**	**3.4**		
						K_{ciw} after djusted						**0.9**							

ANNEX 4- CALIBRATION OF HDM 4 ROAD DETERIORATION MODELS

Prediction and calibration of wide cracking initiation for Overalid Sections

$$ICW = K_{ciw}\, Max[(a_0 + a_1 ICA), a_2 ICA]$$

Lane	Cracking Section			All cracking coeff.							Wide cracking coeff.												
		YE4	SNP	a0	a1	a2	a3	a4	HSNEW(mm)	PCRW(%)	a0	a1	a2	CDS	Predicted Initiation time(years)	Predicted wide cracking initiation age(years)	Wide cracking prediction adjusted by factor	Observed all cracking(%)	Observed wide cracking	surfacing age	Observed all intiation	Observed wide intiation	Error^2
Right	4(82+900-83+200)	0.61	6.61	4.21	0.14	-17	30	0.03	20	30	2.46	0.93	0	1	0.5	2.93	4.68	0.0	0.0	13	13.0	13.0	69.2
Left	4(82+900-83+200)	0.63	6.81	4.21	0.14	-17	30	0.03	20	30	2.46	0.93	0	1	8.66	10.5	16.8	1.1	1.1	13	12.9	12.9	15.4
Right	3(87+400-87+700)	0.61	4.5	4.21	0.14	-17	30	0.03	20	30	2.46	0.93	0	1	4.72	6.85	11	0.6	0.1	13	12.9	13.0	4.1
Left	3(87+400-87+700)	0.63	4.37	4.21	0.14	-17	1	0.03	20	30	2.46	0.93	0	1	4.42	6.57	10.5	7.9	2.0	13	12.2	12.8	5.3
Right	4(87+700-88+000)	0.61	5.23	4.21	0.14	-17	30	0.03	20	30	2.46	0.93	0	1	5.98	8.02	12.8	3.4	2.6	13	12.7	12.7	0.0
Left	4(87+700-88+000)	0.63	5.85	4.21	0.14	-17	30	0.03	20	30	2.46	0.93	0	1	6.97	8.94	14.3	19.0	3.1	13	11.1	12.7	2.6
											Sum					43.8					74.8	77.1	96.7
											Mean					7.3					12.5	12.9	16.1
											K_{ciw} before djusted					1.76						16.1	
											K_{ciw} after djusted					1.6					RMSE	4.01	

ANNEX 4- CALIBRATION OF HDM 4 ROAD DETERIORATION MODELS

Analysis for fitting of Sigmod Curve

$$y = \frac{(cc + a)}{(1 + e^{x_o - x})/b}$$

Lane	Cracking Section	Age since crack initiation(years)	Observed area of cracking(%)	Best fit sigmoidal curve	(Pr-obs)^2
		cc	a	xo	b
		45.61229	25.61231	1.475293	0.061705
Left	2(52+300-52+600)	0.4	8.5	1.52094	48.78373
Right	1(135+000-135+300)	1.9	7.0	5.92416	1.189793
Left	1(135+000-135+300)	1.9	2.1	6.13531	15.94193
Right	1(52+000-52+300)	2.1	2.3	7.29704	24.86283
Left	2(135+300-135+600)	2.2	5.1	8.35673	10.38787
Right	4(135+900-136+200)	2.6	12.2	11.4103	0.641124
Right	3(135+600-135+900)	0.9	5.5	2.49581	9.147447
Left	4(135+900-136+200)	3.0	27.7	15.8439	140.2714
Right	2(87+100-87+400)	3.5	16.2	23.4111	51.95895
Left	5(136+200-136+500)	3.8	18.8	26.9351	66.77489
Left	1(86+800-87+100)	4.3	53.5	36.307	295.9196
Left	2(87+100-87+400)	6.2	58.5	61.9186	11.36743
				Sum	677.247
				mean	32.24986
				RMSE	5.678896

ANNEX 4- CALIBRATION OF HDM 4 ROAD DETERIORATION MODELS

Prediction of the time to 30% of area cracking progression

$$\mathbf{t_{ci} = \frac{[(1 - Z_a)50^{a_1} + Z_a SCA^{a_1} - 0.5^{a_1}]}{a_0 a_1}}$$

Direction	Chainage	Age	Predicted initiation age	Calibrated initiation age	Age since initiation	Observed area of cracking	Z	ZZ	SCR_{it}	a	b	t_{30}
Left	2(52+300-52+600)	14	8.751	13.83	0.4	8.5	1	1	30	1.84	0.45	4.696
Right	1(135+000-135+300	12	6.099	9.636	1.9	7.0	1	1	30	1.84	0.45	4.696
Left	1(135+000-135+300	12	6.541	10.34	1.9	2.1	1	1	30	1.84	0.45	4.696
Right	1(52+000-52+300)	14	6.062	9.578	2.1	2.3	1	1	30	1.84	0.45	4.696
Left	2(135+300-135+600	12	5.8	9.165	2.2	5.1	1	1	30	1.84	0.45	4.696
Right	4(135+900-136+200	12	5.314	8.396	2.6	12.2	1	1	30	1.84	0.45	4.696
Right	3(135+600-135+900	12	5.613	8.869	3.0	5.5	1	1	30	1.84	0.45	4.696
Left	4(135+900-136+200	12	4.416	6.977	3.0	27.7	1	1	30	1.84	0.45	4.696
Right	2(87+100-87+400)	0.945	7.684	12.14	3.5	16.2	1	1	30	1.84	0.45	4.696
Left	5(136+200-136+500	12	5.822	9.199	3.8	18.8	1	1	30	1.84	0.45	4.696
Left	1(86+800-87+100)	13	6.517	10.3	4.3	53.5	1	1	30	1.84	0.45	4.696
Left	2(87+100-87+400)	13	6.295	9.946	6.2	58.5	1	1	30	1.84	0.45	4.696

ANNEX 4- CALIBRATION OF HDM 4 ROAD DETERIORATION MODELS

Rutting Due to Intitial Desnfication

$$\mathbf{RDO} = \mathbf{K_{rid}}\left[\mathbf{a_0}(\mathbf{YE4}\ \mathbf{10^6})^{(\mathbf{a_1}+\mathbf{a_2}\mathbf{DEF})}\mathbf{SNP}^{\mathbf{a3}}\mathbf{COMP}^{\mathbf{a_4}}\right]$$

Segement	Section	Sub-Section		Lane	Observed mean Rut depth	Standard deviation of rut depth	YE4	SNP	DEF	COMP	a_0	a_1	a_2	a_3	a_4	Predicted Rutting(mm)
		Start	End													
1	1	52+000	52+300	Right	10.4	3.0	1	4.51	0.584	95	51740	0.09	0.0384	-0.502	-2.3	3.24503
		52+300	52+600	Right	13.1	1.7	1	4.78	0.533	95	51740	0.09	0.0384	-0.502	-2.3	3.06756
		52+600	52+900	Right	12.7	1.9	1	5.43	0.434	95	51740	0.09	0.0384	-0.502	-2.3	2.73015
		52+900	53+200	Right	9.9	1.6	1	5.16	0.484	95	51740	0.09	0.0384	-0.502	-2.3	2.87624
		52+000	52+300	Left	12.8	1.9	2.94	4.1	0.679	95	51740	0.09	0.0384	-0.502	-2.3	4.05741
		52+300	52+600	Left	14.0	1.7	2.94	5.01	0.494	95	51740	0.09	0.0384	-0.502	-2.3	3.30063
		52+600	52+900	Left	13.3	1.9	2.94	5.92	0.377	95	51740	0.09	0.0384	-0.502	-2.3	2.83889
		0.945136	53+200	Left	12.8	5.2	2.94	5.2	0.464	95	51740	0.09	0.0384	-0.502	-2.3	3.18442
	2	55+200	55+500	Right	12.9	5.5	1	5.09	0.48	95	51740	0.09	0.0384	-0.502	-2.3	2.88989
		55+500	55+800	Right	9.6	5.2	1	5.47	0.476	95	51740	0.09	0.0384	-0.502	-2.3	2.7814
		55+800	56+200	Right	15.4	4.2	1	5.23	0.461	95	51740	0.09	0.0384	-0.502	-2.3	2.82221
		55+200	55+500	Left	8.8	3.3	2.94	4.54	0.573	95	51740	0.09	0.0384	-0.502	-2.3	3.62824
		55+500	55+800	Left	10.2	3.7	2.94	4.81	0.556	95	51740	0.09	0.0384	-0.502	-2.3	3.49043
		55+800	56+200	Left	11.1	3.4	2.94	5.85	0.383	95	51740	0.09	0.0384	-0.502	-2.3	2.86571
2	1	82+000	82+300	Right	13.6	6.2	0.61	5.8	0.39	95	51740	0.09	0.0384	-0.502	-2.3	2.44986
		82+300	82+600	Right	11.8	4.9	0.61	6.26	0.346	95	51740	0.09	0.0384	-0.502	-2.3	2.3053
		82+600	82+900	Right	8.0	4.9	0.61	6.23	0.348	95	51740	0.09	0.0384	-0.502	-2.3	2.31323
		82+900	83+200	Right	6.4	1.6	0.61	6.61	0.302	95	51740	0.09	0.0384	-0.502	-2.3	2.19327
		82+000	82+300	Left	13.2	5.9	0.63	5.56	0.417	95	51740	0.09	0.0384	-0.502	-2.3	2.54589
		82+300	82+600	Left	9.3	3.6	0.63	6.13	0.358	95	51740	0.09	0.0384	-0.502	-2.3	2.35192
		82+600	82+900	Left	8.5	2.5	0.63	6.78	0.307	95	51740	0.09	0.0384	-0.502	-2.3	2.17817
	2	82+900	83+200	Left	9.0	9.4	0.63	6.81	0.297	95	51740	0.09	0.0384	-0.502	-2.3	2.16224
		86+800	87+100	Right	6.1	2.7	0.61	6.1	0.362	95	51740	0.09	0.0384	-0.502	-2.3	2.35465
		87+100	87+400	Right	8.7	4.4	0.61	5.3	0.451	95	51740	0.09	0.0384	-0.502	-2.3	2.64453
		87+400	87+700	Right	9.8	3.8	0.61	4.5	0.59	95	51740	0.09	0.0384	-0.502	-2.3	3.08249
		87+100	87+400	Left	11.6	4.6	0.63	4.37	0.615	95	51740	0.09	0.0384	-0.502	-2.3	3.18008

Rutting Due to Intitial Desnfication

$$\mathbf{RDO} = \mathbf{K_{rid}}\left[\mathbf{a_0}(\mathbf{YE4}\ \mathbf{10^6})^{(\mathbf{a_1}+\mathbf{a_2}\mathbf{DEF})}\mathbf{SNP^{a3}COMP^{a_4}}\right]$$

Segement	Section	Sub-Section		Lane	Observed mean Rut depth	Standard deviation of rut depth	YE4	SNP	DEF	COMP	a_0	a_1	a_2	a_3	a_4	Predicted Rutting(mm)
		Start	End													
		87+400	87+700	Left	8.2	3.5	0.63	4.37	0.614	95	51740	0.09	0.0384	-0.502	-2.3	3.17845
		87+700	88+000	Left	9.2	3.6	0.63	5.85	0.646	95	51740	0.09	0.0384	-0.502	-2.3	2.79095
3	1&2	135+000	135+300	Right	4.3	1.2	0.62	5.58	0.385	95	51740	0.09	0.0384	-0.502	-2.3	2.49575
		135+300	135+600	Right	4.9	2.4	0.62	6.29	0.342	95	51740	0.09	0.0384	-0.502	-2.3	2.29893
		135+600	135+900	Right	4.7	2.0	0.62	5.16	0.47	95	51740	0.09	0.0384	-0.502	-2.3	2.71124
		135+900	136+200	Right	4.4	2.9	0.62	5.3	0.451	95	51740	0.09	0.0384	-0.502	-2.3	2.64915
		136+200	136+500	Right	4.3	1.7	0.62	4.32	0.626	95	51740	0.09	0.0384	-0.502	-2.3	3.21073
		136+500	136+800	Right	9.0	4.6	0.62	3.45	0.895	95	51740	0.09	0.0384	-0.502	-2.3	4.12539
		136+800	137+000	Right	7.9	7.7	0.62	4.1	0.681	95	51740	0.09	0.0384	-0.502	-2.3	3.39026
		135+000	135+300	Left	8.7	3.2	0.36	4.93	0.506	95	51740	0.09	0.0384	-0.502	-2.3	2.66245
		135+300	135+600	Left	5.7	2.2	0.36	4.79	0.529	95	51740	0.09	0.0384	-0.502	-2.3	2.73193
		135+600	135+900	Left	9.7	3.1	0.36	5.78	0.403	95	51740	0.09	0.0384	-0.502	-2.3	2.33683
		135+900	136+200	Left	5.2	3.0	0.36	4.48	0.591	95	51740	0.09	0.0384	-0.502	-2.3	2.91263
		136+200	136+500	Left	3.7	1.7	0.36	4.18	0.659	95	51740	0.09	0.0384	-0.502	-2.3	3.1182
		136+500	136+800	Left	5.0	2.1	0.36	4.44	0.598	95	51740	0.09	0.0384	-0.502	-2.3	2.93585
		136+800	137+000	Left	3.3	1.2	0.36	3.55	0.856	95	51740	0.09	0.0384	-0.502	-2.3	3.72866

ANNEX 4- CALIBRATION OF HDM 4 ROAD DETERIORATION MODELS

Rutting Due to Strutcural Deformation after cracking

$$\Delta RDST_{crk} = K_{rst}\left(a_0 SNP^{a_1} YE4^{a_2} COMP^{a_3} CRX_a^{a_4}\right)$$

Segement	Section	Sub-Section		Lane	Observed mean Rut depth(mm)	Standard deviation of rut depth(mm)	YE4	SNP	COMP	MMP	$ACX_{a(\%)}$	a_0	a_1	a_2	a_3	a_4	Rutting after Cracking(mm)	Years since initiation(mm)	Rutting after initiation(mm)
		Start	End																
1	2	52+000	52+300	Right	10.4	3.0	1	4.51	95	71	1.6	2E-05	-0.84	0.14	1.07	1.11	0.0011	0.23	0.00
		52+300	52+600	Right	13.1	1.7	1	4.78	95	71	3.9	2E-05	-0.84	0.14	1.07	1.11	0.0029	0.85	0.00
		52+600	52+900	Right	12.7	1.9	1	5.4	95	71	3.1	2E-05	-0.84	0.14	1.07	1.11	0.002	0.30	0.00
		52+900	53+200	Right	9.9	1.6	1	5.1	95	71	9.1	2E-05	-0.84	0.14	1.07	1.11	0.007	0.92	0.01
		52+000	52+300	Left	12.8	1.9	2.93	4.1	95	71	3.5	2E-05	-0.84	0.14	1.07	1.11	0.0034	0.35	0.00
		52+300	52+600	Left	14.0	1.7	2.93	5.01	95	71	7.1	2E-05	-0.84	0.14	1.07	1.11	0.0063	0.71	0.00
		52+600	52+900	Left	13.3	1.9	2.93	5.92	95	71	0.6	2E-05	-0.84	0.14	1.07	1.11	0.0003	0.06	0.00
		0.945136	53+200	Left	12.8	5.2	2.93	5.2	95	71	11.5	2E-05	-0.84	0.14	1.07	1.11	0.0104	1.15	0.01
	2	55+200	55+500	Right	12.9	5.5	1	5.09	95	71	31.2	2E-05	-0.84	0.14	1.07	1.11	0.0275	3.12	0.09
		55+500	55+800	Right	9.6	5.2	1	5.47	95	71	17.0	2E-05	-0.84	0.14	1.07	1.11	0.0132	1.70	0.02
		55+800	56+200	Right	15.4	4.2	1	5.23	95	71	44.3	2E-05	-0.84	0.14	1.07	1.11	0.0397	4.43	0.18
		55+200	55+500	Left	8.8	3.3	2.93	4.54	95	71	12.2	2E-05	-0.84	0.14	1.07	1.11	0.0124	1.22	0.02
		55+500	55+800	Left	10.2	3.7	2.93	4.81	95	71	38.8	2E-05	-0.84	0.14	1.07	1.11	0.0427	3.88	0.17
		55+800	56+200	Left	11.1	3.4	2.93	5.85	95	71	25.7	2E-05	-0.84	0.14	1.07	1.11	0.023	2.57	0.06
2	1	82+000	82+300	Right	13.6	6.2	0.59	5.8	95	82	69.3	2E-05	-0.84	0.14	1.07	1.11	0.0649	7.34	0.48
		82+300	82+600	Right	11.8	4.9	0.59	6.26	95	82	84.4	2E-05	-0.84	0.14	1.07	1.11	0.0757	8.80	0.67
		82+600	82+900	Right	8.0	4.9	0.59	6.23	95	82	25.5	2E-05	-0.84	0.14	1.07	1.11	0.0201	2.55	0.05
		82+900	83+200	Right	6.4	1.6	0.59	6.61	95	82	0.0	2E-05	-0.84	0.14	1.07	1.11	0	0.00	0.00
		82+000	82+300	Left	13.2	5.9	0.62	5.56	95	82	58.7	2E-05	-0.84	0.14	1.07	1.11	0.0563	6.22	0.35
		82+300	82+600	Left	9.3	3.6	0.62	6.13	95	82	80.3	2E-05	-0.84	0.14	1.07	1.11	0.0734	7.98	0.59
		82+600	82+900	Left	8.5	2.5	0.62	6.78	95	82	22.5	2E-05	-0.84	0.14	1.07	1.11	0.0164	2.26	0.04
	2	82+900	83+200	Left	9.0	9.4	0.62	6.81	95	82	1.1	2E-05	-0.84	0.14	1.07	1.11	0.0006	0.11	0.00
		86+800	87+100	Right	6.1	2.7	0.59	6.1	95	82	17.4	2E-05	-0.84	0.14	1.07	1.11	0.0134	1.87	0.03

Rutting Due to Strutcural Deformation after cracking

$$\Delta RDST_{crk} = K_{rst}\left(a_0 SNP^{a_1} YE4^{a_2} COMP^{a_3} CRX_a^{a_4}\right)$$

Segement	Section	Sub-Section		Lane	Observed mean Rut depth(mm)	Standard deviation of rut depth(mm)	YE4	SNP	COMP	MMP	$ACX_{a(\%)}$	a_0	a_1	a_2	a_3	a_4	Rutting after Cracking(mm)	Years since initiation(mm)	Rutting after initiation(mm)
		Start	End																
		87+100	87+400	Right	8.7	4.4	0.59	5.3	95	82	15.5	2E-05	-0.84	0.14	1.07	1.11	0.0133	1.62	0.02
		86+800	87+100	Left	12.7	7.3	0.62	5.06	95	82	53.9	2E-05	-0.84	0.14	1.07	1.11	0.0554	5.35	0.30
		87+100	87+400	Left	11.6	4.6	0.62	4.37	95	82	52.2	2E-05	-0.84	0.14	1.07	1.11	0.0606	5.85	0.35
		87+400	87+700	Left	8.2	3.5	0.62	4.37	95	82	4.7	2E-05	-0.84	0.14	1.07	1.11	0.0042	0.79	0.00
		87+700	88+000	Left	9.2	3.6	0.62	5.85	95	82	9.3	2E-05	-0.84	0.14	1.07	1.11	0.007	1.90	0.01
3	1&2	135+000	135+300	Right	4.3	1.2	0.6	5.58	95	61.6	4.3	2E-05	-0.84	0.14	1.07	1.11	0.0023	0.70	0.00
		135+300	135+600	Right	4.9	2.4	0.6	6.29	95	61.6	2.6	2E-05	-0.84	0.14	1.07	1.11	0.0012	0.44	0.00
		135+600	135+900	Right	4.7	2.0	0.6	5.16	95	61.6	2.5	2E-05	-0.84	0.14	1.07	1.11	0.0013	0.55	0.00
		135+900	136+200	Right	4.4	2.9	0.6	5.3	95	61.6	6.8	2E-05	-0.84	0.14	1.07	1.11	0.0039	1.22	0.00
		136+200	136+500	Right	4.3	1.7	0.6	4.32	95	61.6	11.8	2E-05	-0.84	0.14	1.07	1.11	0.0086	1.84	0.02
		136+500	136+800	Right	9.0	4.6	0.6	3.45	95	61.6	18.6	2E-05	-0.84	0.14	1.07	1.11	0.0172	3.41	0.06
		136+800	137+000	Right	7.9	7.7	0.6	4.1	95	61.6	5.3	2E-05	-0.84	0.14	1.07	1.11	0.0037	1.23	0.00
		135+000	135+300	Left	8.7	3.2	0.35	4.93	95	61.6	2.1	2E-05	-0.84	0.14	1.07	1.11	0.0011	0.21	0.00
		135+300	135+600	Left	5.7	2.2	0.35	4.79	95	61.6	5.2	2E-05	-0.84	0.14	1.07	1.11	0.0029	0.51	0.00
		135+600	135+900	Left	9.7	3.1	0.35	5.78	95	61.6	1.4	2E-05	-0.84	0.14	1.07	1.11	0.0006	0.14	0.00
		135+900	136+200	Left	5.2	3.0	0.35	4.48	95	61.6	24.3	2E-05	-0.84	0.14	1.07	1.11	0.0173	2.77	0.05
		136+200	136+500	Left	3.7	1.7	0.35	4.18	95	61.6	17.6	2E-05	-0.84	0.14	1.07	1.11	0.0128	1.88	0.02
		136+500	136+800	Left	5.0	2.1	0.35	4.44	95	61.6	61.4	2E-05	-0.84	0.14	1.07	1.11	0.0486	7.25	0.35
		136+800	137+000	Left	3.3	1.2	0.35	3.55	95	61.6	8.0	2E-05	-0.84	0.14	1.07	1.11	0.0061	1.23	0.01

ANNEX 4- CALIBRATION OF HDM 4 ROAD DETERIORATION MODELS

Rutting Due to Strutcural Deformation after cracking

$$\Delta RDPD = K_{rpd} CDS^3 a_0 YE4\ Sh^{a_1} HS^{a_2}$$

Sub-Section		Lane	Observed mean Rut depth(mm)	Standard deviation of rut depth(mm)	YE4	SNP	HS	SH(Speed of Heavy vehicle-km/h)	CDS	a0	a1	a2	Age	Plastic Rutting(mm)
52+000	52+300	Right	10.3516129	3.02239	1	4.51	100	60	1	2.46	-0.78	0.71	14	2.65
52+300	52+600	Right	13.0755161	1.65868	1	4.78	100	60	1	2.46	-0.78	0.71	14	2.65
52+600	52+900	Right	12.6779032	1.89528	1	5.4	100	60	1	2.46	-0.78	0.71	14	2.65
52+900	53+200	Right	9.90177419	1.55524	1	5.1	100	60	1	2.46	-0.78	0.71	14	2.65
52+000	52+300	Left	12.7929677	1.87231	2.93	4.1	100	60	1	2.46	-0.78	0.71	14	7.78
52+300	52+600	Left	14.0145484	1.6921	2.93	5.01	100	60	1	2.46	-0.78	0.71	14	7.78
52+600	52+900	Left	13.3074516	1.94209	2.93	5.92	100	60	1	2.46	-0.78	0.71	14	7.78
52+900	53+200	Left	12.773625	5.20443	2.93	5.2	100	60	1	2.46	-0.78	0.71	14	7.78
55+200	55+500	Right	12.9284516	5.49665	1	5.09	100	60	1	2.46	-0.78	0.71	14	2.65
55+500	55+800	0.9451	9.57035484	5.19615	1	5.47	100	60	1	2.46	-0.78	0.71	14	2.65
55+800	56+200	Right	15.404122	4.17037	1	5.23	100	60	1	2.46	-0.78	0.71	14	2.65
55+200	55+500	Left	8.81325806	3.33487	2.93	4.54	100	60	1	2.46	-0.78	0.71	14	7.78
55+500	55+800	Left	10.2231935	3.66941	2.93	4.81	100	60	1	2.46	-0.78	0.71	14	7.78
55+800	56+200	Left	11.0576098	3.39065	2.93	5.85	100	60	1	2.46	-0.78	0.71	14	7.78
82+000	82+300	Right	13.5723226	6.15262	0.59	5.8	100	60	1	2.46	-0.78	0.71	13	1.57
82+300	82+600	Right	11.7687419	4.90318	0.59	6.26	100	60	1	2.46	-0.78	0.71	13	1.57
82+600	82+900	Right	8.00416129	4.92002	0.59	6.23	100	60	1	2.46	-0.78	0.71	13	1.57
82+900	83+200	Right	6.44845161	1.63243	0.59	6.61	100	60	1	2.46	-0.78	0.71	13	1.57
82+000	82+300	Left	13.2437419	5.93151	0.62	5.56	100	60	1	2.46	-0.78	0.71	13	1.65
82+300	82+600	Left	9.28370968	3.55193	0.62	6.13	100	60	1	2.46	-0.78	0.71	13	1.65
82+600	82+900	Left	8.50574194	2.48736	0.62	6.78	100	60	1	2.46	-0.78	0.71	13	1.65
82+900	83+200	Left	9.02316129	9.3768	0.62	6.81	100	60	1	2.46	-0.78	0.71	13	1.65
86+800	87+100	Right	6.12754839	2.67932	0.59	6.1	100	60	1	2.46	-0.78	0.71	13	1.57
87+100	87+400	Right	8.73245161	4.39271	0.59	5.3	100	60	1	2.46	-0.78	0.71	13	1.57
87+400	87+700	Right	9.80354839	3.82515	0.59	4.5	100	60	1	2.46	-0.78	0.71	13	1.57
87+700	88+000	Right	11.0899677	3.50408	0.59	5.23	100	60	1	2.46	-0.78	0.71	13	1.57

Rutting Due to Strutcural Deformation after cracking

$$\Delta RDPD = K_{rpd} CDS^3 a_0 YE4\ Sh^{a_1} HS^{a_2}$$

Sub-Section		Lane	Observed mean Rut depth(mm)	Standard deviation of rut depth(mm)	YE4	SNP	HS	SH(Speed of Heavy vehicle-km/h)	CDS	a0	a1	a2	Age	Plastic Rutting(mm)
87+400	87+700	Left	8.15787097	3.48076	0.62	4.37	100	60	1	2.46	-0.78	0.71	13	1.65
87+700	88+000	Left	9.17058065	3.63737	0.62	5.85	100	60	1	2.46	-0.78	0.71	13	1.65
135+000	135+300	Right	4.25451613	1.16831	0.6	5.58	100	60	1	2.46	-0.78	0.71	12	1.59
135+300	135+600	Right	4.91093548	2.37593	0.6	6.29	100	60	1	2.46	-0.78	0.71	12	1.59
135+600	135+900	Right	4.68793548	2.04366	0.6	5.16	100	60	1	2.46	-0.78	0.71	12	1.59
135+900	136+200	Right	4.358	2.89114	0.6	5.3	100	60	1	2.46	-0.78	0.71	12	1.59
136+200	136+500	Right	4.26409677	1.74977	0.6	4.32	100	60	1	2.46	-0.78	0.71	12	1.59
136+500	136+800	Right	8.95016129	4.63829	0.6	3.45	100	60	1	2.46	-0.78	0.71	12	1.59
136+800	137+000	Right	7.8702381	7.70569	0.6	4.1	100	60	1	2.46	-0.78	0.71	12	1.59
135+000	135+300	Left	8.73551613	3.16345	0.35	4.93	100	60	1	2.46	-0.78	0.71	12	0.93
135+300	135+600	Left	5.68467742	2.2034	0.35	4.79	100	60	1	2.46	-0.78	0.71	12	0.93
135+600	135+900	Left	9.70764516	3.13109	0.35	5.78	100	60	1	2.46	-0.78	0.71	12	0.93
135+900	136+200	Left	5.18096774	3.02413	0.35	4.48	100	60	1	2.46	-0.78	0.71	12	0.93
136+200	136+500	Left	3.72370968	1.68523	0.35	4.18	100	60	1	2.46	-0.78	0.71	12	0.93
136+500	136+800	Left	5.02622581	2.14382	0.35	4.44	100	60	1	2.46	-0.78	0.71	12	0.93
136+800	137+000	Left	3.2572381	1.21994	0.35	3.55	100	60	1	2.46	-0.78	0.71	12	0.93

ANNEX 4- CALIBRATION OF HDM 4 ROAD DETERIORATION MODELS

Total Rut Depth													
Sub-Section		Lane	Observed mean Rut depth(mm)	log(OMRD)	Standard deviation of rut	YE4	SNP	Intial densification(mm)	Strucural before cracking(mm)	Structural after cracking(mm)	Plastic deformation(mm)	Sum(mm)	LOG(PRD)
Start	End												
52+000	52+300	Right	10.4	1.0	3.0	0.97	4.51	3.24503	2.97	0.00026	2.6544658	8.8656	0.9
52+300	52+600	Right	13.1	1.1	1.7	0.97	4.78	3.06756	2.78	0.00246	2.6544658	8.50011	0.9
52+600	52+900	Right	12.7	1.1	1.9	0.97	5.43	2.73015	2.42	0.00061	2.6544658	7.80057	0.9
52+900	53+200	Right	9.9	1.0	1.6	0.97	5.16	2.87624	2.58	0.00642	2.6544658	8.1151	0.9
52+000	52+300	Left	12.8	1.1	1.9	2.86	4.1	4.05741	3.72	0.0012	7.7775847	15.5589	1.2
52+300	52+600	Left	14.0	1.1	1.7	2.86	5.01	3.30063	2.96	0.00445	7.7775847	14.0448	1.1
52+600	52+900	Left	13.3	1.1	1.9	2.86	5.92	2.83889	2.45	1.9E-05	7.7775847	13.0654	1.1
52+900	53+200	Left	12.8	1.1	5.2	2.86	5.2	3.18442	2.84	0.0119	7.7775847	13.813	1.1
55+200	55+500	Right	12.9	1.1	5.5	0.97	5.09	2.88989	2.58	0.08593	2.6544658	8.21404	0.9
55+500	55+800	Right	9.6	1.0	5.2	0.97	5.47	2.7814	2.38	0.02242	2.6544658	7.83842	0.9
55+800	56+200	Right	15.4	1.2	4.2	0.97	5.23	2.82221	2.51	0.17581	2.6544658	8.15753	0.9
55+200	55+500	0.94514	8.8	0.9	3.3	2.86	4.54	3.62824	3.31	0.01513	7.7775847	14.7352	1.2
55+500	55+800	Left	10.2	1.0	3.7	2.86	4.81	3.49043	3.10	0.16566	7.7775847	14.5367	1.2
55+800	56+200	Left	11.1	1.0	3.4	2.86	5.85	2.86571	2.48	0.05901	7.7775847	13.1847	1.1
82+000	82+300	Right	13.6	1.1	6.2	0.59	5.8	2.44986	1.95	0.47679	1.5661348	6.43916	0.8
82+300	82+600	Right	11.8	1.1	4.9	0.59	6.26	2.3053	1.78	0.66634	1.5661348	6.32196	0.8
82+600	82+900	Right	8.0	0.9	4.9	0.59	6.23	2.31323	1.79	0.05128	1.5661348	5.72462	0.8
82+900	83+200	Right	6.4	0.8	1.6	0.59	6.61	2.19327	1.68	0	1.5661348	5.43629	0.7
82+000	82+300	Left	13.2	1.1	5.9	0.62	5.56	2.54589	2.05	0.35038	1.6457688	6.59173	0.8
82+300	82+600	Left	9.3	1.0	3.6	0.62	6.13	2.35192	1.83	0.58605	1.6457688	6.41761	0.8
82+600	82+900	Left	8.5	0.9	2.5	0.62	6.78	2.17817	1.63	0.03709	1.6457688	5.49586	0.7
82+900	83+200	Left	9.0	1.0	9.4	0.62	6.81	2.16224	1.63	6.1E-05	1.6457688	5.43469	0.7
86+800	87+100	Right	6.1	0.8	2.7	0.59	6.1	2.35465	1.84	0.025	1.5661348	5.78341	0.8
87+100	87+400	Right	8.7	0.9	4.4	0.59	5.3	2.64453	2.16	0.02154	1.5661348	6.38925	0.8
87+400	87+700	Right	9.8	1.0	3.8	0.59	4.5	2.64453	2.16	0.02154	1.5661348	6.38925	0.8
87+700	88+000	Right	11.1	1.0	3.5	0.59	5.23	3.08249	2.60	1E-05	1.5661348	7.24802	0.9
86+800	87+100	Left	12.7	1.1	7.3	0.62	5.06	2.77344	2.19	0.00062	1.5661348	6.53018	0.8
87+100	87+400	Left	11.6	1.1	4.6	0.62	4.37	2.76392	2.28	0.29648	1.6457688	6.98831	0.8

Total Rut Depth

Sub-Section		Lane	Observed mean Rut depth(mm)	log(OMRD)	Standard deviation of rut	YE4	SNP	Intial densification(mm)	Strucural before cracking(mm)	Structural after cracking(mm)	Plastic deformation(mm)	Sum(mm)	LOG(PRD)
Start	End												
87+400	87+700	Left	8.2	0.9	3.5	0.62	4.37	3.18008	2.70	0.35454	1.6457688	7.87766	0.9
87+700	88+000	Left	9.2	1.0	3.6	0.62	5.85	3.17845	2.70	0.00333	1.6457688	7.52482	0.9
135+000	135+300	Right	4.3	0.6	1.2	0.6	5.58	2.49575	1.87	0.00158	1.5926795	5.95793	0.8
135+300	135+600	Right	4.9	0.7	2.4	0.6	6.29	2.29893	1.63	0.00051	1.5926795	5.52164	0.7
135+600	135+900	Right	4.7	0.7	2.0	0.6	5.16	2.71124	2.04	0.00073	1.5926795	6.34686	0.8
135+900	136+200	Right	4.4	0.6	2.9	0.6	5.3	2.64915	1.98	0.0048	1.5926795	6.22745	0.8
136+200	136+500	Right	4.3	0.6	1.7	0.6	4.32	3.21073	2.50	0.01584	1.5926795	7.32	0.9
136+500	136+800	Right	9.0	1.0	4.6	0.6	3.45	4.12539	3.23	0.05864	1.5926795	9.00823	1.0
136+800	137+000	Right	7.9	0.9	7.7	0.6	4.1	3.39026	2.65	0.00449	1.5926795	7.64171	0.9
135+000	135+300	Left	8.7	0.9	3.2	0.35	4.93	2.66245	2.03	0.00023	0.929063	5.61805	0.7
135+300	135+600	Left	5.7	0.8	2.2	0.35	4.79	2.73193	2.09	0.00151	0.929063	5.75646	0.8
135+600	135+900	Left	9.7	1.0	3.1	0.35	5.78	2.33683	1.69	8.7E-05	0.929063	4.95624	0.7
135+900	136+200	Left	5.2	0.7	3.0	0.35	4.48	2.91263	2.26	0.04777	0.929063	6.14939	0.8
136+200	136+500	Left	3.7	0.6	1.7	0.35	4.18	3.1182	2.45	0.02399	0.929063	6.51699	0.8
136+500	136+800	Left	5.0	0.7	2.1	0.35	4.44	2.93585	2.28	0.35263	0.929063	6.50069	0.8
136+800	137+000	Left	3.3	0.5	1.2	0.35	3.55	3.72866	2.95	0.00744	0.929063	7.61156	0.9
			8.5	41.0								7.55175	38.6

Observed mean Rut depth	8.5
Predicted mean rut depth	7.55
Calibraton factor	1.12583
Observed sum of log of mean rut depth	41
Predicted sum of mean rut depth	38.6
Calibraton factor	1.06218

0.88434

ANNEX 4- CALIBRATION OF HDM 4 ROAD DETERIORATION MODELS

Linear Regression of log(observed) Versus log(Predicted) Rut Depth

Observed	Predicted	Linear regressed	error^2
1.02	0.95	1.02	0.00
1.12	0.93	1.12	0.00
1.10	0.89	1.10	0.00
1.00	0.91	1.00	0.00
1.11	1.19	1.11	0.00
1.15	1.15	1.15	0.00
1.12	1.12	1.12	0.00
1.11	1.14	1.11	0.00
1.11	0.91	1.11	0.00
0.98	0.89	0.98	0.00
1.19	0.91	1.19	0.00
0.95	1.17	0.95	0.00
1.01	1.16	1.01	0.00
1.04	1.12	1.04	0.00
1.13	0.81	1.13	0.00
1.07	0.80	1.07	0.00
0.90	0.76	0.90	0.00
0.81	0.74	0.81	0.00
1.12	0.82	1.12	0.00
0.97	0.81	0.97	0.00
0.93	0.74	0.93	0.00
0.96	0.74	0.96	0.00
0.79	0.76	0.79	0.00
0.94	0.81	0.94	0.00
0.99	0.86	0.99	0.00
1.04	0.81	1.04	0.00
1.10	0.84	1.10	0.00
1.07	0.90	1.07	0.00
0.91	0.88	0.91	0.00
0.69	0.74	0.69	0.00
0.67	0.80	0.67	0.00
0.64	0.79	0.64	0.00
0.63	0.86	0.63	0.00
0.95	0.95	0.95	0.00
0.90	0.88	0.90	0.00
0.94	0.75	0.94	0.00
0.75	0.76	0.75	0.00
0.99	0.70	0.99	0.00
0.71	0.79	0.71	0.00
0.57	0.81	0.57	0.00
0.70	0.81	0.70	0.00
0.51	0.88	0.51	0.00
39.39	37.05	Sum	0.00
		Mean	0.00
		RMSE	0.00

ANNEX 4- CALIBRATION OF HDM 4 ROAD DETERIORATION MODELS

Roughness Prediction and Calibration with Section length of 300m

Section	Sub-Section		Lane	Observed avearge r	ESAL(cumulative)	SNP	COMP	ACRA	ACXa	RDS	HSNEW	$PACX_a$	HSOLD	AGE3	Coeff. for Dsnpk			Coef. Structural	Coeff. cracking	Coefficient Rutting	Dsnpk	Enivronm. coeficent-m	ΔRI_s	ΔRI_r	ΔRIc	ΔRI_s	Sum	Summary Rughness model
	Start	End				inch	%	mm	%	mm	mm	%	mm		a_0	a_1	a_2	a_0	a_0	a_0	inch							(IRI m/km)
1	52+000	52+300	Right	1.7	17.75	4.51	95	2.3	1.6	3.0	100.0	0.0	0.0	14.0	0	63	40	134	0.0066	0.088	0.01	0.00612	0.733	0.266	0.015	0.454	2.47	2.595918399
	52+300	52+600	Right	1.7	17.75	4.78	95	8.5	3.9	1.7	100.0	0.0	0.0	14.0	0	63	40	134	0.0066	0.088	0.03	0.014826	0.455	0.146	0.056	0.454	2.11	2.236880696
	52+600	52+900	Right	1.9	17.75	5.4	95	3.0	3.1	1.9	100.0	0.0	0.0	14.0	0	63	40	134	0.0066	0.088	0.02	0.017266	0.273	0.167	0.02	0.454	1.91	2.278018836
	52+900	53+200	Right	2.3	17.75	5.1	95	9.2	9.1	1.6	100.0	0.0	0.0	14.0	0	63	40	134	0.0066	0.088	0.07	0.034442	0.348	0.137	0.061	0.454	2	2.249981203
	52+000	52+300	Left	1.9	51.92	4.1	95	3.5	3.5	1.9	100.0	0.0	0.0	14.0	0	63	40	134	0.0066	0.088	0.03	0.000765	0.851	0.165	0.023	0.454	2.49	2.887928917
	52+300	52+600	Left	1.9	51.92	5.01	95	7.1	7.1	1.7	100.0	0.0	0.0	14.0	0	63	40	134	0.0066	0.088	0.05	-0.006429	0.374	0.149	0.047	0.454	2.02	3.077073812
	52+600	52+900	Left	2.0	51.92	5.92	95	0.6	0.6	1.9	100.0	0.0	0.0	14.0	0	63	40	134	0.0066	0.088	0	-0.003442	0.185	0.171	0.004	0.454	1.81	3.259245319
	52+900	53+200	Left	3.3	51.92	5.2	95	11.5	11.5	5.2	100.0	0.0	0.0	14.0	0	63	40	134	0.0066	0.088	0.09	0.026658	0.321	0.458	0.076	0.454	2.31	3.638316913
	55+200	55+500	Right	3.5	17.75	5.09	95	31.2	31.2	5.5	100.0	0.0	0.0	14.0	0	63	40	134	0.0066	0.088	0.24	0.054891	0.351	0.484	0.206	0.454	2.49	2.948129749
	55+500	55+800	Right	4.4	17.75	5.47	95	17.0	17.0	5.2	100.0	0.0	0.0	14.0	0	63	40	134	0.0066	0.088	0.13	0.076334	0.259	0.457	0.112	0.454	2.28	2.838502707
	55+800	56+200	Right	3.2	17.75	5.23	95	44.3	44.3	4.2	100.0	0.0	0.0	14.0	0	63	40	134	0.0066	0.088	0.34	0.047952	0.313	0.367	0.292	0.454	2.43	2.859423843
	0.94514	55+500	Left	3.3	51.92	4.54	95	12.2	12.2	3.3	100.0	0.0	0.0	14.0	0	63	40	134	0.0066	0.088	0.09	0.035064	0.563	0.293	0.08	0.454	2.39	3.242774513
	55+500	55+800	Left	3.9	51.92	4.81	95	38.8	38.8	3.7	100.0	0.0	0.0	14.0	0	63	40	134	0.0066	0.088	0.29	0.043119	0.444	0.323	0.256	0.454	2.48	3.523324904
2	55+800	56+200	Left	3.0	51.92	5.85	95	25.7	25.7	3.4	100.0	0.0	0.0	13.0	0	63	40	134	0.0066	0.088	0.19	0.021054	0.189	0.298	0.17	0.422	2.08	3.521495717
	82+000	82+300	Right	3.9	9.2	5.8	95	73.4	69.3	6.2	100.0	0.0	0.0	13.0	0	63	40	134	0.0066	0.088	0.48	0.068597	0.196	0.541	0.485	0.422	2.64	3.081644544
	82+300	82+600	Right	3.1	9.2	6.26	95	88.0	84.4	4.9	100.0	0.0	0.0	13.0	0	63	40	134	0.0066	0.088	0.48	0.041819	0.141	0.431	0.581	0.422	2.57	3.019976825
	82+600	82+900	Right	2.6	9.2	6.23	95	25.5	25.5	4.9	100.0	0.0	0.0	13.0	0	63	40	134	0.0066	0.088	0.19	0.039404	0.144	0.433	0.168	0.422	2.17	2.604829005
	82+900	83+200	Right	1.7	9.2	6.61	95	0.0	0.0	1.6	100.0	0.0	0.0	13.0	0	63	40	134	0.0066	0.088	0	0.022289	0.111	0.144	0	0.422	1.68	1.987876181
	82+000	82+300	Left	4.6	9.91	5.56	95	62.2	58.7	5.9	100.0	0.0	0.0	13.0	0	63	40	134	0.0066	0.088	0.45	0.086866	0.234	0.522	0.41	0.422	2.59	2.985278744
	82+300	82+600	Left	3.8	9.91	6.13	95	79.8	80.3	3.6	100.0	0.0	0.0	13.0	0	63	40	134	0.0066	0.088	0.48	0.070465	0.154	0.313	0.527	0.422	2.42	2.791265037
	82+600	82+900	Left	2.4	9.91	6.78	95	22.6	22.5	2.5	100.0	0.0	0.0	13.0	0	63	40	134	0.0066	0.088	0.17	0.040978	0.1	0.219	0.149	0.422	1.89	2.285785973
1	82+900	83+200	Left	2.0	9.91	6.81	95	1.1	1.1	9.4	100.0	0.0	0.0	13.0	0	63	40	134	0.0066	0.088	0.01	-0.015524	0.098	0.825	0.007	0.422	2.35	3.109192315
	86+800	87+100	Right	1.9	9.2	6.1	95	18.7	17.4	2.7	100.0	0.0	0.0	13.0	0	63	40	134	0.0066	0.088	0.13	0.019697	0.158	0.236	0.123	0.422	1.94	2.24078078
	87+100	87+400	Right	2.8	9.2	5.3	95	16.2	15.5	4.4	100.0	0.0	0.0	13.0	0	63	40	134	0.0066	0.088	0.12	0.050238	0.287	0.387	0.107	0.422	2.2	2.43559029
	87+400	87+700	Right	3.0	9.2	4.5	95	0.6	0.3	3.8	100.0	0.0	0.0	13.0	0	63	40	134	0.0066	0.088	0	0.064443	0.565	0.337	0.004	0.422	2.33	2.223000214
	87+700	88+000	Right	2.3	9.2	5.23	95	3.4	2.6	3.5	100.0	0.0	0.0	13.0	0	63	40	134	0.0066	0.088	0.02	0.038521	0.303	0.308	0.022	0.422	2.06	2.223255619
	86+800	87+100	Left	3.2	9.91	5.06	95	53.5	53.9	7.3	100.0	0.0	0.0	13.0	0	63	40	134	0.0066	0.088	0.41	0.043768	0.348	0.645	0.353	0.422	2.77	3.103334821
	87+100	87+400	Left	4.1	9.91	4.37	95	58.5	52.2	4.6	100.0	0.0	0.0	13.0	0	63	40	134	0.0066	0.088	0.4	0.082579	0.637	0.402	0.386	0.422	2.85	2.724546306
2	87+400	87+700	Left	3.7	9.91	4.37	95	7.9	4.7	3.5	100.0	0.0	0.0	13.0	0	63	40	134	0.0066	0.088	0.04	0.083213	0.637	0.306	0.052	0.422	2.42	2.234003109
	135+000	135+300	Right	2.0	8.8	5.58	95	7.0	4.3	1.2	100.0	0.0	0.0	12.0	0	63	40	134	0.0066	0.088	0.03	0.039108	0.223	0.103	0.046	0.389	1.76	1.868365445
	135+300	135+600	Right	1.4	8.8	6.29	95	4.4	2.6	2.4	100.0	0.0	0.0	12.0	0	63	40	134	0.0066	0.088	0.02	-0.003206	0.134	0.209	0.029	0.389	1.76	2.044050542
	135+600	135+900	Right	1.1	8.8	5.16	95	5.5	2.5	2.0	100.0	0.0	0.0	12.0	0	63	40	134	0.0066	0.088	0.02	-0.019717	0.311	0.18	0.036	0.389	1.92	1.967090491
	135+900	136+200	Right	1.7	8.8	5.3	95	12.2	6.8	2.9	100.0	0.0	0.0	12.0	0	63	40	134	0.0066	0.088	0.05	0.012214	0.278	0.254	0.081	0.389	2	2.135105887

Roughness Prediction and Calibration with Section length of 300m

Section	Sub-Section		Lane	Observed avearge r	ESAL(cumulative)	SNP	COMP	ACRA	ACXa	RDS	HSNEW	$PACX_a$	HSOLD	AGE3	Coeff. for Dsnpk			Coef. Structural	Coeff. cracking	Coefficient Rutting	Dsnpk	Enivronm. coeficent-m	ΔRI_s	ΔRI_r	ΔRIc	ΔRI_s	Sum	Summary Rughness model
	Start	End				inch	%	mm	%	mm	mm	%	mm		a_0	a_1	a_2	a_0	a_0	a_0	inch							(IRI m/km)
	136+200	136+500	Right	2.1	8.8	4.32	95	18.4	11.8	1.7	100.0	0.0	0.0	12.0	0	63	40	134	0.0066	0.088	0.09	0.042274	0.646	0.154	0.122	0.389	2.31	1.984050552
	136+500	136+800	Right	3.2	8.8	3.45	95	34.1	18.6	4.6	100.0	0.0	0.0	12.0	0	63	40	134	0.0066	0.088	0.14	0.0718	1.578	0.408	0.225	0.389	3.6	2.464500056
	136+800	137+000	Right	2.2	8.8	4.1	95	12.3	5.3	7.7	100.0	0.0	0.0	12.0	0	63	40	134	0.0066	0.088	0.04	0.017033	0.798	0.678	0.081	0.389	2.95	2.770191592
	135+000	135+300	Left	1.5	5.32	4.93	95	2.1	2.1	3.2	100.0	0.0	0.0	12.0	0	63	40	134	0.0066	0.088	0.02	0.008802	0.376	0.278	0.014	0.389	2.06	2.015762378
	135+300	135+600	Left	1.7	5.32	4.79	95	5.1	5.2	2.2	100.0	0.0	0.0	12.0	0	63	40	134	0.0066	0.088	0.04	0.025186	0.423	0.194	0.034	0.389	2.04	1.898335866
	135+600	135+900	Left	1.2	5.32	5.78	95	1.4	1.4	3.1	100.0	0.0	0.0	12.0	0	63	40	134	0.0066	0.088	0.01	-0.01614	0.192	0.276	0.01	0.389	1.87	2.023697241
	135+900	136+200	Left	2.8	5.32	4.48	95	27.7	24.3	3.0	100.0	0.0	0.0	12.0	0	63	40	134	0.0066	0.088	0.18	0.064101	0.557	0.266	0.183	0.389	2.4	2.157410478
	136+200	136+500	Left	2.6	5.32	4.18	95	18.8	17.6	1.7	100.0	0.0	0.0	12.0	0	63	40	134	0.0066	0.088	0.13	0.066065	0.739	0.148	0.124	0.389	2.4	1.904269134
	136+500	136+800	Left	4.5	5.32	4.44	95	72.5	61.4	2.1	100.0	0.0	0.0	12.0	0	63	40	134	0.0066	0.088	0.47	0.107704	0.578	0.189	0.479	0.389	2.63	2.332171219
1&2	136+800	137+000	Left	2.3	5.32	3.55	95	12.3	8.0	1.2	100.0	0.0	0.0	12.0	0	63	40	134	0.0066	0.088	0.06	0.056951	1.412	0.107	0.081	0.389	2.99	1.783115824
			Mean	2.6																	Sum	1.578148					Mean	2.54780214
					0bs/Pred	1.038															Mean	0.035867						

ANNEX 4- CALIBRATION OF HDM 4 ROAD DETERIORATION MODELS

Estimation of Environmental coefficient and prediction of the roughness using a summary model for 1-1.2km length section

$$\mathbf{m} = \frac{\{\ln[1.02\mathbf{RI_t} - (0.143\mathbf{RDS} + 0.0068\mathbf{ACRX} + 0.056\mathbf{APAT})] - \ln[\mathbf{RI_0} + 263\mathbf{NE}(1+\mathbf{SNP})^{-5}]\}}{\mathbf{AGE3}}$$

$$\mathbf{RI_t} = 0.98\left[e^{\mathbf{AGE3}*\mathbf{m}}(\mathbf{RI_o} + 263\mathbf{NE}(1+\mathbf{SNP})^{-5}) + 0.143\mathbf{RDS} + 0.0068\mathbf{ACRX} + 0.056\mathbf{APAT}\right]$$

Segement	Section	Sub-Section		Lane	Observed avearge roughness(IRI)	NE	SNP	COMP	ACRA	ACXa	RDS	HSNEW	$PACX_a$	HSOLD	AGE3	Coefficients for Dsnpk			Coef. Structural	Coefficient cracking	Coefficient Rutting	Dsnpk	Enivronmental coeficent-m	Average m/section/direction	Predicted roughness
	1	Start	End		IRI(m/km)	millions/lane	inch	%	mm	%	mm	mm	%	mm		a_0	a_1	a_2	a_0	a_0	a_0	inch			
		52+000	53+200	Right	1.9	17.75	4.95	95	5.8	4.4	2.1	100.0	0.0	0.0	14.0	0	63	40	134	0.007	0.088	0.03358	0.01671829	0.03478104	2.45
		52+000	53+300	Left	2.3	51.92	5.06	95	5.7	5.7	2.8	100.0	0.0	0.0	14.0	0	63	40	134	0.007	0.088	0.04321	0.002267693		3.49
	2	55+200	56+200	Right	3.5	17.75	5.08	95	30.8	30.8	5.0	100.0	0.0	0.0	14.0	0	63	40	134	0.007	0.088	0.23346	0.052843787		2.97
1		0.945136	56+200	Left	3.4	51.92	5.07	95	25.6	25.6	3.5	100.0	0.0	0.0	14.0	0	63	40	134	0.007	0.088	0.19405	0.030365039	0.01631637	3.70
	1	82+000	83+200	Right	2.8	9.2	6.23	95	46.7	44.8	4.4	100.0	0.0	0.0	13.0	0	63	40	134	0.007	0.088	0.33958	0.037864227	0.03963816	2.73
		82+000	83+200	Left	4.6	9.91	6.32	95	41.4	40.7	5.4	100.0	0.0	0.0	13.0	0	63	40	134	0.007	0.088	0.30813	0.086347059		2.83
	2	86+800	88+000	Right	2.5	9.2	5.3	95	9.7	9.0	3.6	100.0	0.0	0.0	13.0	0	63	40	134	0.007	0.088	0.06784	0.041412096		2.36
2		86+800	88+000	Left	3.7	9.91	4.91	95	34.7	30.0	4.8	100.0	0.0	0.0	13.0	0	63	40	134	0.007	0.088	0.2274	0.07063479	0.07849092	2.63
	1&2	135+000	137+000	Right	2.0	8.8	4.88	95	13.4	7.4	3.2	100.0	0.0	0.0	12.0	0	63	40	134	0.007	0.088	0.05609	0.02300073	0.01941158	2.21
3		135+000	137+000	Left	2.4	5.32	4.93	95	20.0	17.2	1.9	100.0	0.0	0.0	12.0	0	63	40	134	0.007	0.088	0.13038	0.053556509	0.04979524	2.04
				Mean	2.9																		Mean	0.03973889	2.74
							0bs/Pred		1.1													Kge	Mean/0.023	1.72777763	

ANNEX 4- CALIBRATION OF HDM 4 ROAD DETERIORATION MODELS

Roughness Calibration					
Segement		Observed IRI(m/km)	Predicted IRI(m/km)	Predicted IRI(m/km)	Error^2
Start Chainage	End Chainage				
52+000	53+200	1.90	2.45	2.59864632	0.5
52+000	53+300	2.28	3.49	3.69648409	2.0
55+200	56+200	3.54	2.97	3.14296542	0.2
55+200	56+200	3.40	3.70	3.91915974	0.3
82+000	83+200	2.80	2.73	2.89230659	0.0
82+000	83+200	4.61	2.83	3.00357648	2.6
86+800	88+000	2.50	2.36	2.50467893	0.0
86+800	88+000	3.70	2.63	2.79283174	0.8
135+000	137+000	1.97	2.21	2.33979381	0.1
135+000	137+000	2.40	2.04	2.16535824	0.1
Average		2.91	2.74		0.7
Calibration factor		0.945136			0.808